UNIVERSIDADE FEDERAL DE SANTA CATARINA
DEPARTAMENTO DE ENGENHARIA MECÂNICA

Leonardo Mejia Rincon

WRENCH CAPABILITY OF PLANAR MANIPULATORS

Florianópolis

2016

Leonardo Mejia Rincon

WRENCH CAPABILITY OF PLANAR MANIPULATORS

Tese submetida ao Programa de Pós-Graduação em Engenharia Mecânica para a obtenção do Grau de Doutor em Engenharia Mecânica.
Orientador: Prof. Daniel Martins, Dr. Eng.
Coorientador: Prof. Henrique Simas, Dr. Eng.

Florianópolis

2016

Catalogação na fonte elaborada pela biblioteca da
Universidade Federal de Santa Catarina

A ficha catalográfica é confeccionada pela Biblioteca Central.

Tamanho: 7cm x 12 cm

Fonte: Times New Roman 9,5

Maiores informações em:
http://www.bu.ufsc.br/design/Catalogacao.html

Leonardo Mejia Rincon

WRENCH CAPABILITY OF PLANAR MANIPULATORS

Esta Tese foi julgada aprovada para a obtenção do Título de "Doutor em Engenharia Mecânica", e aprovada em sua forma final pelo Programa de Pós-Graduação em Engenharia Mecânica.

Florianópolis, 15 de Abril 2016.

Prof. Armando Albertazzi Gonçalves Jr, Dr. Eng.
Coordenador do Curso

Prof. Daniel Martins, Dr. Eng.
Orientador

Prof. Henrique Simas, Dr. Eng.
Coorientador

Banca Examinadora:

Prof. Daniel Martins, Dr. Eng.
Presidente

Prof. Tarcisio Hess Coelho, Dr. Eng.

Prof. Anibal Alexandre Campos Bonilla, Dr. Eng.

Prof. Edson Roberto de Pieri, Dr. Eng.

Prof. Lucas Weihmann, Dr. Eng.

Prof. Eduardo Alberto Fancello, Dr. Eng.

To my princess Magali, the reason to wake-up each morning.

AGRADECIMENTOS

Aos meus inesquecíveis avós Maria B. Carrascal (In Memorian), Carlos D. Rincon e Isabel Rincon (In Memorian), exemplos de amor, simplicidade, honestidade, sabedoria, dedicação ao próximo e figuras de grande importância em minha formação e de quem eu sinto muita saudade.

Aos meus pais George e Mildred, às minhas irmãs, Sandra e Sor Margit, por todo amor, carinho, educação, compreensão, ajuda e por fazerem dos meus sonhos os seus sonhos.

Aos meus sobrinhos por se tornarem o motor da minha história.

À minha esposa Magali, quem de forma especial e carinhosa me deu força e coragem, me apoiando nos momentos de dificuldades. Muito obrigado pela sua paciência e capacidade de me trazer paz na correria de cada dia.

Aos meus tios e primos pelo apoio incondicional ao longo da minha vida.

Ao Prof. Daniel Martins pelas contribuições e valiosas conversas, e ao Prof. Henrique Simas pela paciência e ajuda fornecida.

Ao pessoal do Laboratório de Robótica da Universidade Federal de Santa Catarina (LAR): Anelize, Estevan, Julio Frantz, Andrea, Fabiola, Gonzalo, Roberto, Julio Golin, Daniel Ponce e outros, pelas discussões e aportes feitos ao trabalho e pelas discussões e conversas conclusivas ou não.

À CNPq pelo apoio financeiro.

"When you change the way you look at things, the things you look at change".

Max Planck

RESUMO

Robôs são amplamente utilizados em fábricas, e novas aplicações no espaço, nos oceanos, nas indústrias nucleares e em outros campos estão sendo ativamente desenvolvidas. A criação de robôs autónomos que podem aprender a agir em ambientes imprevisíveis tem sido um objetivo de longa data da robótica, da inteligência artificial, e das ciências cognitivas.

Um passo importante para a autonomia dos robôs é a necessidade de dotá-los com um certo nível de independência, a fim de enfrentar as mudanças rápidas no ambiente circundante; para obter robôs que operem fora de ambientes rigidamente estruturados, tais como centros de investigação ou instalações de universidades e sem precisar da supervisão de engenheiros ou especialistas, é necessário enfrentar diferentes desafios tecnológicos, entre eles, o desenvolvimento de estratégias que permitam que os robôs interajam com o ambiente. Neste contexto, quando um contacto físico com o ambiente é estabelecido, uma força específica precisa de ser exercida e esta força tem de ser controlada em relação ao processo a fim de evitar a sobrecarga ou danificar o manipulador ou os objetos a serem manipulados.

O principal objetivo deste trabalho é apresentar novas metodologias desenvolvidas para determinar a máxima carga que um mecanismo ou manipulador planar pode aplicar ou suportar (capacidade de carga), sejam eles paralelos, seriais ou híbridos e com redundância ou não. A fim de resolver o problema da capacidade de carga, neste trabalho foram propostas duas novas abordagens com base no método do fator de escala clássico e nos métodos clássicos de otimização. Essas novas abordagens deram como resultado um novo método chamado de método de fator de escala modificado utilizado para resolver a capacidade de carga em manipuladores seriais planares e quatro modelos matemáticos para resolver o problema de capacidade de carga em manipuladores paralelos planares com um grau líquido de restrição igual três, quatro, cinco ou seis ($C_N = 3$, $C_N = 4$, $C_N = 5$ ou $C_N = 6$).

Palavras-chave: Capacidade de carga. Mecanismos. Robôs. Redundância cinemática. Redundância de atuação. Teoria de Helicoides. Método de Davies.

ABSTRACT

Robots are now widely used in factories, and new applications of robots in space, the oceans, nuclear industries, and other fields are being actively developed. Creating autonomous robots that can learn to act in unpredictable environments has been a long-standing goal of robotics, artificial intelligence, and cognitive sciences.

An important step towards the autonomy of robots is the need to provide them with a certain level of independence in order to face quick changes in the environment surrounding them; to get robots operating outside rigidly structured environments, such as research centres or universities facilities and beyond the supervision of engineers or experts, it is necessary to face different technological challenges, amongst them, the development of strategies that allow robots to interact with the environment. In this context, when a physical contact with the the environment is established, a process-specific force need to be exerted and this force has to be controlled in relation to the particular process in order to prevent overloading or damaging the manipulator or the objects to be manipulated.

The main objective of this work is to present new methodologies developed for determining the maximum wrench that can be applied or sustained (wrench capability) in planar mechanisms and manipulators, whether it be serial parallel or hybrid and with redundancy or not. In order to solve the wrench capability problem, in this work two new approaches were proposed based in the classic scaling factor method and in classical optimization methods. These new approaches gave as result a new method called the modified scaling factor method used to solve the wrench capability in planar serial manipulators and four mathematical closed-form solutions to solve the wrench capability problem in planar parallel manipulators with a net degree of constraint equal to three, four, five or six ($C_N = 3$, $C_N = 4$, $C_N = 5$ ou $C_N = 6$).

Keywords: Wrench Capability. Mechanisms. Robots. Kinematic redundancy. Actuation redundancy. Screw theory. Davies method.

LIST OF FIGURES

LIST OF TABLES

LIST OF ABBREVIATIONS

DOF	Degree of freedom
DE	Differential evolution
IFR	International federation of robotics
LAR	Laboratory of robotic (UFSC)
MAV	Maximum available value
MIV	Maximum isotropic value
GA	Genetic algorithms
EC	Evolutionary computation
GGT	General graph theory
PM	Planar manipulator
PPM	Planar parallel manipulator
KKT	Karush-Kuhn-Tucker
SVD	Singular Value Decomposition
DH	Denavit Hartenberg

LIST OF SYMBOLS

x, y	Cartesian coordinates
\$	Screw
$\widehat{\$}$	Normalized screw
h	Pitch of a screw
λ	Screw system dimension
n	Number of links in a mechanism
j	Number of joints in a mechanisms
v	Number of the independent circuits in a graph
R	Revolute joint
$\underline{\text{R}}$	Actuated revolute joint
P	Prismatic joint
$\underline{\text{P}}$	Actuated prismatic joint
S	Spheric joint
U	Universal joint
M	Mobility
k	Number of cuts in a graph
C	Number of cords in a graph
e	Number of direct couplings in a graph
O_{xyz}	Origin of a coordinate system
$\$^J$	Wrench
$\widehat{\$}^J$	Normalized wrench
ψ_i	Scaling factor for a saturated joint i
Ψ	Generalized scaling factor
ϕ	Orientation of the end effector of a manipulator
C_N	Net degree of constraint
G_A	Action graph
G_C	Coupling graph
J	Jacobian
v	Linear velocity
w	Angular velocity
f	Pure force
m	Moment

τ	Primary action in a joint
$\tau_{i_{ext}}$	Extreme action Capability in a joint
$\tau_{i_{min}}$	Minimum action Capability in a joint
$\tau_{i_{max}}$	Maximum action Capability in a joint
$[Q_N]_{k,e}$	Cut-set matrix
$[A_N]_{3k,e}$	Action matrix
$[\widehat{A}_N]_{3k,e}$	Unitary action matrix
$[A]$	Coeficient matrix of the static solution
$a_{m,n}$	element m, n of the coeficient matrix of the static solution
F_x	Force in x
F_y	Force in y
F_z	Force in z
M_x	Moment in x
M_y	Moment in y
M_z	Moment in z
${}^{i-1}T_i$	Homogeneous tansformation matrix
f_{obj}	Objective function
x_n	Variables of the objective function
$h_i(x)$	Equality constraints
$g_i(x)$	Inequality constraints
n_e	Total number of equality constraints
n_g	Total number of inequality constraints
$\mathcal{L}$	Lagrangian function
θ	Angle of application of the force
F_{av}	Maximum available force
F_{is}	Maximum isotropic force
F_{app}	Maximum force with a prescribed moment
F_m	Maximum force that can be applied with zero moment

CONTENTS

1 INTRODUCTION

Robots are now widely used in factories, and applications of robots in space, the oceans, nuclear industries, and other fields are being actively developed. Also, nowadays, the use of robots in every facet of society, including the home, is being seriously considered. In this context, creating autonomous robots that can learn to act in unpredictable environments has been a long-standing goal of robotics, artificial intelligence, and cognitive sciences.

An important step towards the autonomy of robots is the need to provide them with a certain level of independence in order to face quick changes in the environment surrounding them; to get robots operating outside rigidly structured environments, such as research centres or universities facilities and beyond the supervision of engineers or experts, it is necessary to face different technological challenges, amongst them, the development of strategies that allow robots to interact with the environment (ROMANELLI, 2011).

In regard to the nature of the interaction between a robot and its environment, robotic applications can be categorized in two classes. The first class is referred to ***non-contact tasks*** (unconstrained motion in a free space, without any environmental influence on the robot). In these tasks, the robot dynamics is the most important aspect as regards its performance, several industrial applications such as pick-and-place, spray painting, gluing, and arc or spot welding belong to this category.

In contrast to the non-contact tasks, many complex advanced robotic applications (packaging, assembling, or machining) require the manipulator to be coupled with other objects which can move (ROMANELLI, 2011), this kind of applications can be categorized as ***contact tasks***.

The ***contact tasks*** can be furthermore divided into two subclasses: ***essential force tasks*** and ***compliant motion tasks***. The first subclass requires the end-effector to establish a physical contact with the objects in the environment and exert a process-specific force. In these tasks, a synergy between the control of the end-effector position and interaction forces is required; some examples of this kind of tasks are deburring, roughing, bending, polishing, and so forth. In these tasks, the force has to be controlled in relation to the particular process in order to prevent overloading or damaging the tool or the objects to be manufactured. In the second subclass, the tasks focus on the end-effector motion, which has to be realized close to the con-

strained surfaces, and it must be compliant (i.e., capable to reacting to the interaction forces). In this second subclass, the problem of controlling the robot is joined to the problem of accurate positioning (as in part-mating process) (ROMANELLI, 2011). In the future of robotics, the interaction with the environment is fundamental and more and more tasks will include and require interaction.

In this work, we will focus on the contact task class; within this context, the *wrench capability* in planar manipulators is studied herein and generalized methods to solve the *wrench capability* problem in planar mechanisms and manipulators are proposed.

The ***wrench capability*** is defined as the maximum wrench (force and moment) that can be applied (or sustained) for a given pose, based on the limits of its actuators (NOKLEBY et al., 2005). The *wrench capability* of a manipulator is dependent on its design, posture, actuation limits and redundancies (WEIHMANN; MARTINS; COELHO, 2011). By considering all possible directions of the applied wrench, a wrench capability plot can be generated for the given pose (NOKLEBY et al., 2005, 2007).

The wrench capability analysis is essential for the design and performance evaluation of manipulators. For a given pose, the end-effector is required to move with a desired force/moment or to sustain a specified wrench. Thus, the information of the joint torques that will produce such conditions could be investigated. These study is referred to as the inverse static force problem. An extended problem can be formulated as the analysis of the maximum wrench that the end-effector can apply into the wrench spaces.

In robotics, although the terms ***wrench capability*** and ***force capability*** of a manipulator can be used as synonymous, in the current document is preferably used the term *wrench capability* because it is broader.

1.1 LITERATURE REVIEW ON THE WRENCH CAPABILITY

The idea of measuring the manipulating ability of manipulators was first introduced in (YOSHIKAWA, 1985b), where the velocity manipulability ellipsoid and the force manipulability ellipsoid were defined. To date, three different approaches for determining force capabilities have been proposed in the literature: wrench ellipsoid, wrench polytope and constrained optimization (FIRMANI et al., 2008b).

1.1.1 Wrench ellipsoid

The wrench ellipsoid approach is based on bounding the actuator torque vector by a unit sphere $\tau^T\tau \leq 1$. The torques are mapped into the wrench space by using $\tau = J^T F$, yielding a force ellipsoid $F^T J J^T F \leq 1$. If Singular Value Decomposition (SVD) is applied to J i.e., $J = U \sum V^T$, the principal axes of the ellipsoid can be determined as u_k/σ_k where σ_k is the k^{th} singular value and u_k is the k^{th} column of matrix U . These axes can be employed as wrench performance indices of the manipulator. This approach was introduced by Yoshikawa (YOSHIKAWA, 1985b, 1985a) with the manipulability (twist) ellipsoid and proposed manipulability measurements. Also, Yoshikawa (YOSHIKAWA, 1990) presented the duality between the twist and wrench ellipsoids concluding that axes of the ellipsoids coincide but their lengths are inversely proportional.

For cooperating manipulators, Chiacchio *et al* (CHIACCHIO; VERCELLI; PIERROT, 1996) presented a complete analysis of wrench ellipsoids for multiple-arm systems, which involves external and internal forces. Lee and Kim (LEE; KIM, 1991) (velocity problem) and Chiacchio et al. (CHIACCHIO; VERCELLI; PIERROT, 1997) (static force problem) proposed to normalize the joint space variables (joint velocities and joint torques, respectively) when the actuators do not produce the same output. As a result, the resulting ellipsoid is defined as the pre-image of the unit sphere in the scaled joint variable space.

The wrench ellipsoid approach can be implemented easily and the required computation is immediate. However, this approach is an approximation because the joint torques are normalized ($\tau^T\tau \leq 1$) yielding a hypersphere in the torque space. The correct model of the joint torques must be an m-dimensional parallelepiped in the torque space due to the nature of the extreme torque capabilities of each actuator, i.e., $\tau_{i_{min}}$ or $\tau_{i_{max}}$.

1.1.2 Wrench polytope

The wrench polytope approach considers the complete region in which the actuator can operate. A comparison between the ellipsoid approach and the polytope approach is shown in Fig. (1). Assume a manipulator with two actuated revolute joints whose extreme capabilities are $\tau_{i_{ext}} = \pm 1$ [Nm], for $i = 1, 2$. Fig. (1.a) shows the generation of an ellipse (in general, an ellipsoid) as a result of mapping a circle (in

general, a hypersphere). Fig. (1.b) shows the generation of a polygon (in general, a polytope) as a result of mapping a square (in general, a hypercube). Each plot contains two coordinate systems.

The inner circle of Fig. (1.a) and the inner square of Fig. (1.b) describe the torque limits in the torque space (bottom and left axes); whereas, the outer ellipse and polygon describe the wrench capabilities in the wrench space (top and right axes). The lines that connect the inner to the outer shapes illustrate the linear transformation. Note how the edges and vertices of the square and polygon correspond in both spaces. The areas comprised by these geometrical shapes represent the feasible capabilities in their corresponding spaces. The square is an exact representation of the torque capabilities; while, the circle is an approximation. For example, the upper-right vertex of the square is $\tau_1 = \tau_2 = 1$ [Nm]; although this torque combination is feasible, the circle model does not include it. Thus, modeling the torque capabilities as a square is better than as a circle. Fig. (1.c) shows how the circle and ellipse are inscribed within the square and polygon, respectively. It is important to mention that the principal axes of the ellipse are directed towards the vertices of the polygon.

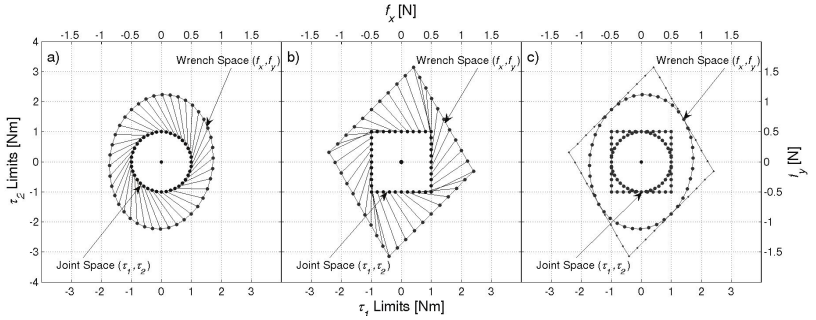

Figure 1 – Mapping of ellipsoids and polytopes from the joint space to the task space.

In general, each actuator torque defines an orthonormal axis in $\mathbb{R}^m$. The extremes of each torque constrain the torque space with a pair of parallel planes along each axis. The feasible region in which the manipulator can operate is bounded by these pairs of parallel planes yielding an m-dimensional parallelepiped.

A linear transformation, such as the equation of the direct static force ($\tau = J^T F$), maps vector τ from $\mathbb{R}^m$ (joint torque space) to $\mathbb{R}^n$ (wrench space). Rockafellar (ROCKAFELLAR, 1997) studied the prop-

erties of convex polyhedral sets. From his analysis, the following relationship is held through a linear transformation: Let τ be the m-dimensional parallelepiped (a convex set) and J^{-T} be the linear transformation from $\mathbb{R}^m$ to $\mathbb{R}^n$. Then the resulting transformation $J^{-T}\tau$ leads to another convex polyhedral set (F) in $\mathbb{R}^n$ and it contains a finite number of facets.

Kokkinis and Paden (KOKKINIS; PADEN, 1989) introduced the concept of twist and wrench convex polytopes. The analysis was applied to a single serial manipulator and to two cooperating manipulators. Chiacchio *et al.* (CHIACCHIO, 1997) analyzed the wrench polytopes of redundant serial manipulators. Finotello *et al.* (FINOTELLO et al., 1998) introduced two sets of indices that can be implemented to twist and wrench polytopes: the maximum isotropic value (MIV) and the maximum available value (MAV). These indices will be discussed in detail in Chapter 2. For 6-DOF manipulators, Finotello *et al.* (FINOTELLO et al., 1998) proposed to analyze these indices with force and moment as separate entities. Gallina *et al.* (GALLINA; ROSATI; ROSSI, 2001) analyzed the manipulability of a 3-DOF wire driven planar haptic device using polytopes. Lee and Shim (LEE; SHIM, 2004) expanded the concept to dynamic manipulability of multiple cooperating manipulators resulting in acceleration polytopes.

Krut et al. (KRUT; COMPANY; PIERROT, 2004b) analyzed twist ellipsoids and polytopes in redundant parallel manipulators and established performance indices. They showed that there is another ellipsoid, besides the one derived with SVD, which is larger in volume and is fully inscribed within the polytope. Krut et al. (KRUT; COMPANY; PIERROT, 2004a) also studied force performance indices of redundant parallel manipulators and determined the isotropic wrench workspaces of planar wire-driven manipulators with multiple actuated limbs. Firmani *et al.* (FIRMANI et al., 2008a) derived a set of wrench performance indices for PPMs.

1.1.3 Constrained optimization

In general, the constrained optimization approach involves: an objective function that maximizes either the magnitude of the force (F) or the moment (M_z); one equality constraint ($F = J^{-T}\tau$); and a set of inequality constraints ($\tau_{i_min} \leq \tau_i \leq \tau_{i_max}$), indicating the actuator output capabilities. Several studies that used this approach are related below.

Kumar and Waldron (KUMAR; WALDRON, 1988) investigated the force distribution in redundantly-actuated closed-loop kinematic chains and concluded that there would be zero internal forces using the Moore-Penrose pseudo-inverse solution. Tao and Luh (TAO; LUH, 1989) developed an algorithm to determine the minimum torque required to sustain a common load between two joint-redundant cooperating manipulators. Nahon and Angeles (NAHON; ANGELES, 1992) described the problem of a hand grasping an object as a redundantly-actuated kinematic chain, by minimizing the internal forces in the system using quadratic programming (QP).

Weihmann *et al.*(WEIHMANN; MARTINS; COELHO, 2011) and Mejia *et al.* (MEJIA; SIMAS; MARTINS, 2014b, 2014c) proposed methodologies to evaluate the wrench capability of planar parallel manipulators using differential evolution algorithms *(DE)*. Buttolo and Hannaford (BUTTOLO; HANNAFORD, 1995) analyzed the force capabilities of a redundant planar parallel manipulator. Torques were optimized using the $\infty - norm$ resulting in higher force capabilities when compared to the pseudo-inverse solution.

Nokleby *et al.* (NOKLEBY et al., 2005) developed a methodology to optimize the force capabilities of redundantly-actuated planar parallel manipulators using an n-norm, for large values of n, and a scaling factor. After, Nokleby *et al.* (NOKLEBY et al., 2007) used these methods to obtain results for 3-RRR, 3-RPR and 3-PRR parallel architectures with redundant and non-redundant actuation. Zibil *et al.* (ZIBIL et al., 2007) implemented this approach to spatial parallel manipulators.

In general, the methods that use the constrained optimization as primary tool are usually slow due to the numerical nature of the algorithm and the inaccuracies due to the existence of local minima. Based on these limitations, in this work two new approaches to solve the wrench capability problem are proposed as an attempt to reduce the time and the effort needed to solve such a problem avoiding simultaneously the use of optimization algorithms or iterative processes. The proposed methods are based in the classic scaling factor method and in classical gradient-based optimization methods.

First, some improvements are proposed on the classic scaling factor method proposed by Nokleby *et al.* (NOKLEBY et al., 2005) in order to avoid the use of an optimization algorithm. These improvements result in the obtention of a modified scaling factor method that solves the wrench capabilities problem in an easier, faster and more direct way. When used in conjunction with the Davies method, the modified scaling factor method proposed herein constitutes a powerful

tool used to solve the wrench capability problem when the net degree of constraint in a mechanism or manipulator is equal to three ($C_N = 3$).

In the other hand, when the net degree of constraint in a mechanism or manipulator is greater than or equal to three ($C_N \geq 3$), mathematical closed-form solutions to obtain the wrench capability of manipulators are obtained.

The proposed generalized scaling factor method and the mathematical closed-form solutions to obtain the wrench capability of manipulators are the main results obtained in this work and can be used to solve the wrench capability in most of planar mechanisms or manipulators.

1.2 OBJECTIVES

The main objective of this work is to develop new strategies to solve the wrench capability problem in general planar manipulators in contact with the environment, taking advantage in an efficient way of the kinematic redundancy and the actuation redundancy when they are present. Some specific objectives are listed below:

i. To analyse the factors which influence in the behavior of the wrench capability in planar manipulator;

ii. To develop new strategies to solve the wrench capability problem in planar manipulators;

iii. To compare the new proposed strategies to solve the wrench capability problem with other approaches found in the literature.

1.3 MOTIVATION

As previously mentioned, the increased complexity of the tasks of industrial manipulators requires further studies on robots interaction with the environment. The task space capabilities of a manipulator to perform motion and/or to exert forces and moments are of fundamental importance in robotics. Their evaluation can be useful to determine the structure and the size of a manipulator that best fit the designer's requirements or they can be used to find a better configuration or a better operation point for a manipulator to perform a given task (CHIACCHIO; VERCELLI; PIERROT, 1996).

The main problem related to the wrench capability optimization problem is that the presence of geometric variable parameters generates non-linear and non-convex functions over the search space. This condition allows that global optimization methods should be used (WEIHMANN; MARTINS; COELHO, 2011). The global optimization problem is not easy to solve and it is still an open challenge for researchers since an analytical optimal solution is difficult to obtain, even for relatively simple application problems. Based in this idea, several methods have been proposed in the literature using constrained optimization algorithms.

As previously mentioned, the methods that use the constrained optimization as primary tool are usually slow due to the numerical nature of the algorithm. This fact, is the main motivation of this thesis, and encouraged the study of alternatives to solve the wrench capability problem but without using optimization algorithms or numerical algorithms in order to reduce the time and the effort needed to solve such a problem.

1.4 OVERVIEW OF THIS WORK

This work is organized as summarized below:

Chapter 1 is an introduction to the wrench capability problem and presents a deep literature review. The objectives and motivation of this work are also presented in this chapter.

Chapter 2 studies the fundamentals of the wrench capability problem. In this chapter it is also included a brief revision about redundancy in manipulators and wrench performance indices.

Chapter 3 presents the wrench capability problem in general planar serial manipulators and presents the first result obtained in this thesis: "the modified scaling factor method".

Chapter 4 presents the wrench capability problem in general planar parallel manipulators and presents the second result obtained in this thesis: "The closed form-solutions to solve the wrench capability problem in manipulators with a net degree of constraint equal to three, four, five or six".

Chapter 5 presents the conclusions and topics for further works.

Additionally to the five main chapters described previously, three appendices were included in order to support the comprehension of the

thesis, these appendices are organized as summarized below:

Appendix A introduces some fundamental concepts of the theory of mechanisms, necessary in order to help the reader in the understanding of the main chapters. In this appendix the direct and inverse kinematic problem of manipulators also is presented and some examples are developed.

Appendix B studies the static problem in mechanisms and manipulators. Several concepts related to the Screw Theory are presented and finally the main mathematical tool to solve the static in mechanisms and manipulators (The Davies method) is presented.

Appendix C presents several concepts related to the global optimization process, these concepts are important for the understanding of the proposed procedure to solve the wrench capability problem in Chapter 4.

2 WRENCH CAPABILITY

2.1 INSTANTANEOUS TWIST AND WRENCH CAPABILITIES

The instantaneous twist and wrench capability analysis are essential for the design and performance evaluation of serial and parallel manipulators (FIRMANI et al., 2008b). An instantaneous twist is a screw quantity that contains both angular and translational velocities of the end-effector, i.e., $V = \{\omega^T; v^T\}^T$. Whereas, a wrench is a screw quantity that contains the forces and moments acting on the end-effector, i.e., $F = \{f^T; m^T\}^T$. For a given pose, the required task of the end-effector is to move with a desired twist and to sustain (or apply) a specific wrench (FIRMANI et al., 2008b). These kinematic conditions are achieved with corresponding joint velocities ($\dot{q}$) and joint torques (τ) respectively. The relationship between the task and joint spaces is defined by the well known linear transformations:

$$\dot{x} = J\dot{q} \tag{2.1}$$

$$\tau = J^T F \tag{2.2}$$

where J is referred to as the Jacobian matrix.

In addition, an extended problem can be formulated as the analysis of the maximum twist or wrench that the end-effector can perform in the twist or wrench spaces, respectively. The knowledge of maximum twist and wrench capabilities is an important tool for achieving the optimum design of manipulators (FIRMANI et al., 2008b). For instance, by being able to graphically visualize the twist and wrench capabilities, comparisons between different design parameters, such as the actuator torque capabilities and the dimensions of the links, can be explored. Also, the performance of an existing manipulator can be improved by identifying the optimal capabilities based on the configuration of the branches and the pose of the end-effector (FIRMANI et al., 2008b).

This work focuses on the wrench capabilities of planar manipulators, whether they are serial, parallel or hybrid and with actuation redundancy or not. In this work, two new approaches are proposed based in the classic scaling factor method and in classical optimization methods. These methods will be discussed in detail in Chapters 3 and 4.

Before to introduce the proposed methods to solve the wrench

capability problem, we will discuss briefly the redundancies found in manipulators due that most of the proposed solutions herein are applicable when this phenomenon appears in planar manipulators. In this chapter we also introduce the concept of wrench capability polytope and include a description of the most common wrench capability indices found in the literature.

2.2 REDUNDANCY

2.2.1 Types of redundancy

Merlet (MERLET, 1996) described that the inclusion of redundancy may lead to improvements in various analyses such as direct kinematics, singular configurations, optimal force control, and calibration. Lee and Kim (LEE; KIM, 1993) defined a redundant parallel manipulator as one that has an infinite number of choices for either generating motion or resisting external forces. Also, Lee and Kim (LEE; KIM, 1993) presented an analysis of different types of redundancy. Ebrahimi et al. (EBRAHIMI; CARREYERO; BORDREAU, 2007) classified redundancy into two categories: kinematic and actuation redundancy.

2.2.2 Kinematic redundancy

A manipulator is termed kinematically redundant when at least one of the branches can have self-motion while keeping the mobile platform fixed (FIRMANI et al., 2008b). Thus, there is an infinite number of possible solutions to the inverse displacement problem. This is the typical case of redundant serial manipulators. For parallel manipulators, this redundancy happens when the number of joints of at least one branch is greater than the number of joints that are required to provide the desired mobility of the mobile platform. This type of redundancy allows self-motion of the redundantly-jointed branch(es) improving the dexterity and workspace of the manipulator (FIRMANI et al., 2008b).

A draw back of this type of redundancy is the increase of mass and/or inertia due to the addition of actuators on the mobile links. Despite the redundancy, there is only one vector force per branch acting on the mobile platform. Thus, the load capability cannot be optimized, but as an alternative, the direction of the branch forces can be optimized by changing the posture of the redundantly-jointed branch(es).

With this type of redundancy, each actuator can be manipulated independently and there are no internal forces that could damage the device. Kinematic redundancy can be employed to reduce or even eliminate singular configurations. Wang and Gosselin (WANG; GOSELIN, 2004) added an extra revolute joint to one branch of the 3-RPR PPM yielding a RRPR-2RPR layout. The singularity conditions were identified and the singularity loci were reduced. Ebrahimi et al. (EBRAHIMI; CARREYERO; BORDREAU, 2007) proposed the 3-PRRR PPM, a layout that contains joint redundancy in every branch. This manipulator can provide singularity free paths and obstacle avoidance by properly manipulating the actuated joints.

2.2.3 Actuation redundancy

A parallel manipulator is termed redundantly actuated when an infinite number of resultant force combinations can span the system of external forces. Thus, there is an infinite number of solutions to the inverse static force problem. The implementation of this redundancy requires a reliable control system because a small variation in the displacement may cause severe damage to the manipulator. There are two types of actuation redundancy: in-branch redundancy and branch redundancy.

In-Branch Redundancy:

Passive joints are replaced by active joints. For every redundant actuator added within branch(es), the number of the forces resisting an external load is augmented by one. This type of redundancy can be easily incorporated into an existing device. Nokleby et al. (NOKLEBY et al., 2005) developed a methodology to optimize the force capabilities of the 3-RRR PPM using a high norm and a scaling factor. Zibil et al. (ZIBIL et al., 2007) determined the force capabilities of the 3-RRR PPM by using an analytical based method. Nokleby et al. (NOKLEBY et al., 2007) investigated the force-moment capabilities of different in-branch redundancy architectures. With in-branch redundancy, there is no change in the workspace of the manipulator. However, there is an increase of mass and/or inertia due to the addition of actuators. Firmani and Podhorodeski (FIRMANI; PODHORODESKI, 2004) eliminated families of singular configurations by adding a redundant actuator to the 3-RRR PPM, yielding a RRR-2RRR layout.

Branch Redundancy:

An additional actuated branch is added to the system. For every additional actuated branch incorporated into the system, the number of forces acting on the mobile platform is augmented by one. Buttolo and Hannaford (BUTTOLO; HANNAFORD, 1995) designed and analyzed the force capabilities of a 2-DOF 3-RRR PPM haptic device, where all three branches are pinned together. Gallina et al. (GALLINA; ROSATI; ROSSI, 2001) analyzed the maximum force and moment of a fourwire driven 3-DOF planar haptic device. Krut et al. (KRUT; COMPANY; PIERROT, 2004b) implemented performance indices, previously developed in Krut et al. (KRUT; COMPANY; PIERROT, 2004a) for velocity analysis, to 2-DOF parallel wire-driven manipulators. Different analyses of multi-actuated wires were considered. Nokleby et al. (NOKLEBY et al., 2007) investigated the force-moment capabilities of the 4-RRR, 4-RPR, and 4-PRR PPMs. Firmani and Podhorodeski (FIRMANI; PODHORODESKI, 2004) presented a methodology to identify singular configurations of planar parallel manipulators with redundant branches. The main problem of manipulators with branch redundancy is the reduction of their dexterity and workspace.

2.3 WRENCH POLYTOPE ANALYSIS

2.3.1 Joint space parallelepiped

In order to introduce the concept, consider a manipulator working into an specific task space and being controlled by a known number of actuators. Let n be the DOF of the task space coordinates and m be the number of actuated joints. The i^{th} joint torque variable, which is bounded by $\tau_{i_{min}}$ and $\tau_{i_{max}}$, can be represented in the joint torque space as two parallel planes in $\mathbb{R}^m$. With m joints, there are $2m$ planes or m pairs of parallel planes. An m-dimensional parallelepiped is formed with the combination of all of these parallel planes yielding the region of joint torque capabilities (FIRMANI et al., 2008b). If all the torque capabilities were equal, the m-dimensional parallelepiped would result in a hypercube. Also, if the magnitude of the extreme torques were equal, i.e., $|\tau_{i_{min}}| = |\tau_{i_{max}}|$, the parallelepiped would be center-symmetric; otherwise it would be skewed.

A vertex of the m-dimensional parallelepiped defines the inter-

section of m extreme torque planes. Thus, a vertex occurs when all joint torques are at their extreme capabilities, i.e.,

$$\upsilon = [\tau_{1_{ext}}, \tau_{2_{ext}}, \cdots, \tau_{m_{ext}}] \tag{2.3}$$

where $\tau_{i_{ext}}$ denotes the extreme capabilities of the i^{th} actuator, i.e., $\tau_{i_{min}}$ or $\tau_{i_{max}}$.

2.3.2 Linear transformation

Visvanathan and Milor (VISVANATHAN; MILOR, 1986) investigated the problems in analog integrated circuits while accounting for the tolerance variations of the principal process parameters. The problem involved the mapping of a parallelepiped under a linear transformation. Their mathematical formulation is similar to the one used for analyzing wrench capabilities. Let the coordinates of the vertices of a parallelepiped in $\mathbb{R}^m$ be υ_j, for $j = 1, ..., 2^m$.

Be , υ_j for j = 1, ..., 2 . m through a linear transformation from $\mathbb{R}^m$ to $\mathbb{R}^n$, such as $F = J^{-T}\tau$, the m-dimensional parallelepiped becomes a polytope (VISVANATHAN; MILOR, 1986). A polytope is a convex region, i.e., any two points inside the polytope can be connected by a line that completely fits inside the polytope. An n-dimensional convex polytope is bounded by $(n-1)$-dimensional facets or hyperplanes, e.g., linear edges in $\mathbb{R}^2$ bounding a polygon or planar facets in $\mathbb{R}^3$ bounding a polyhedron.

A polytope P can be completely characterized by mapping all the vertices of the parallelepiped and enclosing them in a convex hull, i.e.,

$$P = convh\{J^{-T}\upsilon_j, \;\; j = 1, ..., 2^m\} \tag{2.4}$$

where *convh* denotes a convex hull operator which encloses all the extreme points forming the feasible region of the torque space in the wrench space. A closed bounded convex set is the convex hull of its extreme points (ROCKAFELLAR, 1997). The total number of vertices in the polytope υ_{T_n} depends on the dimension of the two spaces.

2.3.3 Polytopes in Non-redundant planar manipulators

For non-redundant manipulators ($n = m$) the number of vertices in the polytope equals the number of vertices in the m-dimensional parallelepiped, i.e., $v_{T_m} = v_{T_n} = 2^m$, an the vertices of the polytope are the image of the vertices of the m-dimensional parallelepiped (CHIACCHIO; VERCELLI; PIERROT, 1996), i.e.,

$$p_j = J^{-T} v_j \tag{2.5}$$

where p_j and v_j are the vertices of the polytope and parallelepiped, respectively. The linear transformation between the two spaces also makes that the edges and facets of the polytope are the corresponding image of the edges and facets of the m-dimensional parallelepiped.

For a planar parallel manipulator the vertices of the wrench polytope are found as follows:

$$p_j = J^{-T} v_j \tag{2.6}$$

$$\begin{bmatrix} F_x \\ F_y \\ M_z \end{bmatrix} = \begin{bmatrix} a_{1,1} & a_{1,2} & a_{1,3} \\ a_{2,1} & a_{2,2} & a_{2,3} \\ a_{3,1} & a_{3,2} & a_{3,3} \end{bmatrix} \cdot \begin{bmatrix} \tau_{1_{ext}} \\ \tau_{2_{ext}} \\ \tau_{3_{ext}} \end{bmatrix} \tag{2.7}$$

where $a_{i,j}$ denotes the elements of J^{-T}. There are eight vertices 2^3 due to the combination of the extreme torque capabilities, i.e., $\tau_{i_{ext}}$ can be either $\tau_{i_{min}}$ or $\tau_{i_{max}}$.

Fig. 2 illustrates the linear transformation of the torque capabilities of a non-redundant planar parallel manipulator from the torque space to the wrench space. Fig. 2 also shows the corresponding image of the vertices, edges, and facets between the parallelepiped and the polytope.

The resulting wrench polytope of a non-redundant manipulator has the following characteristics:

i. Any point outside the polytope is a wrench that cannot be applied or sustained;

ii. Any point inside the polytope is achieved with actuators that are not working at their extreme capabilities;

iii. Any point on a facet of the polytope has one actuator working at an extreme capability;

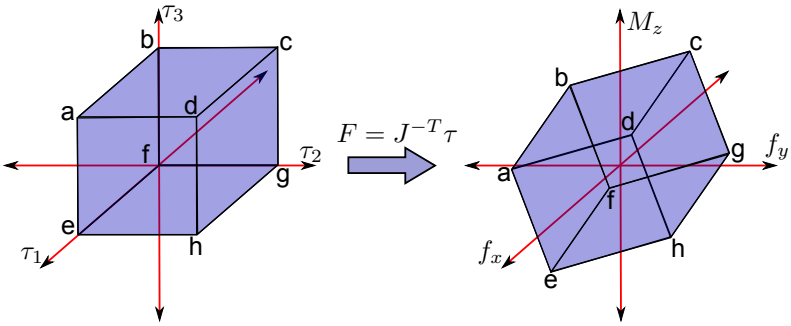

Figure 2 – Linear transformation of a parallelepiped to a polytope of a non-redundant PPM and image projection of vertices, edges, and facets.

iv. Any point on an edge of the polytope has two actuators working at their extremes;

v. Any vertex of the polytope has all three actuators working at their extremes.

2.3.4 Polytopes in redundant planar manipulators

For redundant manipulators ($n < m$) the number of vertices in the polytope is less than the vertices of the m-dimensional parallelepiped, i.e., $\upsilon_{Tn} < \upsilon_{Tm}$. In this case, the vertices of the polytope are formed with the mapping of some of the vertices of the m-dimensional parallelepiped, i.e. (FIRMANI et al., 2008b),

$$p_k \subset J^{-T}\upsilon_j \tag{2.8}$$

with $k < j$. The points that do not form the vertices of the polytope are internal points in P. Let the potential vertices (p_j) of the polytope be all the projected vertices of the m-dimensional parallelepiped in $\mathbb{R}^n$. Thus, the potential vertices are determined as follows:

$$p_j = J^{-T}\upsilon_j \tag{2.9}$$

$$\begin{bmatrix} F_x \\ F_y \\ M_z \end{bmatrix} = \begin{bmatrix} a_{1,1} & a_{1,2} & \cdots & a_{1,m} \\ a_{2,1} & a_{2,2} & \cdots & a_{2,m} \\ a_{3,1} & a_{3,2} & \cdots & a_{3,m} \end{bmatrix} \cdot \begin{bmatrix} \tau_{1_{ext}} \\ \tau_{2_{ext}} \\ \vdots \\ \tau_{m_{ext}} \end{bmatrix} \tag{2.10}$$

The number of vertices of the wrench polytope depends on the pose of the manipulator, which defines the elements of the linear transformation matrix, J^{-T} and it may vary from case to case.

Finding the external vertices of a polytope can be computationally expensive. Generating a polytope through a convex hull has been studied thoroughly in the field of computational geometry and the goal has been to make a more efficient algorithm. Chand and Kapur (CHAND; KAPUR, 1970) proposed the so-called gift wrapping algorithm, where the facets of a polytope are found by determining the angles between one vertex and the rest of the points. The minimum and maximum angles correspond to the hyperplanes passing through that point. Visvanathan and Milor (VISVANATHAN; MILOR, 1986) proposed an algorithm that searches in the directions that are orthogonal to each of the known hyperplanes. New vertices and hyperplanes are formed and the process is repeated. Bicchi et al. (BICCHI; MELCHIORRI; BALLUCHI, 1995) presented an algorithm that involves slack variables that transform the inequality constraints of the actuator limits into equality constraints. Lee (LEE, 1997) proposed a method for determining the vertices of twist polytopes using vector algebra. Hwang et al. (HWANG; LEE; HSIA, 2000) developed a recursive algorithm that removes all the internal points when first encountered. Hwang et al. (HWANG; LEE; HSIA, 2000) also showed that even though the number of potential vertices grows exponentially 2^m the number of external points increases linearly.

The resulting wrench polytope of a redundant manipulator has the following characteristics:

i. Any point outside the polytope is a wrench that cannot be applied or sustained;

ii. Any point inside the polytope is achieved with actuators that may or may not work at their extreme capabilities;

iii. Any point on a facet of the polytope has $m - 2$ actuators working at their extremes;

iv. Any point on an edge of the polytope has $m-1$ actuators working at their extremes;

v. Any vertex of the polytope has all m actuators working at their extremes.

2.4 WRENCH PERFORMANCE INDICES

2.4.1 Operational conditions

A wrench polytope represents the region in which the manipulator can apply feasible wrenches. Unfortunately, a major drawback of this approach compared to the ellipsoid approach is the efficiency of the algorithm. Determining the axes of the ellipsoid by applying Singular Value Decomposition (SVD) to J is definitely more efficient than constructing a polytope. A small eigenvalue indicates that the manipulator requires large actuator torques to sustain an exerted wrench.

Nonetheless, the best representation, from a design perspective, may not be the polytope itself, but rather a set of indices that characterize it. These points may lie on facets, edges, or vertices of the wrench polytope, and represent maximum/minimum values of either moments or forces. Thus, these points, which are referred to as wrench performance indices, allow the determination of either force or moment ranges.

Under operational conditions, the manipulator performance is dictated by the requirements of the application. These requirements establish some parameters of moments and forces acting on the manipulator. This is, the range of forces can be determined based on moment requirements; similarly, the range of moments can be determined based on force requirements. For the force analysis, there are two ranges of forces that can be determined. Finotello et al. (FINOTELLO et al., 1998) defined these forces as maximum available value (MAV) and maximum isotropic value (MIV). Herein, MAV and MIV are denoted as F_{av} and F_{is} respectively.

Assume a wrench with a constant moment, thus the polytope is reduced to a polygon, i.e., the polytope is sliced at the constant moment yielding a polygon. The area enclosed by the polygon represents the force capabilities of the manipulator. The maximum available force (F_{av}) is the farthest distance from the center of the force space to the polygon. This force can be only applied in a particular direction and

corresponds to a vertex of the polygon.

The maximum isotropic force (F_{is}) is the shortest distance from the center of the force space to the polygon. Fig. 3 illustrates the force polygon of a 3- $\underline{\text{R}}$RR PPM, where the underline denotes the actuated joints and is indicated in the figure with τ_1, τ_2 and τ_3. For an arbitrary direction α, the distance from the center of the force space to any point within the polygon is proportional to the magnitude of the force that can be applied or sustained. Fig. 3 also shows an arbitrary force vector $f = [f_x, f_y]^T = [f\cos(\alpha), f\sin(\alpha)]^T$ and the maximum available (F_{av}) and isotropic (F_{is}) forces.

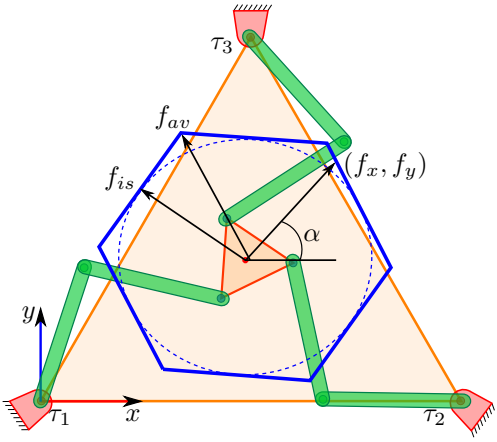

Figure 3 – Force polygon in a 3$\underline{\text{R}}$RR planar parallel manipulator

Firmani et al. (FIRMANI et al., 2008b) described six different scenarios of operational conditions in which the forces and moments interact are presented. Table 1 summarizes the six operational conditions which lead to two force analyses and four moment analyses presented by Firmani et al. (FIRMANI et al., 2008b).

Additionally, Firmani et al. (FIRMANI et al., 2008b) describe six different indices to evaluate the wrench performance of a manipulator. The performance index can be determined by verifying the maximum f or m_z among all of the combinations. If the problem involves finding a torque in transition, it is important to verify that this torque does not exceed its torque output capabilities.

The performance indices presented by Firmani et al. (FIRMANI et al., 2008b) are described below and are valid for both non-redundant

Table 1 – Operational condition and corresponding analyses.

Operational Condition	Analysis
Prescribed Moment	Force Analysis: Find Range of Available and Isotropic Forces
Largest Allowable Force with an Associated Moment	
Prescribed Force (magnitude and direction)	Moment Analysis: Find Range of Moments
Largest Allowable Moment with an Associated Force	
Prescribed Isotropic Force (magnitude)	
Prescribed Available Force (magnitude)	

and redundant planar parallel manipulators.

Maximum Force with a Prescribed Moment:

If the moment must be preserved (M_z must be specified as a constant) in the requirements of the application, either zero or any other value, the polytope is reduced to a polygon.

The maximum available force (${}^{pm}F_{av}$) corresponds to the largest value of f that is evaluated with the combinations, where $f = \sqrt{f_x^2 + f_y^2}$. The maximum isotropic force (${}^{pm}F_{is}$) is determined as the shortest distance from the center of the force space to the polygon. ${}^{pm}F_{av}$ and ${}^{pm}F_{is}$ represent a point on an edge and a point on a facet of the polytope.

The maximum available value (MAV) presented by Finotello *et al.* (FINOTELLO et al., 1998) and the maximum force with a prescribed moment (F_{app}) presented by Firmani *et al.* (FIRMANI et al., 2008a) are similar force capability performance indices and they are defined as the maximum force that can be applied (or sustained) by a manipulator with a prescribed moment (WEIHMANN; MARTINS; COELHO, 2011). If this prescribed moment is zero, it yields a pure force analysis. For a given direction, the maximum force that can be applied with zero moment will be denoted as F_m (WEIHMANN; MARTINS; COELHO, 2011).

From this point, it will be adopted the notation presented by Firmani *et al.* (FIRMANI et al., 2008a) in order to maintain a concordance with the author's previously published papers. In this manner,

the notation F_{app} will be considered for the cases where the maximum force that can be applied (or sustained) by a manipulator have a prescribed constant moment different to zero and the notation F_m will be considered for the cases where the maximum force that can be applied (or sustained) by a manipulator have a prescribed moment equal to zero.

Maximum Allowable Force with an Associated Moment:

If a moment does not affect the requirement of the application, the manipulator can reach the largest available and isotropic forces. To achieve these forces a particular moment must be associated with them. A force polygon may be generated by projecting the vertices of the polytope on the force plane, or in other words, a force polygon can be obtained as the upper view of the wrench capability polytope (FIRMANI et al., 2008b).

Maximum Moment with a Prescribed Force:

For a fully described force (f *and* α), the force vector may be drawn within the polytope and the set of moments ${}^{pf}M_z$ that can be reached with this force can be determined. The largest and smallest M_z that can be obtained while keeping the torques in transition within their capabilities define the range of ${}^{pf}M_z$ (FIRMANI et al., 2008b).

Maximum Allowable Moment with an Associated Force:

If the force does not affect the application, the maximum range of moments (${}^{af}M_z$) has an associated force, i.e., a specific force must be applied to achieve the largest moment. To find the maximum moment all the actuators are set to their maximum capabilities. The highest and lowest vertices of the polytope represent this performance index (FIRMANI et al., 2008b).

Maximum Moment with a Prescribed Isotropic Force:

Assume that the manipulator is required to apply or sustain the same force in all directions, i.e., an isotropic force f_{is}. The region of moments that can attain this force may be seen as a cylinder of radius f_{is} that is fully contained within the polytope and intersects facets of the polytope. The maximum and minimum ${}^{pif}M_z$ are determined by

comparing the resulting isotropic moment associated with every plane of the polytope. Isotropy is ensured with the plane that yields the minimum of the maximum M_z moment (FIRMANI et al., 2008b).

Maximum Moment with a Prescribed Available Force:

Assume that the manipulator is required to apply a large force regardless of its direction, i.e., available force f_{av}. This case may be seen as the intersection of a cylinder of radius f_{av} with a point on the polytope which is the farthest away from the $M_z = 0$ plane. The cylinder usually intersects an edge of the polytope, but in some particular cases the intersection may happen with a facet of a vertex of the polytope (FIRMANI et al., 2008b).

3 WRENCH CAPABILITY IN MANIPULATORS USING A MODIFIED SCALING FACTOR METHOD

In this chapter a modified scaling factor method to obtain the maximum force with a prescribed moment in planar manipulators with a net degree of constraint equal to three ($C_N = 3$) is presented. The method proposed in this chapter is based on the scaling factor method presented by Nokleby et al. [2005], but includes several modifications which allow the use of optimization algorithms to be avoided. These modifications lead to a reduction in the computing time and effort required to evaluate the force capability in planar mechanisms, enabling the proposed method to be used in real-time applications such as machining, grasping and manipulation. The modified scaling factor method proposed herein is general and can be applied to any planar manipulator satisfying the condition $C_N = 3$.

The ***scaling factor method*** was originally proposed by Nokleby *et al.* (NOKLEBY et al., 2005) as an attempt to solve the force capability problem in planar manipulators, but, this ***original scaling factor method*** (NOKLEBY et al., 2005) does not allow the desired moment at the manipulator end effector to be included in an explicit mathematical expression, and an optimization process is required in order to solve the force capability problem. In addition, the computation of the maximum allowed moment is not presented. In this chapter some improvements to the ***original scaling factor method*** will be described in order to address these issues, resulting in the proposed ***modified scaling factor method***.

The novelty of this ***modified scaling factor method*** lies in the fact that herein does not require the use of an optimization algorithm, in contrast to the original scaling factor method. Instead, explicit equations are used in order to solve the force capability problem. The avoidance of optimization algorithms results in a simpler, faster and more direct solution to obtain the force capability of manipulators compared with other solutions for the same problem found in the literature.

The modified scaling factor method proposed in this chapter is one of the results presented in this thesis and, in combination with the Davies method, it constitutes a powerful tool to solve the force capability problem in any mechanism or manipulator (whether it be serial, parallel or hybrid) with a net degree of constraint equal to three ($C_N = 3$).

3.1 STATIC MODELS OF MECHANISMS AND MANIPULATORS WITH $C_N = 3$

In planar manipulators with $C_N = 3$, once the Davies method has been applied to obtain the inverse statics, it is possible to represent the N primary actions $[\tau_1, \tau_2, ..., \tau_N]^T$ as a generalized function of a coefficient matrix $[A]$ and the wrenches at the end effector $[F_x, F_y, M_z]^T$, as shown in Eq. (3.1).

$$\begin{bmatrix} \tau_1 \\ \tau_2 \\ \vdots \\ \tau_N \end{bmatrix} = \begin{bmatrix} a_{1,1} & a_{1,2} & a_{1,3} \\ a_{2,1} & a_{2,2} & a_{2,3} \\ \vdots & \vdots & \vdots \\ a_{n,1} & a_{n,2} & a_{n,3} \end{bmatrix} \cdot \begin{bmatrix} F_x \\ F_y \\ M_z \end{bmatrix} \tag{3.1}$$

In Eq. (3.1) the elements $a_{1,1}, \ldots, a_{n,3}$ represent kinematic expressions as a function of the manipulator joint positions, the elements $\tau_1, \tau_2, ..., \tau_N$ represent the primary actions (force or moment) of the actuated joints and the elements F_x, F_y, M_z represent the wrenches at the end effector. Thus, the serial manipulator shown in Fig. 4 (which is a 3 DoF manipulator), can be statically modelled as shown in Eq. (3.2), and the serial manipulator shown in Fig. 5 (which is a 6 DoF manipulator), can be statically modelled as shown in Eq. (3.3).

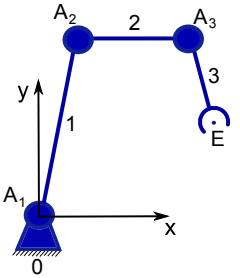

Figure 4 – Planar serial manipulator with 3 DoF.

$$\begin{bmatrix} \tau_{A_1} \\ \tau_{A_2} \\ \tau_{A_3} \end{bmatrix} = \begin{bmatrix} a_{1,1} & a_{1,2} & a_{1,3} \\ a_{2,1} & a_{2,2} & a_{2,3} \\ a_{3,1} & a_{3,2} & a_{3,3} \end{bmatrix} \cdot \begin{bmatrix} E_{F_x} \\ E_{F_y} \\ E_{M_z} \end{bmatrix} \tag{3.2}$$

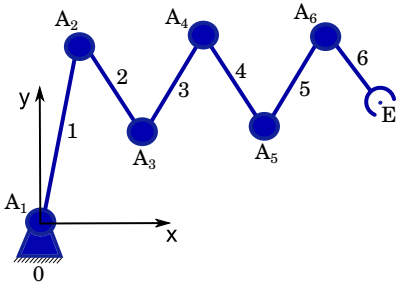

Figure 5 – Planar serial manipulator with 6 DoF.

$$\begin{bmatrix} \tau_{A_1} \\ \tau_{A_2} \\ \tau_{A_3} \\ \tau_{A_4} \\ \tau_{A_5} \\ \tau_{A_6} \end{bmatrix} = \begin{bmatrix} a_{1,1} & a_{1,2} & a_{1,3} \\ a_{2,1} & a_{2,2} & a_{2,3} \\ a_{3,1} & a_{3,2} & a_{3,3} \\ a_{4,1} & a_{4,2} & a_{4,3} \\ a_{5,1} & a_{5,2} & a_{5,3} \\ a_{6,1} & a_{6,2} & a_{6,3} \end{bmatrix} \cdot \begin{bmatrix} E_{F_x} \\ E_{F_y} \\ E_{M_z} \end{bmatrix} \tag{3.3}$$

The modified scaling factor method proposed in this paper is applicable only when the manipulator evaluated has the property $C_N = 3$. Manipulators with C_N values which are not three ($C_N \neq 3$) will be treated in Chapter 4 and are not addressed in this chapter.

3.2 SCALING FACTOR METHOD

The scaling factor method, originally presented by Nokleby *et al.* in Ref. (NOKLEBY et al., 2005), is a numerical force-moment computational method that allows the actuator limits to be easily incorporated into the problem of determining the force-moment capabilities of manipulators (GARG; NOKLEBY; CARRETERO,). The method is explained in this section and some improvements to the method are proposed in Section 3.2.

In the original scaling factor method, a unit wrench $\$_F$ is used to represent the desired wrench direction as shown in Eq. (3.4). In this equation f_{app} is the wrench intensity of F_{app} (NOKLEBY et al., 2005).

$$F_{app} = f_{app}\$_F \tag{3.4}$$

Using the unit wrench $\$_F = [\cos(\theta), \sin(\theta), 0]^T$ in order to represent the desired direction of the force, the inverse statics equation shown in Eq. (3.1) can be rewritten as:

$$\begin{bmatrix} \tau_1 \\ \tau_2 \\ \vdots \\ \tau_N \end{bmatrix} = \begin{bmatrix} a_{1,1} & a_{1,2} & a_{1,3} \\ a_{2,1} & a_{2,2} & a_{2,3} \\ \vdots & \vdots & \vdots \\ a_{n,1} & a_{n,2} & a_{n,3} \end{bmatrix} \cdot \begin{bmatrix} \cos(\theta) \\ \sin(\theta) \\ 0 \end{bmatrix} \tag{3.5}$$

Note that in Eq. (3.5) the prescribed moment is zero ($M_z = 0$) and it yields a pure force analysis (F_m). By expanding Eq. (3.5), the primary actions (τ_1, τ_2,..., τ_N) can be calculated as a function of θ as shown below.

$$\tau_i(\theta) = a_{i,1} \cdot \cos(\theta) + a_{i,2} \cdot \sin(\theta) + a_{i,3} \cdot 0 \qquad i = 1, 2, ..., N \tag{3.6}$$

Since all maximum actuated joint torque/force limits ($\tau_{i_{max}}$) are known for all actuated joints i, scaling factors for each actuated joint can be found using Eq. (3.7) (NOKLEBY et al., 2005).

$$\psi_i = \left| \frac{\tau_{i_{max}}}{\tau_i(\theta)} \right| \qquad i = 1, 2, ..., N \tag{3.7}$$

where ψ_i is the scaling factor for each actuated joint i, and $\tau_i(\theta)$ is the torque/force of the i^{th} actuated joint for a unit wrench in the desired force direction, obtained from Eq. (3.6).

The scaling factors of Eq. (3.7) can be placed in a set. The scaling factor (Ψ) in this set with the minimum value is the maximum factor which all joint torques/forces can be scaled by and still remain at or below their corresponding maximum values (NOKLEBY et al., 2005), i.e.:

$$\Psi = \min(\psi_i) \qquad i = 1, 2, ..., N \tag{3.8}$$

Since $\$_F = [\cos(\theta), \sin(\theta), 0]^T$ is a unit wrench with a prescribed moment equal to zero ($M_z = 0$), the method corresponds to a pure force case, allowing us to rewrite Eq. (3.4) as:

$$F_m = f_m \$_F \tag{3.9}$$

where f_m is the wrench intensity of F_m, and its maximum possible

value is:

$$f_m = \Psi \tag{3.10}$$

By multiplying both sides of the *inverse statics* equation shown in Eq. (3.5) by the scaling factor (Ψ), it is possible to highlight the effects of apply the scaling factor, as shown in Eq. (3.11).

$$\begin{bmatrix} \Psi \cdot \tau_1(\theta) \\ \Psi \cdot \tau_2(\theta) \\ \vdots \\ \Psi \cdot \tau_N(\theta) \end{bmatrix} = \begin{bmatrix} a_{1,1} & a_{1,2} & a_{1,3} \\ a_{2,1} & a_{2,2} & a_{2,3} \\ \vdots & \vdots & \vdots \\ a_{n,1} & a_{n,2} & a_{n,3} \end{bmatrix} \cdot \begin{bmatrix} \Psi \cdot \cos(\theta) \\ \Psi \cdot \sin(\theta) \\ \Psi \cdot 0 \end{bmatrix} \tag{3.11}$$

In Eq. (3.11) it can be noted that the use of the scaling factor implies that the torques at the actuated joints of the manipulator (which solve the unit wrench problem) will be scaled by a value of Ψ, and the unit force (initially imposed) will be scaled by the same value of Ψ, but the moment at the end effector of the manipulator remains equal to zero ($M_z = \Psi \cdot 0 = 0$).

At this point it is important to highlight that in the original scaling factor method, when a desired moment which differs from zero ($M_z \neq 0$) is imposed within the unit wrench ($\$_F$), the application of a scaling factor amplifies both the unit force and the desired moment (M_z). In order to better understand this, consider the unit wrench $\$_F = [\cos(\theta), \sin(\theta), M_z]^T$. On applying the original scaling factor method using this unit wrench, Eq. (3.11) is modified as shown in Eq. (3.12).

$$\begin{bmatrix} \Psi \cdot \tau_1(\theta, M_z) \\ \Psi \cdot \tau_2(\theta, M_z) \\ \vdots \\ \Psi \cdot \tau_N(\theta, M_z) \end{bmatrix} = \begin{bmatrix} a_{1,1} & a_{1,2} & a_{1,3} \\ a_{2,1} & a_{2,2} & a_{2,3} \\ \vdots & \vdots & \vdots \\ a_{n,1} & a_{n,2} & a_{n,3} \end{bmatrix} \cdot \begin{bmatrix} \Psi \cdot \cos(\theta) \\ \Psi \cdot \sin(\theta) \\ \Psi \cdot M_z \end{bmatrix} \tag{3.12}$$

It can be observed in Eq. (3.12) that when a desired moment at the end-effector which differs from zero ($M_z \neq 0$) is applied, it will be scaled Ψ times together with the unit force, and this represents an undesirable situation because the final value for the desired moment is Ψ times higher than the desired value. In order to solve this problem

it is necessary to find an initial value for the moment (M_{I_z}) within the unit wrench ($\$_F$) in order to satisfy the condition $\Psi \cdot M_{I_z} = M_z$ as shown in Eq. (3.13).

$$\begin{bmatrix} \Psi \cdot \tau_1(\theta, M_{I_z}) \\ \Psi \cdot \tau_2(\theta, M_{I_z}) \\ \vdots \\ \Psi \cdot \tau_N(\theta, M_{I_z}) \end{bmatrix} = \begin{bmatrix} a_{1,1} & a_{1,2} & a_{1,3} \\ a_{2,1} & a_{2,2} & a_{2,3} \\ \vdots & \vdots & \vdots \\ a_{n,1} & a_{n,2} & a_{n,3} \end{bmatrix} \cdot \begin{bmatrix} \Psi \cdot \cos(\theta) \\ \Psi \cdot \sin(\theta) \\ \Psi \cdot M_{I_z} \end{bmatrix} \quad (3.13)$$

This original scaling factor method uses an optimization algorithm in order to obtain the appropriate values for M_{I_z} and Ψ (the Broyden-Fletcher-Goldfarb-Shanno (BFGS) quasi-Newton algorithm with a mixed quadratic and cubic line search (NOKLEBY et al., 2005) (ZIBIL et al., 2007)). This leads to a significant increase in the time required to solve the force capability problem. In addition, the computation of the maximum allowed moment is not an easy task.

As shown in Section 3.2, the original scaling factor method is applicable when the imposed moment at the end effector is zero ($M_z = 0$), but when a different value for the imposed moment is defined it is necessary to use an optimization algorithm in order to solve the force capability problem.

Herein we apply some algebraic modifications to the original scaling factor method proposed by Nokleby *et al.* in Ref. (NOKLEBY et al., 2005). These modifications require the use of a new unit wrench imposed at the end effector of the manipulator and a systematic solution for the associated variables. The proposed modifications allow us to avoid the use of optimization algorithms, reducing considerably the time required to solve the force capability problem.

In the proposed modified scaling factor method, the unit wrench $\$_F$ must include an associated value σ as the component of the moment in z. The new unit wrench is represented as $\$_F = [\cos(\theta), \sin(\theta), \sigma]^T$, and Eq. (3.1) can be rewritten as shown in Eq. (3.14).

$$\begin{bmatrix} \tau_1 \\ \tau_2 \\ \vdots \\ \tau_N \end{bmatrix} = \begin{bmatrix} a_{1,1} & a_{1,2} & a_{1,3} \\ a_{2,1} & a_{2,2} & a_{2,3} \\ \vdots & \vdots & \vdots \\ a_{n,1} & a_{n,2} & a_{n,3} \end{bmatrix} \cdot \begin{bmatrix} \cos(\theta) \\ \sin(\theta) \\ \sigma \end{bmatrix} \quad (3.14)$$

The associated value σ must be such that when multiplied by a scaling factor (ψ) the desired moment is obtained:

$$M_z = \psi \cdot \sigma \tag{3.15}$$

As in Section 3.2, an expansion for Eq. (3.14) can be obtained as:

$$\tau_i(\theta, \sigma) = a_{i,1} \cdot \cos(\theta) + a_{i,2} \cdot \sin(\theta) + a_{i,3} \cdot \sigma \qquad i = 1, 2, ..., N \tag{3.16}$$

Considering the direction θ as a constant, Eq. (3.16) can be rewritten in a simplified way as a function only of σ, as shown in Eq. (3.17). In this equation the element $m_i(\theta)$ is dependent on the chosen constant angle θ (i.e.: $m_i(\theta) = a_{i,1}\cos(\theta) + a_{i,2}\sin(\theta)$; $\quad i = 1, 2, ..., N$).

$$\tau_i(\sigma) = m_i(\theta) + a_{i,3} \cdot \sigma \qquad i = 1, 2, ..., N \tag{3.17}$$

As in Section 3.2, since all maximum actuated joint torque/force limits ($\tau_{i_{max}}$) are known for all actuated joints i, scaling factors for each actuated joint can be found, but this time using Eq. (3.18).

$$\psi_i(\sigma) = \left| \frac{\tau_{i_{max}}}{\tau_i(\sigma)} \right| = \left| \frac{\tau_{i_{max}}}{m_i(\theta) + a_{i,3}\sigma} \right| \quad i = 1, 2, ..., N \tag{3.18}$$

where, $\psi_i(\sigma)$ is the scaling factor for each actuated joint i, and $\tau_i(\sigma)$ is the torque/force of the i^{th} actuated joint for a unit wrench in the desired force direction (θ), obtained from Eq. (3.17).

Note that the scaling factors $\psi_i(\sigma)$ for each actuated joint i are now dependent on the value of the unknown value σ since the value of θ is a constant. Rewriting Eq. (3.15) as ${M_z}^2 = (\psi_i(\sigma) \cdot \sigma)^2$, and substituting Eq. (3.18) into this rewritten equation using the property of the absolute value $|f|^2 = f^2$, we obtain Eq. (3.19). This new equation is a quadratic equation whose solution allows us to ascertain the values of σ which satisfy Eqs. (3.15) and (3.18) simultaneously.

$${M_z}^2 = \left(\frac{\tau_{i_{max}}}{m_i(\theta) + a_{i,3}\sigma} \right)^2 \cdot \sigma^2 \quad i = 1, 2, ..., N \tag{3.19}$$

Equation (3.19) can be algebraically manipulated as shown in Eq. (3.20) in order to facilitate the obtention of the root values.

$$A\sigma^2 + B\sigma + C = 0; \qquad i = 1, 2, ..., N \tag{3.20}$$

where

$$A = ((M_z \cdot a_{i,3})^2 - \tau_{i_{max}}^2) \quad (3.21)$$

$$B = (2 \cdot M_z^2 \cdot a_{i,3} \cdot m_i(\theta)) \quad (3.22)$$

$$C = (M_z \cdot m_i(\theta))^2 \quad (3.23)$$

On solving the quadratic equation (3.20) two roots for σ are obtained for each value of i ($i = 1, 2, ..., N$). In total we will have $2N$ different roots and the obtained roots must be used in Eq. (3.15) in order to obtain $2N$ scaling factors, one scaling factor for each root (σ) obtained.

As in section 3.2, the scaling factors can be placed in a set. The scaling factor (Ψ) in this set with the minimum value is the maximum factor which all joint torques/forces can be scaled by and still remain at or below their corresponding maximum values (NOKLEBY et al., 2005), i.e.:

$$\Psi = \min(\psi_i(\sigma_1), \psi_i(\sigma_2)) \quad i = 1, 2, ..., N \quad (3.24)$$

where σ_1 and σ_2 are the two roots of σ obtained for each value of $i = 1, 2, ..., N$.

Since $\$_F = [\cos(\theta), \sin(\theta), \sigma]^T$ represents a unit force with an initial moment in z, the maximum possible wrench intensity f_{app} of the screw quantity F_{app} in Eq. (3.4) is:

$$f_{app} = \Psi \quad (3.25)$$

Multiplying the scaling factor by both sides of the inverse statics equation allows better observation of the effects of the scaling factor, as shown in Eq. (3.26).

$$\begin{bmatrix} \Psi \cdot \tau_1(\theta) \\ \Psi \cdot \tau_2(\theta) \\ \vdots \\ \Psi \cdot \tau_N(\theta) \end{bmatrix} = \begin{bmatrix} a_{1,1} & a_{1,2} & a_{1,3} \\ a_{2,1} & a_{2,2} & a_{2,3} \\ \vdots & \vdots & \vdots \\ a_{n,1} & a_{n,2} & a_{n,3} \end{bmatrix} \cdot \begin{bmatrix} \Psi \cdot \cos(\theta) \\ \Psi \cdot \sin(\theta) \\ \Psi \cdot \sigma \end{bmatrix} \quad (3.26)$$

In Eq. (3.26) the first element in the right vector represents the component in x of the maximum force at the end effector of the manipulator ($F_x = \Psi \cdot \cos(\theta)$), the second element in the right vector

represents the component in y of the maximum force at the end effector of the manipulator ($F_y = \Psi \cdot \sin(\theta)$) and the last element in the right vector represents the imposed moment at the end effector of the manipulator ($M_z = \Psi \cdot \sigma$), as shown previously in Eq. (3.15).

The modified scaling factor method proposed in this section is an important result obtained in this thesis, and in combination with the Davies method it constitutes a powerful tool that can be used in order to solve the force capability problem in any mechanism or manipulator with a net degree of constraint equal to three ($C_N = 3$).

At this point it is important to note that the modified scaling factor method proposed herein solves the main problem associated with the original scaling factor method, that is, it avoid the use of optimization algorithms and allows the desired moment at the manipulator end effector to be included in an explicit mathematical expression.

It is also important to emphasize that although the modified scaling factor method proposed herein allow us to include a determined value for the moment at the manipulator end effector, the interval in which the moment can change is still unknown. In order to solve this problem, an additional approach can be considered, as will be shown in Section 3.2.1.

3.2.1 Maximum imposed moment

As shown in Section 3.2, the proposed modified scaling factor method involves imposing a desired moment at the end effector of the manipulator (M_z). This imposed moment can not take values outside the acceptable range $[M_{z_{min}} \leq M_z \leq M_{z_{max}}]$, and the calculation of the elements $M_{z_{min}}$ and $M_{z_{max}}$ is carried out by following the same logic applied in the previous sections, but now a unit wrench is imposed at the end effector with an unit moment at z ($M_z = 1$) and without forces in x or y. The new unit wrench is imposed as $\$_F = [0, 0, 1]^T$ and Eq. (3.1) can be rewritten as Eq. (3.27).

$$\begin{bmatrix} \tau_1 \\ \tau_2 \\ \vdots \\ \tau_N \end{bmatrix} = \begin{bmatrix} a_{1,1} & a_{1,2} & a_{1,3} \\ a_{2,1} & a_{2,2} & a_{2,3} \\ \vdots & \vdots & \vdots \\ a_{n,1} & a_{n,2} & a_{n,3} \end{bmatrix} \cdot \begin{bmatrix} 0 \\ 0 \\ 1 \end{bmatrix} \tag{3.27}$$

Expanding Eq. (3.27) provides the values of τ_1,..., τ_N. The

expansion of Eq. (3.27) is shown below in Eq. (3.28).

$$\tau_i = a_{i,3} \quad i = 1, 2, ..., N \tag{3.28}$$

Once again, since all maximum actuated joint torque/force limits ($\tau_{i_{max}}$) are known for all actuated joints i, scaling factors for each actuated joint can be found, in this case using Eq. (3.29) (NOKLEBY et al., 2005).

$$\psi_i = \left| \frac{\tau_{i_{max}}}{\tau_i} \right| \quad i = 1, 2, ..., N \tag{3.29}$$

where ψ_i is the scaling factor for each actuated joint i, and τ_i is the torque/force of the i^{th} actuated joint for a unit wrench in the desired force direction, obtained from Eq. (3.28).

Once again, the scaling factors of Eq. (3.29) can be placed in a set. The scaling factor (Ψ) in this set with the minimum value is the maximum factor which all joint torques/forces can be scaled by and still remain at or below their corresponding maximum values (NOKLEBY et al., 2005), i.e.:

$$\Psi = \min(\psi_i) \quad i = 1, 2, ..., N \tag{3.30}$$

Since $\$_F = [0, 0, 1]^T$ is a wrench with a unit moment at z, the maximum possible moment intensity $M_{z_{max}}$ of the screw quantity is:

$$M_{z_{max}} = \Psi \tag{3.31}$$

Multiplying the scaling factor by both sides of the inverse statics equation provides better observation of the effects of the scaling factor, as shown in Eq. (3.32).

$$\begin{bmatrix} \Psi \cdot \tau_1 \\ \Psi \cdot \tau_2 \\ \vdots \\ \Psi \cdot \tau_N \end{bmatrix} = \begin{bmatrix} a_{1,1} & a_{1,2} & a_{1,3} \\ a_{2,1} & a_{2,2} & a_{2,3} \\ \vdots & \vdots & \vdots \\ a_{n,1} & a_{n,2} & a_{n,3} \end{bmatrix} \cdot \begin{bmatrix} \Psi \cdot 0 \\ \Psi \cdot 0 \\ \Psi \cdot 1 \end{bmatrix} \tag{3.32}$$

By repeating this procedure using the unit wrench $\$_F = [0, 0, -1]^T$ it is possible to obtain the minimum moment at the end effector of the manipulator as $M_{z_{min}} = -M_{z_{max}}$, allowing us to determine the acceptable range of imposed moments where: $[M_{z_{min}} \leq M_z \leq M_{z_{max}}]$.

3.3 APPLICATIONS AND RESULTS

In order to validate the method proposed in this chapter, four cases were studied. The first is a 3 DoF planar serial manipulator, the second is a 6 DoF planar serial manipulator, the third is a 3 DoF 3$\underline{\text{R}}$RR planar parallel manipulator and the fourth is a 4 DoF $PRRR$ planar serial manipulator.

3.3.1 3 DoF planar serial manipulator

The schematic representation of the manipulator studied is shown in Fig. 6. This is a planar serial manipulator with mobility equal to three ($M = 3$) and with a net degree of constraint equal to three ($C_N = 3$). The statics of the manipulator was solved using the formalism described by Davies (DAVIES, 1983c). The inverse statics solution for this manipulator can be generalized as shown in Eq. (3.33).

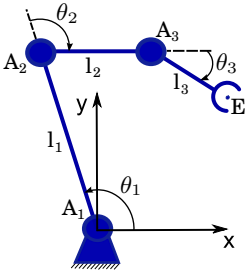

Figure 6 – Planar serial manipulator with 3 DoF.

$$\begin{bmatrix} \tau_{A_1} \\ \tau_{A_2} \\ \tau_{A_3} \end{bmatrix} = \begin{bmatrix} a_{1,1} & a_{1,2} & a_{1,3} \\ a_{2,1} & a_{2,2} & a_{2,3} \\ a_{3,1} & a_{3,2} & a_{3,3} \end{bmatrix} \cdot \begin{bmatrix} E_{Fx} \\ E_{Fy} \\ E_{Mz} \end{bmatrix} \tag{3.33}$$

The graphical results were obtained using arbitrary topological information for the links: $l_1 = 0.4$ [m], $l_2 = 0.25$ [m] and $l_3 = 0.15$ [m], the end effector position $E = (E_x, E_y) = (0.1498\text{ [m]}, 0.3355\text{ [m]})$, the angles $[\theta_1, \theta_2, \theta_3] = [120°, -100°, -60°]$ and the maximum torques in the actuated joints $\tau_{1max} = \tau_{2max} = \tau_{3max} = \pm\ 10$ [Nm].

As previously discussed (Sections 3.2 and 3.2), the maximum

force at the manipulator end effector is a function of the direction of the force (θ) and the prescribed moment (M_z). Graphical results were firstly obtained using the proposed modified scaling factor method with a prescribed moment $M_z = 0$ [Nm] and varying the θ angle within the interval $[0°, 360°]$. This allows us to obtain a force capability polygon, as shown in Fig. 7.

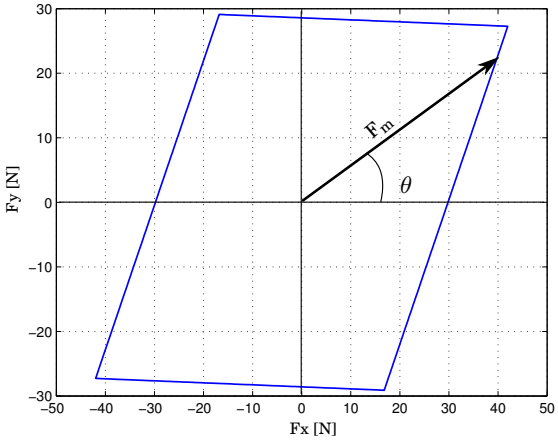

Figure 7 – Force capability polygon in a 3 DoF serial manipulator.

As shown in Section 3.2.1, it is possible to determine the interval in which the moment can be modified without hindering the normal performance of the manipulator. This interval was calculated as: $[-M_{max}, M_{max}] = [-10\ [\text{Nm}], 10\ [\text{Nm}]]$.

By varying the value of the prescribed moment within the previously computed range of moments it is possible to obtain the force capability polytope, as shown in Fig. 8. Note that the force capability polytope is obtained as a set of individual force capability polygons. In order to illustrate this, it can be observed that the force capability polygon shown as a red-dashed line in Fig. 8, where the prescribed moment is $M_z = 0$ [Nm], is the same as the force capability polygon shown in Fig. 7.

Aditionally, in Fig. 9 are shown thee diferent force capability polygons which prescribed moments are $M_z = -10$ [Nm], $M_z = 0$ [Nm] and $M_z = 10$ [Nm] respectively. Such polygons are the same as the force capability polygons shown in Fig. 8 and represented as a continuous green line and a a red-dashed line. Observe that the force capability

polygons with prescribed moments $M_z = -10$ [Nm] and $M_z = 10$ [Nm] cannot apply forces in all the directions but only in a certain interval.

At this point it is important to emphasize that a force capability polygon is not an spherical representation of all the forces and moments at the end effector of the manipulator but a superposition of polar representations that allow identify the behavior of the forces F_x and F_y trough the imposition of a prescribed moment M_z.

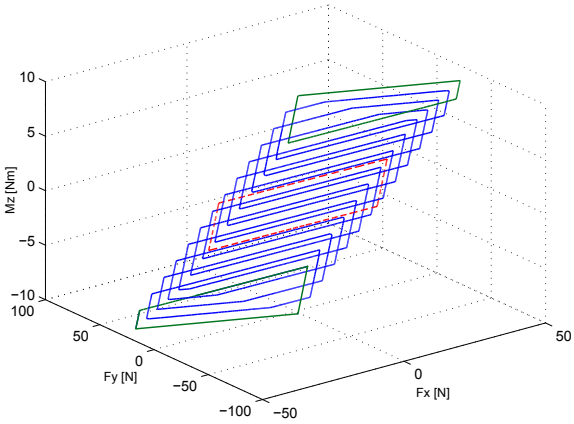

Figure 8 – Force capability polytope in a 3 DoF serial manipulator.

3.3.2 6 DoF planar serial manipulator

The schematic representation of the manipulator studied is shown in Fig. 10. This is a planar serial manipulator with mobility equal to six ($M = 6$) and with a net degree of constraint equal to three ($C_N = 3$). As in the last case, the statics of the manipulator was solved using the formalism described by Davies (DAVIES, 1983c). The inverse statics solution for this manipulator can be generalized as shown in Eq. (3.34).

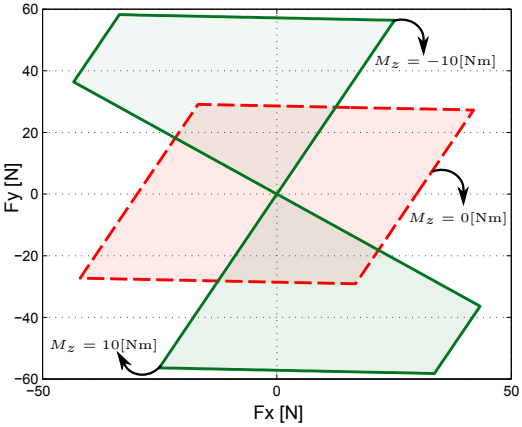

Figure 9 – Force capability polygons with different prescribed moments ($M_z = -10$, $M_z = 0$ and $M_z = 10$) in a 3 DoF serial manipulator.

$$\begin{bmatrix} \tau_{A_1} \\ \tau_{A_2} \\ \tau_{A_3} \\ \tau_{A_4} \\ \tau_{A_5} \\ \tau_{A_6} \end{bmatrix} = \begin{bmatrix} a_{1,1} & a_{1,2} & a_{1,3} \\ a_{2,1} & a_{2,2} & a_{2,3} \\ a_{3,1} & a_{3,2} & a_{3,3} \\ a_{4,1} & a_{4,2} & a_{4,3} \\ a_{5,1} & a_{5,2} & a_{5,3} \\ a_{6,1} & a_{6,2} & a_{6,3} \end{bmatrix} \cdot \begin{bmatrix} E_{Fx} \\ E_{Fy} \\ E_{Mz} \end{bmatrix} \tag{3.34}$$

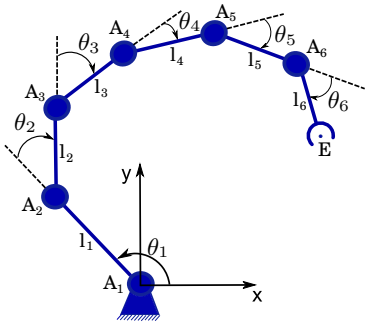

Figure 10 – Planar serial manipulator with 6 DoF.

The graphical results were obtained using arbitrary topological information for the links: $l_1 = 0.4$ [m], $l_2 = l_3 = l_4 = l_5 = 0.25$ [m] and $l_6 = 0.15$ [m], the end effector position $E = (E_x, E_y) = (0.3200\text{ [m]}, 0.5899\text{ [m]})$, the angles $\theta_1 = 140°$, $\theta_2 = -40°$ $\theta_3 = -40°$, $\theta_4 = -40°$, $\theta_5 = -40°$ and $\theta_6 = -40°$ and the maximum torques in the actuated joints $\tau_{1max} = \tau_{2max} = \tau_{3max} = \tau_{4max} = \tau_{5max} = \tau_{6max} = \pm\ 10$ [Nm].

As previously discussed (Sections 3.2 and 3.2), the maximum force at the manipulator end effector is a function of the direction of the force (θ) and the prescribed moment (M_z). In order to obtain graphical results in this study case, the proposed modified scaling factor method was used with a prescribed moment $M_z = 0$ [Nm] and with the θ angle varying within the interval $[0°, 360°]$. This allows us to obtain a force capability polygon, as shown in Fig. 11.

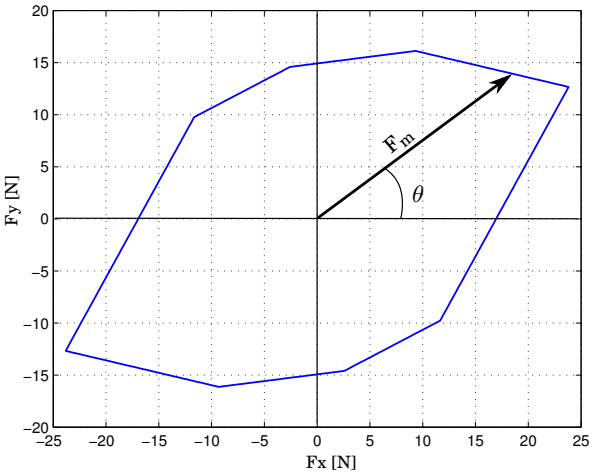

Figure 11 – Force capability polygon in a 6 DoF serial manipulator.

As shown in Section 3.2.1, it is possible to determine the interval in which the moment can be modified without hindering the normal performance of the manipulator. This interval was calculated as: $[-M_{max}, M_{max}] = [-10\text{ Nm}, 10\text{ Nm}]$.

By varying the value of the prescribed moment within the previously computed range of moments it is possible to obtain the force capability polytope, as shown in Fig. 12. Note that the force capability polytope is obtained as a set of individual force capability polygons. In order to illustrate this, it can be observed that the force capability

polygon shown as a red-dashed line in Fig. 12, where the prescribed moment is $M_z = 0$ [Nm], is the same as the force capability polygon shown in Fig. 11.

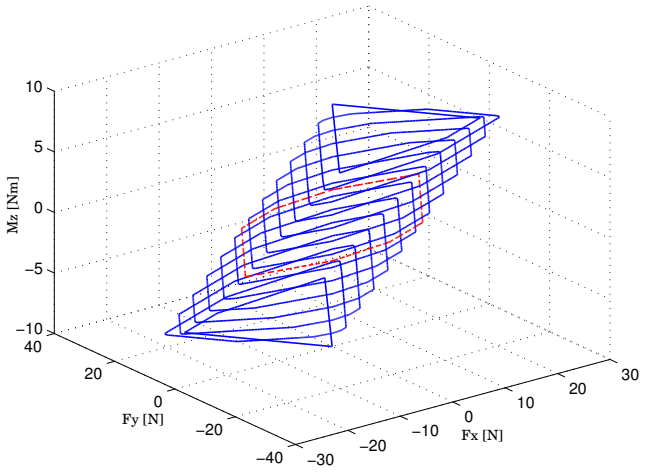

Figure 12 – Force capability polytope in a 6 DoF serial manipulator.

At this point it is very important to note that the results shown in Figs. 7 and 11 can not be directly compared since the manipulators studied in the two cases are different and their kinematic position and orientation at the end effector differ. Similarly, the results obtained in Figs. 8 and 12 can not be directly compared.

3.3.3 4 DoF *PRRR* planar serial manipulator

The schematic representation of the manipulator studied is shown in Fig. 13. This is a planar serial manipulator with mobility equal to four ($M = 4$) and with a net degree of constraint equal to three ($C_N = 3$). The statics of the manipulator was solved using the formalism described by Davies (DAVIES, 1983c). The inverse statics solution for this manipulator can be generalized as shown in Eq. (3.35).

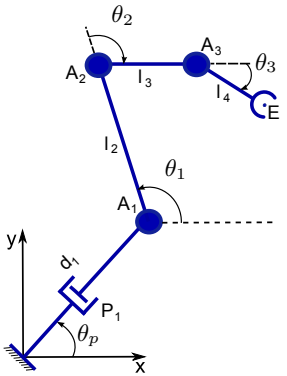

Figure 13 – Planar serial manipulator with 3 DoF.

$$\begin{bmatrix} \tau_{A_1} \\ \tau_{A_2} \\ \tau_{A_3} \\ F_{P_1} \end{bmatrix} = \begin{bmatrix} a_{1,1} & a_{1,2} & a_{1,3} \\ a_{2,1} & a_{2,2} & a_{2,3} \\ a_{3,1} & a_{3,2} & a_{3,3} \\ a_{4,1} & a_{4,2} & a_{4,3} \end{bmatrix} \cdot \begin{bmatrix} E_{Fx} \\ E_{Fy} \\ E_{Mz} \end{bmatrix} \tag{3.35}$$

The graphical results were obtained using arbitrary topological information for the links: $d_1 = 0.2$ [m], $l_1 = 0.4$ [m], $l_2 = 0.25$ [m] and $l_3 = 0.15$ [m], the end effector position $E = (0.1498\ [\text{m}], 0.3355\ [\text{m}])$, the angles $[\theta_p, \theta_1, \theta_2, \theta_3] = [65°, 120°, -100°, -60°]$ and the maximum torques/forces in the actuated joints $\tau_{1max} = \tau_{2max} = \tau_{3max} = \pm\ 10$ [Nm] and $F_{Pmax} = \pm\ 5$ [N].

As previously discussed (Sections 3.2 and 3.2), the maximum force at the manipulator end effector is a function of the direction of the force (θ) and the prescribed moment (M_z). Graphical results were firstly obtained using the proposed modified scaling factor method with a prescribed moment $M_z = 0$ [Nm] and varying the θ angle within the interval $[0°, 360°]$. This allows us to obtain a force capability polygon, as shown in Fig. 14.

As shown in Section 3.2.1, it is possible to determine the interval in which the moment can be modified without hindering the normal performance of the manipulator. This interval was calculated as: $[-M_{max}, M_{max}] = [-10\ [\text{Nm}], 10\ [\text{Nm}]]$.

By varying the value of the prescribed moment within the previously computed range of moments it is possible to obtain the force

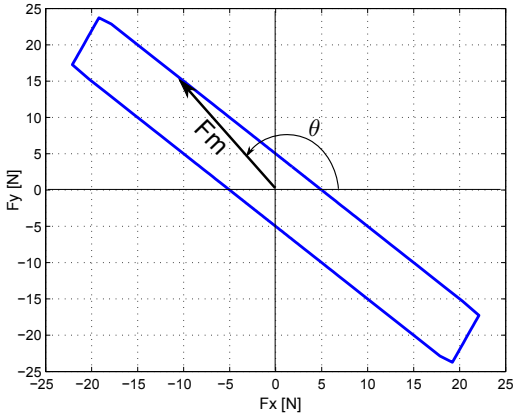

Figure 14 – Force capability polygon in a 4 DoF *PRRR* planar serial manipulator.

capability polytope, as shown in Fig. 15. Note that the force capability polytope is obtained as a set of individual force capability polygons. In order to illustrate this, it can be observed that the force capability polygon shown as a red-dashed line in Fig. 15, where the prescribed moment is $M_z = 0$ [Nm], is the same as the force capability polygon shown in Fig. 14.

Again, at this point it is important to emphasize that a force capability polygon is not an spherical representation of all the forces and moments at the end effector of the manipulator but a superposition of polar representations that allow identify the behavior of the forces F_x and F_y trough the imposition of a prescribed moment M_z.

3.3.4 3$\underline{\text{R}}$RRR parallel manipulator

The schematic representation of the 3$\underline{\text{R}}$RRR parallel manipulator is shown in Fig. 16. As in the last two cases, the statics of the manipulator was solved using the formalism described by Davies (DAVIES, 1983c). The inverse statics solution for this manipulator can be generalized as shown in Eq. (3.36).

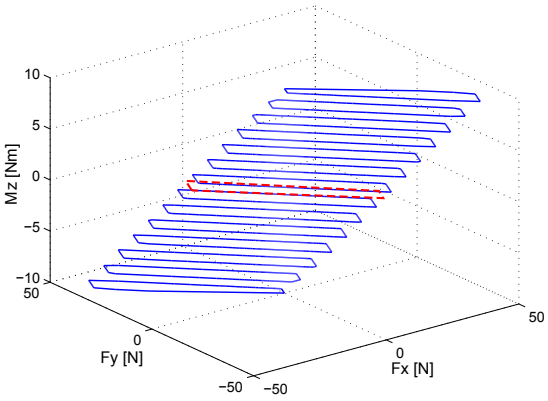

Figure 15 – Force capability polytope in a 3 DoF serial manipulator.

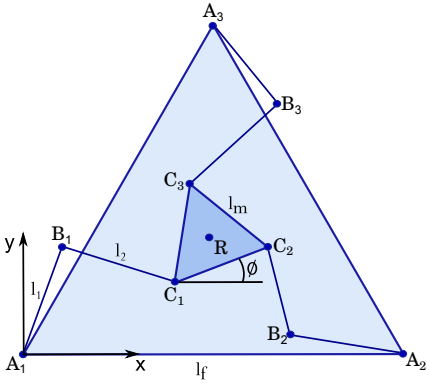

Figure 16 – Schematic representation of a 3RRR parallel manipulator.

$$\begin{bmatrix} \tau_{A_1} \\ \tau_{A_2} \\ \tau_{A_3} \end{bmatrix} = \begin{bmatrix} a_{1,1} & a_{1,2} & a_{1,3} \\ a_{2,1} & a_{2,2} & a_{2,3} \\ a_{3,1} & a_{3,2} & a_{3,3} \end{bmatrix} \cdot \begin{bmatrix} R_{Fx} \\ R_{Fy} \\ R_{Mz} \end{bmatrix} \tag{3.36}$$

In order to validate the results, in this study the topology was the same as that used in Nokleby *et al.* (NOKLEBY et al., 2005) and Mejia *et al.* (MEJIA; SIMAS; MARTINS, 2014b). The graphical results were obtained using the link lengths and platform edge lengths: $l_1 = l_2 = l_m = 0.2$ [m], $l_f = 0.5$ [m], the manipulator end effector is located at (0.25 [m], 0.144 [m]), the mobile platform is oriented at $\phi = 0°$ and the maximum torque allowed in each actuated joint of the manipulator is $\pm$ 4.2 [Nm].

To obtain the graphical results, the proposed modified scaling factor method was used with a prescribed moment $M_z = 0$ [Nm] and with the θ angle varying within the interval $[0°; 360°]$. This allows us to obtain a force capability polygon, as shown in Fig. 17

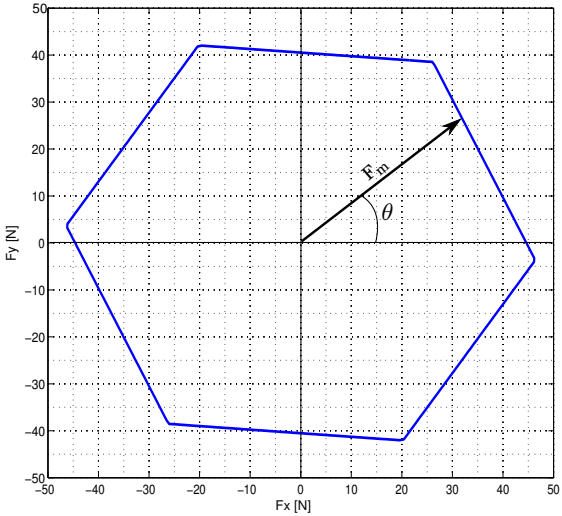

Figure 17 – Force capability polygon in a 3RRR parallel manipulator.

As shown in Section 3.2.1, it is possible to determine the interval in which the moment can be modified without hindering the normal performance of the manipulator. This interval was calculated as: $[-M_{max}, M_{max}] = [-8.3913$ [Nm], 8.3913 [Nm]].

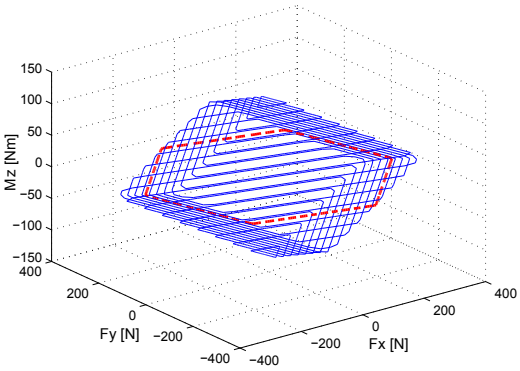

Figure 18 – Force capability polytope in a 3$\underline{\text{R}}$RR parallel manipulator.

Finally, by varying the value of the prescribed moment within the previously computed range, it is possible to obtain the force capability polytope, as shown in Fig. 18. Note that the force capability polytope is obtained as a set of individual force capability polygons. In order to illustrate this, it can be observed that the force capability polygon shown as a red-dashed line in Fig. 18, where the prescribed moment is $M_z = 0$ [Nm], is the same as the force capability polygon shown in Fig. 17.

The results shown in Figs. 17 and 18 are the same as those obtained by Nokleby (NOKLEBY et al., 2005) and Mejia (MEJIA; SIMAS; MARTINS, 2014b) using the original scaling factor method and a differential evolution *(DE)* algorithm. This allowed us to validate the proposed modified scaling factor method. The comparison showed that the force capabilities obtained herein were exactly the same as the reported by Nokleby *et al.* (NOKLEBY et al., 2005) and Mejia *et al.* (MEJIA; SIMAS; MARTINS, 2014b), but an important difference lies in the computing time used to obtain these results.

Using the proposed modified scaling factor method, the force capability analysis for one pose is completed in 0.099731 [s] when running on a P4 2.4 GHz computer. In comparison, on applying the original scaling factor method the force capability analysis for one pose is completed in 15 [s] (ZIBIL et al., 2007), even when run on a faster computer (a P4 3.2 GHz). The same results were obtained by Mejia *et al.* (MEJIA; SIMAS; MARTINS, 2014b) using a differential evolution

Table 2 – Comparison of the computing times required for different approaches to solving the force capability problem.

Method	**Time needed for one pose**	**Time needed for one direction**	**Processor**
(DE) algorithm	> 5400 s	> 18 s	P4 2.4 GHz
Original scaling factor method	15 s	Unknown	P4 3.2 GHz
Modified scaling factor method	0.099731 s	0.000311 s	P4 2.4 GHz

(DE) algorithm, but with a very slow response of more than 5400 [s] when run on a P4 2.4 GHz computer.

Another important issue with regard to the computing time of the proposed modified scaling factor method is that when the force capability of a manipulator is evaluated in a fixed direction, the time used in that operation is only 0.000311 [s] (again, when run on a P4 2.4 GHz computer). This response is very fast and allows us to contemplate applications that require a real-time response in terms of the manipulation of the force, such as grasping, polishing, milling, etc. A comparison of the computing times required to solve the force capability problem is shown in Table 1.

This variation in the computing time required to solve the force capability problem applying different methodologies is easily explained considering that the time needed to evaluate the mathematical functions (as in the case of the proposed modified scaling factor method) is, in general, considerably less than the time required to solve the problem using an optimization algorithm or a numerical solution which requires several iterations or decision processes. An implicit characteristic of the proposed modified scaling factor method is that, in general, it requires less time and effort to evaluate the variables involved.

4 WRENCH CAPABILITY IN GENERAL PLANAR PARALLEL MANIPULATORS

As previously discussed in Chapter 2, *The **wrench capability** of a manipulator is defined as the maximum wrench that can be applied (or sustained) for a given pose, based on the limits of its actuators* (NOKLEBY et al., 2005). The wrench capability phenomenon can be classified by using several wrench capability indices which describe the behavior of the forces and moments present at the manipulator.

One of the most important indices found in literature is the the maximum force with a prescribed moment (F_{app}) presented by Firmani *et al.* If this prescribed moment is zero, it yields a pure force analysis. For a given direction, the maximum force that can be applied with zero moment will be denoted as F_m (WEIHMANN; MARTINS; COELHO, 2011).

The principal aim of this chapter is to present generalized mathematical closed-form solutions to obtain the maximum force with a prescribed moment $\boldsymbol{F_{app}}$ in planar redundantly and not-redundantly actuated mechanisms and manipulators with a net degree of constraint equal to three, four, five and six ($C_N = 3$, $C_N = 4$, $C_N = 5$, $C_N = 6$). The proposed mathematical models are obtained applying classical optimization methods, considering the cases in which the net degree of constraint is equal to the number of actuated joints in the mechanism or manipulator. The mathematical closed form solutions presented in this chapter together with the modified scaling factor method presented in Chapter 3. are the main results obtained in this thesis. In robotics, closed-form solutions are often very desirable, because they are faster than numerical solutions and readily identify all possible solutions (SICILIANO; KHATIB, 2008).

The novelty of the study described herein lies in the fact that our main results are not methods or numerical algorithms, but mathematical closed-form solutions to obtain the force capability in planar redundantly-actuated mechanisms and manipulators with a net degree of constraint equal to three, four, five and six ($C_N = 3$, $C_N = 4$, $C_N = 5$, $C_N = 6$). An equation is said to be a closed-form solution if it solves a given problem in terms of functions and mathematical operations from a given generally-accepted set (CHOW, 1999). This means that the mathematical closed form solutions reported in this chapter are functions that can be used directly without the use of a method, numerical algorithm or optimization process, implying that their use represent simpler, faster and more direct solutions to obtain the force

capability of manipulators compared with other solutions for the same problem found in literature. To validate the mathematical closed-form solutions proposed in this chapter five study cases will be studied in Section 4.8.

4.1 STATIC MODELS OF PARALLEL MANIPULATORS

In the static analysis of manipulators, the goal is to determine the force and moment requirements for the joints in relation to the wrenches applied at the end effector. It is possible to apply forces and moments at the joints of the mechanism to analyze the wrenches obtained at the end effector, or to apply external wrenches at the end effector to calculate the forces and moments required at the joints to balance these external forces.

There are several methodologies which allow us to obtain a complete static analysis of manipulators; however, in this thesis the formalism presented by Davies (DAVIES, 1983c) is used as the primary mathematical tool to analyze the mechanisms statically. In the present study, the Davies method was used because the obtention of the static model of a manipulator or mechanism is simple, easily adaptable and it is not necessary to use a pseudo-inverse as in other methodologies. Additionally, the Davies method together with the proposed mathematical closed-form solutions, constitute a powerful tool that can be used in order to solve the force capability problem in redundantly and not-redundantly actuated parallel manipulators with a net degree of constraint equal to three, four, five and six ($C_N = 3$, $C_N = 4$, $C_N = 5$, $C_N = 6$). for more information about the Davies method reader can review Appendix B where this method was studied.

In parallel planar manipulators, once the Davies method has been applied in order to obtain its static model, it is possible to represent the wrenches at the end effector (F_x, F_y, M_z) as a generalized function of a coefficient matrix $(A_{3\times C_N})$ and the N primary actions $(\tau_1, \tau_2, ..., \tau_N)$, as shown in Eq. (4.1). In order to better understand this idea, consider for example the parallel manipulators shown in Fig. 19.

$$\begin{bmatrix} F_x \\ F_y \\ M_z \end{bmatrix} = \begin{bmatrix} a_{1,1} & a_{1,2} & \cdots & a_{1,N} \\ a_{2,1} & a_{2,2} & \cdots & a_{2,N} \\ a_{3,1} & a_{3,2} & \cdots & a_{3,N} \end{bmatrix} \cdot \begin{bmatrix} \tau_1 \\ \tau_2 \\ \vdots \\ \tau_N \end{bmatrix} \tag{4.1}$$

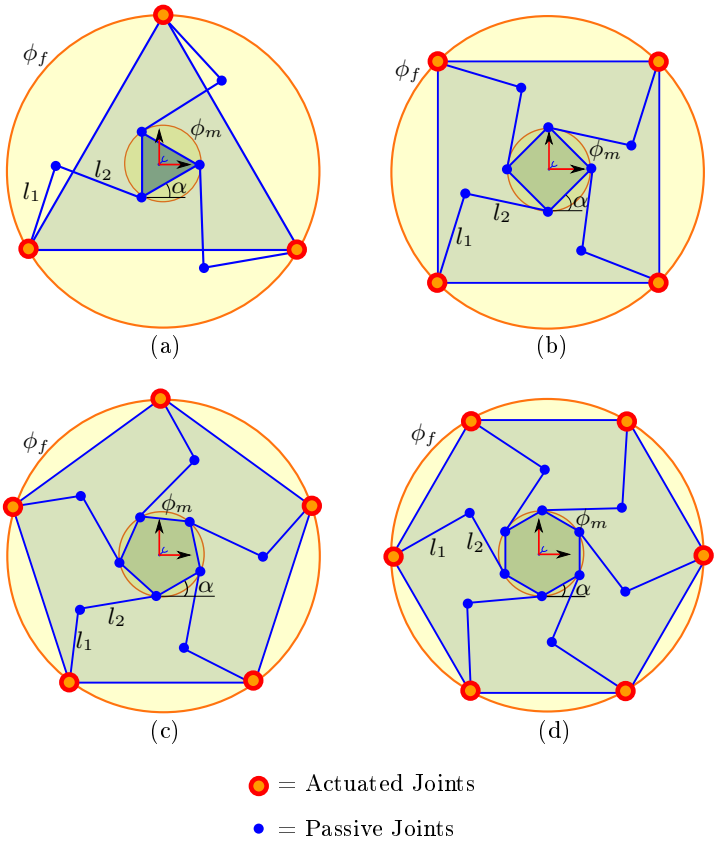

Figure 19 – (a). Non-Redundantly-actuated 3$\underline{\text{R}}$RRR planar parallel manipulator ($C_N = 3$). (b). Redundantly-actuated 4$\underline{\text{R}}$RRR planar parallel manipulator ($C_N = 4$). (c). Redundantly-actuated 5$\underline{\text{R}}$RRR planar parallel manipulator ($C_N = 5$). (d). Redundantly-actuated 6$\underline{\text{R}}$RRR planar parallel manipulator ($C_N = 6$).

In planar manipulators with $C_N = 3$ like the 3$\underline{\text{R}}$RRR parallel manipulator shown in Fig. 19(a), once the Davies method has been applied in order to obtain its static model, it is possible to represent the wrenches at the end effector (F_x, F_y, M_z) as a generalized function of a coefficient matrix $(A_{3\times3})$ and the three primary actions (τ_1, τ_2, τ_3), as shown in Eq. (4.2). In a similar way, in planar manipulators with $C_N = 4$ like the 4$\underline{\text{R}}$RRR parallel manipulator shown in Fig. 19(b), once

the Davies method has been applied in order to obtain its static model, it is possible to represent the wrenches at the end effector (F_x, F_y, M_z) as a generalized function of a coefficient matrix $(A_{3\times4})$ and the four primary actions $(\tau_1, \tau_2, \tau_3, \tau_4)$, as shown in Eq. (4.3). In manipulators with $C_N = 5$ like the 5$\underline{\text{R}}$RRR parallel manipulator shown in Fig. 19(c), the wrenches at the end effector (F_x, F_y, M_z) can be represented statically by using the Davies method as a generalized function of a coefficient matrix $(A_{3\times5})$ and the five primary actions $(\tau_1, \tau_2, \tau_3, \tau_4, \tau_5)$ as shown in Eq. (4.4). Finally, manipulators with $C_N = 6$ like the 6$\underline{\text{R}}$RRR parallel manipulator shown in Fig. 19(d), can have the wrenches at the end effector (F_x, F_y, M_z) represented as a generalized function of a coefficient matrix $(A_{3\times6})$ and the six primary actions $(\tau_1, \tau_2, \tau_3, \tau_4, \tau_5, \tau_6)$ as shown in Eq. (4.5).

At this point it is very important to emphasize that although only especific models were shown for parallel manipulators with $C_N = 3$, $C_N = 4$, $C_N = 5$ and $C_N = 6$, Eq. 4.1 generalizes the static behavior of any parallel manipulator with $C_N \geq 3$.

$$\begin{bmatrix} F_x \\ F_y \\ M_z \end{bmatrix} = \begin{bmatrix} a_{1,1} & a_{1,2} & a_{1,3} \\ a_{2,1} & a_{2,2} & a_{2,3} \\ a_{3,1} & a_{3,2} & a_{3,3} \end{bmatrix} \cdot \begin{bmatrix} \tau_1 \\ \tau_2 \\ \tau_3 \end{bmatrix} \tag{4.2}$$

$$\begin{bmatrix} F_x \\ F_y \\ M_z \end{bmatrix} = \begin{bmatrix} a_{1,1} & a_{1,2} & a_{1,3} & a_{1,4} \\ a_{2,1} & a_{2,2} & a_{2,3} & a_{2,4} \\ a_{3,1} & a_{3,2} & a_{3,3} & a_{3,4} \end{bmatrix} \cdot \begin{bmatrix} \tau_1 \\ \tau_2 \\ \tau_3 \\ \tau_4 \end{bmatrix} \tag{4.3}$$

$$\begin{bmatrix} F_x \\ F_y \\ M_z \end{bmatrix} = \begin{bmatrix} a_{1,1} & a_{1,2} & a_{1,3} & a_{1,4} & a_{1,5} \\ a_{2,1} & a_{2,2} & a_{2,3} & a_{2,4} & a_{2,5} \\ a_{3,1} & a_{3,2} & a_{3,3} & a_{3,4} & a_{3,5} \end{bmatrix} \cdot \begin{bmatrix} \tau_1 \\ \tau_2 \\ \tau_3 \\ \tau_4 \\ \tau_5 \end{bmatrix} \tag{4.4}$$

$$\begin{bmatrix} F_x \\ F_y \\ M_z \end{bmatrix} = \begin{bmatrix} a_{1,1} & a_{1,2} & a_{1,3} & a_{1,4} & a_{1,5} & a_{1,6} \\ a_{2,1} & a_{2,2} & a_{2,3} & a_{2,4} & a_{2,5} & a_{2,6} \\ a_{3,1} & a_{3,2} & a_{3,3} & a_{3,4} & a_{3,5} & a_{3,6} \end{bmatrix} \cdot \begin{bmatrix} \tau_1 \\ \tau_2 \\ \tau_3 \\ \tau_4 \\ \tau_5 \\ \tau_6 \end{bmatrix} \quad (4.5)$$

4.2 OPTIMIZATION OF THE FORCE CAPABILITY IN MANIPULATORS.

The principal aim of this chapter is to present generalized mathematical closed-form solutions to obtain the maximum force with a prescribed moment ($\boldsymbol{F_{app}}$) in manipulators with a net degree of constraint equal to three, four, five and six ($C_N = 3$, $C_N = 4$, $C_N = 5$, $C_N = 6$). In other words, *the force capability optimization problem is defined as the maximization of the force magnitude with a given direction and with a prescribed moment at the end effector in parallel manipulators satisfying the conditions* $C_N = 3$, $C_N = 4$, $C_N = 5$ *or* $C_N = 6$. This condition allow us to think in a solution based in the optimization methods presented in Appendix C.

In this section the procedure to obtain the mathematical closed-form solutions defining the maximum force with a prescribed moment ($\boldsymbol{F_{app}}$) in manipulators with $C_N = 3$ is shown in detail, and the resulting closed-form solution obtained for this kind of manipulators by using this procedure will be shown in Section 4.4.

The optimization process used to obtain the mathematical closed-form solutions for manipulators with $C_N = 4$, $C_N = 5$ and $C_N = 6$ is very similar to such as used in in manipulators with $C_N = 3$, and because of this, only the closed-form solutions for this kind of manipulators will be presented in sections 4.5, 4.6 and 4.7 in order to exemplify. Manipulators with $C_N > 6$ can have their mathematical closed form solutions obtained in a similar way as in manipulators with $C_N = 3$, $C_N = 4$, $C_N = 5$ and $C_N = 6$, however in this study will be not included.

4.3 FORCE CAPABILITY OPTIMIZATION IN MANIPULATORS WITH $C_N = 3$

In order to solve the force capability problem in parallel manipulators with $C_N = 3$, the first consideration that must take into account is that the direction of the application of the force must be known. The imposition of a force direction allows us to determine the relations between the forces F_x and F_y at the manipulator end effector, as shown in Fig. 20. These relations can be expressed mathematically by Eqs. (4.6) and (4.7).

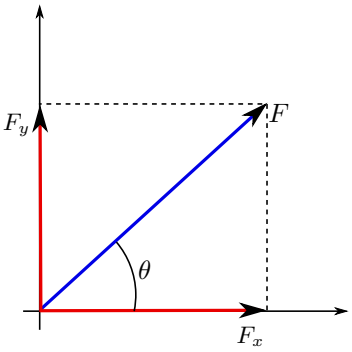

Figure 20 – Prescribed force direction at the manipulator end effector

$$F = \sqrt{{F_x}^2 + {F_y}^2} \tag{4.6}$$

$$F_y = F_x \tan(\theta) \tag{4.7}$$

Equations. (4.6) and (4.7) can be rewritten with the substitution of the elements in Eq. (4.2), as shown in Eqs. (4.8) and (4.9), respectively.

$$F = \sqrt{(a_{1,1}\tau_1 + a_{1,2}\tau_2 + a_{1,3}\tau_3)^2 + (a_{2,1}\tau_1 + a_{2,2}\tau_2 + a_{2,3}\tau_3)^2} \tag{4.8}$$

$$k_a(\theta)\tau_1 + k_b(\theta)\tau_2 + k_c(\theta)\tau_3 = 0 \tag{4.9}$$

where:

$$k_a(\theta) = a_{2,1} - a_{1,1}\tan(\theta) \quad (4.10)$$
$$k_b(\theta) = a_{2,2} - a_{1,2}\tan(\theta) \quad (4.11)$$
$$k_c(\theta) = a_{2,3} - a_{1,3}\tan(\theta) \quad (4.12)$$

The formulation of the force capability optimization problem can be generalized as shown in Eqs. (4.13) to (4.18). For convenience, the objective function is represented in Eq. (4.13) as the negative of the square of the force, in order to maximize the force. Equation (4.14) represents the equality constraint function of the force direction. Equation (4.180) represents the equality constraint function of the prescribed moment ($\boldsymbol{M_{i_z}}$). Equations (4.16), (4.17) and (4.18) represent the inequality constraint functions of the maximum admissible torque in each actuated joint τ_1, τ_2 and τ_3.

$$\begin{aligned} &minimize: \quad f(\tau_1,\tau_2,\tau_3) = -F^2 = -\left(F_x^2 + F_y^2\right) = \ldots \\ &\ldots = -\left((a_{1,1}\tau_1 + a_{1,2}\tau_2 + a_{1,3}\tau_3)^2 + (a_{2,1}\tau_1 + a_{2,2}\tau_2 + a_{2,3}\tau_3)^2\right) \end{aligned} \quad (4.13)$$

$$subject\ to: \quad h_1(\tau_1,\tau_2,\tau_3) : k_a(\theta)\tau_1 + k_b(\theta)\tau_2 + k_c(\theta)\tau_3 = 0 \quad (4.14)$$
$$h_2(\tau_1,\tau_2,\tau_3) : a_{3,1}\tau_1 + a_{3,2}\tau_2 + a_{3,3}\tau_3 - M_{i_z} = 0 \quad (4.15)$$
$$g_1(\tau_1) : -\tau_{1max} \leqslant \tau_1 \leqslant \tau_{1max} \quad (4.16)$$
$$g_2(\tau_2) : -\tau_{2max} \leqslant \tau_2 \leqslant \tau_{2max} \quad (4.17)$$
$$g_3(\tau_3) : -\tau_{3max} \leqslant \tau_3 \leqslant \tau_{3max} \quad (4.18)$$

Note that Eqs. (4.16), (4.17) and (4.18) represent six inequality constraints, because each equation can be decomposed into two independent inequality constraints (e.g. Eq. (4.16) can be decomposed into $g_{1a}(\tau_1) : -\tau_{1max} - \tau_1 \leqslant 0$ and $g_{1b}(\tau_1) : \tau_1 - \tau_{1max} \leqslant 0$).

To solve the force capability optimization problem it is necessary to define a Lagrangian function as a combination of the objective function, the equality constraint functions, the inequality constraint functions, the Lagrange multipliers and the slack variables as shown in deatil in Appendix C.

For convenience, in this chapter the Lagrange multipliers for the equality constraints are represented as λ_1 and λ_2, the Lagrange mul-

tipliers for the inequality constraints are represented as $\mu_1, ..., \mu_6$ and the slack variables are represented as $s_1, ..., s_6$. Equation (4.19) shows the Lagrangian function used to solve the F_{app} optimization problem herein.

$$\begin{aligned}\mathcal{L} = &-\left(k_r {\tau_1}^2 + k_s {\tau_2}^2 + k_t {\tau_3}^2 + k_u \tau_1 \tau_2 + k_v \tau_1 \tau_3 + k_w \tau_2 \tau_3\right) + \dots \\ \dots &+ \lambda_1 \left[k_a(\theta)\tau_1 + k_b(\theta)\tau_2 + k_c(\theta)\tau_3\right] + \lambda_2 \left[a_{3,1}\tau_1 + a_{3,2}\tau_2 + a_{3,3}\tau_3 - M_{i_z}\right] + \dots \\ &\dots + \mu_1 \left[-\tau_{1max} - \tau_1 + {s_1}^2\right] + \mu_2 \left[\tau_1 - \tau_{1max} + {s_2}^2\right] + \dots \\ &\dots + \mu_3 \left[-\tau_{2max} - \tau_2 + {s_3}^2\right] + \mu_4 \left[\tau_2 - \tau_{2max} + {s_4}^2\right] + \dots \\ &\dots + \mu_5 \left[-\tau_{3max} - \tau_3 + {s_5}^2\right] + \mu_6 \left[\tau_3 - \tau_{3max} + {s_6}^2\right] \end{aligned} \quad (4.19)$$

where:

$$k_r = {a_{1,1}}^2 + {a_{2,1}}^2 \quad (4.20)$$

$$k_s = {a_{1,2}}^2 + {a_{2,2}}^2 \quad (4.21)$$

$$k_t = {a_{1,3}}^2 + {a_{3,3}}^2 \quad (4.22)$$

$$k_u = 2a_{1,1}a_{1,2} + 2a_{2,1}a_{2,2} \quad (4.23)$$

$$k_v = 2a_{1,1}a_{1,3} + 2a_{2,1}a_{2,3} \quad (4.24)$$

$$k_w = 2a_{1,2}a_{1,3} + 2a_{2,2}a_{2,3} \quad (4.25)$$

Differentiating the Lagrangian function shown in Eq.(4.19) with respect to τ, λ, μ and s, Eqs. (4.26) to (4.42) are obtained. These equations allow us to construct a mathematical system whose solution will solve the force capability optimization problem.

The partial derivatives of the Lagrangian ($\mathcal{L}$) as a function of the actuated joints (τ_1, τ_2 and τ_3) are obtained as:

$$\frac{\partial \mathcal{L}}{\partial \tau_1} = -\left(2k_r\tau_1 + k_u\tau_2 + k_v\tau_3\right) + \lambda_1 k_a(\theta) + \lambda_2 a_{3,1} - \mu_1 + \mu_2 = 0 \quad (4.26)$$

$$\frac{\partial \mathcal{L}}{\partial \tau_2} = -\left(2k_s\tau_2 + k_u\tau_1 + k_w\tau_3\right) + \lambda_1 k_b(\theta) + \lambda_2 a_{3,2} - \mu_3 + \mu_4 = 0 \quad (4.27)$$

$$\frac{\partial \mathcal{L}}{\partial \tau_3} = -\left(2k_t\tau_3 + k_v\tau_1 + k_w\tau_2\right) + \lambda_1 k_c(\theta) + \lambda_2 a_{3,3} - \mu_5 + \mu_6 = 0 \quad (4.28)$$

The partial derivatives of the Lagrangian ($\mathcal{L}$) as a function of the Lagrange multipliers for equality constraints (λ_1 and λ_2) are obtained as:

$$\frac{\partial \mathcal{L}}{\partial \lambda_1} = k_a(\theta)\tau_1 + k_b(\theta)\tau_2 + k_c(\theta)\tau_3 = 0 \tag{4.29}$$

$$\frac{\partial \mathcal{L}}{\partial \lambda_2} = a_{3,1}\tau_1 + a_{3,2}\tau_2 + a_{3,3}\tau_3 - M_{i_z} = 0 \tag{4.30}$$

The partial derivatives of the Lagrangian ($\mathcal{L}$) as a function of the Lagrange multipliers for inequality constraints (μ_1, μ_2, μ_3, μ_4, μ_1 and μ_6) are obtained as:

$$\frac{\partial \mathcal{L}}{\partial \mu_1} = {s_1}^2 - \tau_{1max} - \tau_1 = 0 \tag{4.31}$$

$$\frac{\partial \mathcal{L}}{\partial \mu_2} = {s_2}^2 - \tau_{1max} + \tau_1 = 0 \tag{4.32}$$

$$\frac{\partial \mathcal{L}}{\partial \mu_3} = {s_3}^2 - \tau_{2max} - \tau_2 = 0 \tag{4.33}$$

$$\frac{\partial \mathcal{L}}{\partial \mu_4} = {s_4}^2 - \tau_{2max} + \tau_2 = 0 \tag{4.34}$$

$$\frac{\partial \mathcal{L}}{\partial \mu_5} = {s_5}^2 - \tau_{3max} - \tau_3 = 0 \tag{4.35}$$

$$\frac{\partial \mathcal{L}}{\partial \mu_6} = {s_6}^2 - \tau_{3max} + \tau_3 = 0 \tag{4.36}$$

Finally, the partial derivatives of the Lagrangian ($\mathcal{L}$) as a function of the slack variables (s_1, s_2, s_3, s_4, s_1 and s_6) are obtained as:

$$\frac{\partial \mathcal{L}}{\partial s_1} = 2s_1\mu_1 = 0 \tag{4.37}$$

$$\frac{\partial \mathcal{L}}{\partial s_2} = 2s_2\mu_2 = 0 \tag{4.38}$$

$$\frac{\partial \mathcal{L}}{\partial s_3} = 2s_3\mu_3 = 0 \tag{4.39}$$

$$\frac{\partial \mathcal{L}}{\partial s_4} = 2s_4\mu_4 = 0 \tag{4.40}$$

$$\frac{\partial \mathcal{L}}{\partial s_5} = 2s_5\mu_5 = 0 \tag{4.41}$$

$$\frac{\partial \mathcal{L}}{\partial s_6} = 2s_6\mu_6 = 0 \tag{4.42}$$

The mathematical system shown in Eqs. (4.26) to (4.42) is solved through the imposition of hypothetical values for s_n and μ_n satisfying the conditions shown in Eqs. (4.37) to (4.42), but avoiding conflicting solutions. The case in which $s_1 = 0$ and $s_2 = 0$ can be considered as an example of such conflicting solutions, because although they are possible solutions for Eqs. (4.37) and (4.38), the solutions obtained for Eqs. (4.31) and (4.32), where $\tau_1 = -\tau_{1max}$ and $\tau_1 = \tau_{1max}$, are physically impossible to put into practice because the maximum positive torque and the maximum negative torque cannot be applied in an actuator at the same time.

4.4 MATHEMATICAL CLOSED-FORM SOLUTION TO OBTAIN THE FORCE CAPABILITY IN MANIPULATORS WITH $C_N = 3$

In this section, one of the main results obtained in this study is presented. First, the closed-form solution to obtain the force capability in mechanisms and manipulators with $C_N = 3$ is shown; then, a closed-form solution to obtain the limits within which the prescribed moment at the manipulator end effector can be changed is presented.

The mathematical closed-form solution to obtain the force capability in manipulators with $C_N = 3$ presented in this section is obtained from the solution of the mathematical system shown in Eqs. (4.26) to (4.42). This solution allows us to obtain the maximum force with a prescribed moment (F_{app}) in planar manipulators with $C_N = 3$ as a function of the desired force direction (θ) and the prescribed moment (M_{i_z}) at the end effector of the manipulator.

The mathematical closed-form solution is shown in Eqs. (4.43) to (4.53) and represents one of the most important results obtained in this study. It should be noted that the nine kinematic variables ($a_{1,1}, ..., a_{3,3}$) were obtained from the solution of the direct static problem presented in Eq. (4.2), and the terms $k_a(\theta)$, $k_b(\theta)$ and $k_c(\theta)$ were previously obtained as shown in Eqs. (4.10), (4.11) and (4.12).

$$F_{app}(\theta, M_{i_z}) = \max[f_e(-\tau_{1max}, \tau_2, \tau_3) \cdot kkt_1; f_e(\tau_{1max}, \tau_2, \tau_3) \cdot kkt_1; \cdots$$
$$\cdots f_e(\tau_1, -\tau_{2max}, \tau_3) \cdot kkt_2; f_e(\tau_1, \tau_{2max}, \tau_3) \cdot kkt_2; \cdots$$
$$\cdots f_e(\tau_1, \tau_2, -\tau_{3max}) \cdot kkt_3; f_e(\tau_1, \tau_2, \tau_{3max}) \cdot kkt_3] \quad (4.43)$$

where

$$f_e(\tau_1, \tau_2, \tau_3) = \left((a_{1,1}\tau_1 + a_{1,2}\tau_2 + a_{1,3}\tau_3)^2 + (a_{2,1}\tau_1 + a_{2,2}\tau_2 + a_{2,3}\tau_3)^2\right)^{\frac{1}{2}} \quad (4.44)$$

$$kkt_1 = \begin{cases} 1 & \Leftrightarrow \quad (-\tau_{2max} \leq \tau_2 \leq \tau_{2max}) \wedge (-\tau_{3max} \leq \tau_3 \leq \tau_{3max}) \\ 0 & \qquad\qquad otherwise \end{cases} \quad (4.45)$$

$$kkt_2 = \begin{cases} 1 & \Leftrightarrow \quad (-\tau_{2max} \leq \tau_2 \leq \tau_{2max}) \wedge (-\tau_{3max} \leq \tau_3 \leq \tau_{3max}) \\ 0 & \qquad\qquad otherwise \end{cases} \quad (4.46)$$

$$kkt_3 = \begin{cases} 1 & \Leftrightarrow \quad (-\tau_{1max} \leq \tau_1 \leq \tau_{1max}) \wedge (-\tau_{3max} \leq \tau_3 \leq \tau_{3max}) \\ 0 & \qquad\qquad otherwise \end{cases} \quad (4.47)$$

In this solution, Eq. (4.43) is represented as the maximum value of six terms. Each term in Eq. (4.43) is obtained as the product of Eq. (4.44) (evaluated with different values of τ_1, τ_2 and τ_3) and a penalization term (kkt_n) as shown in Eqs. (4.45) to (4.47).

To evaluate the first and second terms in Eq. (4.43), the components τ_2 and τ_3 need to be obtained as a function of τ_1 (using $-\tau_{1max}$ and τ_{1max}, respectively), M_{i_z} and θ using Eqs. (4.48) and (4.49). To evaluate the third and fourth terms in Eq. (4.43), the components τ_1 and τ_3 need to be obtained as a function of τ_2 (using $-\tau_{2max}$ and τ_{2max}, respectively), M_{i_z} and θ using Eqs. (4.50) and (4.51). Also, to evaluate the fifth and sixth terms in Eq. (4.43), the components τ_1 and τ_2 need to be obtained as a function of τ_3 (using $-\tau_{3max}$ and τ_{3max}, respectively), M_{i_z} and θ using Eqs. (4.52) and (4.53).

$$\tau_2(\tau_1, M_{i_z}, \theta) = \frac{k_c(\theta)M_{i_z} + (a_{3,2}k_a(\theta) - a_{3,1}k_c(\theta))\tau_1}{a_{3,2}k_c(\theta) - a_{3,2}k_b(\theta)} \quad (4.48)$$

$$\tau_3(\tau_1, M_{i_z}, \theta) = \frac{(a_{3,1}k_b(\theta) - a_{3,2}k_a(\theta))\tau_1 - k_b(\theta)M_{i_z}}{a_{3,2}k_c(\theta) - a_{3,2}k_b(\theta)} \quad (4.49)$$

$$\tau_1(\tau_2, M_{i_z}, \theta) = \frac{k_c(\theta)M_{i_z} + (a_{3,2}k_b(\theta) - a_{3,2}k_c(\theta))\tau_2}{a_{3,1}k_c(\theta) - a_{3,2}k_a(\theta)} \quad (4.50)$$

$$\tau_3(\tau_2, M_{i_z}, \theta) = \frac{(a_{3,2}k_a(\theta) - a_{3,1}k_b(\theta))\tau_2 - k_a(\theta)M_{i_z}}{a_{3,1}k_c(\theta) - a_{3,2}k_a(\theta)} \quad (4.51)$$

$$\tau_1(\tau_3, M_{i_z}, \theta) = \frac{k_b(\theta)M_{i_z} + (a_{3,2}k_c(\theta) - a_{3,2}k_b(\theta))\tau_3}{a_{3,1}k_b(\theta) - a_{3,2}k_a(\theta)} \quad (4.52)$$

$$\tau_2(\tau_3, M_{i_z}, \theta) = \frac{(a_{3,2}k_a(\theta) - a_{3,1}k_c(\theta))\tau_3 - k_a(\theta)M_{i_z}}{a_{3,1}k_b(\theta) - a_{3,2}k_a(\theta)} \quad (4.53)$$

4.4.1 Mathematical closed-form solution for the maximum prescribed moment (M_{max}):

As previously shown in Eq. (4.43), the maximum force at the manipulator end effector is a function of the direction of the force (θ) and the prescribed moment (M_{i_z}). But while the direction of the force (θ) can be prescribed arbitrarily within the interval $[0; 2\pi]$ *rad*, the moment at the manipulator end effector (M_{i_z}) can only be prescribed within the interval $[-M_{max}; M_{max}]$. The value of M_{max} can be obtained using Eq. (4.54). This equation represents other important result obtained in this study.

$$M_{max} = \max[M_m(\tau_{1max}, \tau_2, \tau_3); M_m(\tau_1, \tau_{2max}, \tau_3); M_m(\tau_1, \tau_2, \tau_{3max})] \quad (4.54)$$

where

$$M_m = |a_{3,1}\tau_1 + a_{3,2}\tau_2 + a_{3,3}\tau_3| \quad (4.55)$$

Eq. (4.54) is represented as the maximum value of three terms. Each term in Eq. (4.54) is obtained evaluating Eq. (4.55) with different values of τ_1 , τ_2 and τ_3. To evaluate the first term in Eq. (4.54), the components τ_2 and τ_3 need to be obtained as a function of τ_1 using Eqs. (4.56) and (4.57). To evaluate the second term in Eq. (4.54), the

components τ_1 and τ_3 need to be obtained as a function of τ_2 using Eqs. (4.58) and (4.59). Finally, to evaluate the third term in Eq. (4.54), components τ_1 and τ_2 need to be obtained as a function of τ_3 using Eqs. (4.60) and (4.61).

$$\tau_2(\tau_1) = \frac{\tau_1(a_{1,3}a_{2,1} - a_{1,1}a_{2,3})}{a_{1,2}a_{2,3} - a_{1,3}a_{2,2}} \tag{4.56}$$

$$\tau_3(\tau_1) = \frac{\tau_1(a_{1,1}a_{2,2} - a_{1,2}a_{2,1})}{a_{1,2}a_{2,3} - a_{1,3}a_{2,2}} \tag{4.57}$$

$$\tau_1(\tau_2) = \frac{\tau_2(a_{1,3}a_{2,2} - a_{1,2}a_{2,3})}{a_{1,1}a_{2,3} - a_{1,3}a_{2,1}} \tag{4.58}$$

$$\tau_3(\tau_2) = \frac{\tau_2(a_{1,2}a_{2,1} - a_{1,1}a_{2,2})}{a_{1,1}a_{2,3} - a_{1,3}a_{2,1}} \tag{4.59}$$

$$\tau_1(\tau_3) = \frac{\tau_3(a_{1,2}a_{2,3} - a_{1,3}a_{2,2})}{a_{1,1}a_{2,2} - a_{1,2}a_{2,1}} \tag{4.60}$$

$$\tau_2(\tau_3) = \frac{\tau_3(a_{1,3}a_{2,1} - a_{1,1}a_{2,3})}{a_{1,1}a_{2,2} - a_{1,2}a_{2,1}} \tag{4.61}$$

The interval $[-M_{max}; M_{max}]$ represents the possible values to which the prescribed moment at the manipulator end effector can be changed and this is the second part of the proposed mathematical closed-form solution to obtain the force capability in planar manipulators with $C_N = 3$.

4.5 MATHEMATICAL CLOSED-FORM SOLUTION TO OBTAIN THE FORCE CAPABILITY IN MANIPULATORS WITH $C_N = 4$

In a similar way as in section 4.4, the mathematical closed-form solution to obtain the force capability in manipulators with $C_N = 4$ can be obtained by using an optimization process. In this section the mathematical closed-form solution to obtain the force capability in manipulators with $C_N = 4$ is presented directly as shown in Eqs. (4.62) to (4.81).

$$
\begin{aligned}
F_{app}(\theta, M_{i_z}) = \max[&f_e(-\tau_{1max}, -\tau_{2max}, \tau_3, \tau_4) \cdot kkt_1; \cdots \\
&\cdots f_e(-\tau_{1max}, \tau_{2max}, \tau_3, \tau_4) \cdot kkt_1; f_e(\tau_{1max}, -\tau_{2max}, \tau_3, \tau_4) \cdot kkt_1; \cdots \\
&\cdots f_e(\tau_{1max}, \tau_{2max}, \tau_3, \tau_4) \cdot kkt_1; f_e(-\tau_{1max}, \tau_2, -\tau_{3max}, \tau_4) \cdot kkt_2 \cdots \\
&\cdots f_e(-\tau_{1max}, \tau_2, \tau_{3max}, \tau_4) \cdot kkt_2; f_e(\tau_{1max}, \tau_2, -\tau_{3max}, \tau_4) \cdot kkt_2; \cdots \\
&\cdots f_e(\tau_{1max}, \tau_2, \tau_{3max}, \tau_4) \cdot kkt_2; f_e(-\tau_{1max}, \tau_2, \tau_3, -\tau_{4max}) \cdot kkt_3; \cdots \\
&\cdots f_e(-\tau_{1max}, \tau_2, \tau_3, \tau_{4max}) \cdot kkt_3; f_e(\tau_{1max}, \tau_2, \tau_3, -\tau_{4max}) \cdot kkt_3; \cdots \\
&\cdots f_e(\tau_{1max}, \tau_2, \tau_3, \tau_{4max}) \cdot kkt_3; f_e(\tau_1, -\tau_{2max}, -\tau_{3max}, \tau_4) \cdot kkt_4; \cdots \\
&\cdots f_e(\tau_1, -\tau_{2max}, \tau_{3max}, \tau_4) \cdot kkt_4; f_e(\tau_1, \tau_{2max}, -\tau_{3max}, \tau_4) \cdot kkt_4; \cdots \\
&\cdots f_e(\tau_1, \tau_{2max}, \tau_{3max}, \tau_4) \cdot kkt_4; f_e(\tau_1, -\tau_{2max}, \tau_3, -\tau_{4max}) \cdot kkt_5; \cdots \\
&\cdots f_e(\tau_1, -\tau_{2max}, \tau_3, \tau_{4max}) \cdot kkt_5; f_e(\tau_1, \tau_{2max}, \tau_3, -\tau_{4max}) \cdot kkt_5; \cdots \\
&\cdots f_e(\tau_1, \tau_{2max}, \tau_3, \tau_{4max}) \cdot kkt_5; f_e(\tau_1, \tau_2, -\tau_{3max}, -\tau_{4max}) \cdot kkt_6; \cdots \\
&\cdots f_e(\tau_1, \tau_2, -\tau_{3max}, \tau_{4max}) \cdot kkt_6; f_e(\tau_1, \tau_2, \tau_{3max}, -\tau_{4max}) \cdot kkt_6; \cdots \\
&\cdots f_e(\tau_1, \tau_2, \tau_{3max}, \tau_{4max}) \cdot kkt_6] \quad (4.62)
\end{aligned}
$$

where

$$
\begin{aligned}
f_e(\tau_1, \tau_2, \tau_3, \tau_4) = &\left((a_{1,1}\tau_1 + a_{1,2}\tau_2 + a_{1,3}\tau_3 + a_{1,4}\tau_4\right)^2 + \cdots \\
&\cdots + \left(a_{2,1}\tau_1 + a_{2,2}\tau_2 + a_{2,3}\tau_3 + a_{2,4}\tau_4\right)^2)^{\frac{1}{2}} \quad (4.63)
\end{aligned}
$$

$$
kkt_1 = \begin{cases} 1 & \Leftrightarrow \quad (-\tau_{3max} \le \tau_3 \le \tau_{3max}) \wedge (-\tau_{4max} \le \tau_4 \le \tau_{4max}) \\ 0 & \qquad otherwise \end{cases} \quad (4.64)
$$

$$
kkt_2 = \begin{cases} 1 & \Leftrightarrow \quad (-\tau_{2max} \le \tau_2 \le \tau_{2max}) \wedge (-\tau_{4max} \le \tau_4 \le \tau_{4max}) \\ 0 & \qquad otherwise \end{cases} \quad (4.65)
$$

$$
kkt_3 = \begin{cases} 1 & \Leftrightarrow \quad (-\tau_{2max} \le \tau_2 \le \tau_{2max}) \wedge (-\tau_{3max} \le \tau_3 \le \tau_{3max}) \\ 0 & \qquad otherwise \end{cases} \quad (4.66)
$$

$$
kkt_4 = \begin{cases} 1 & \Leftrightarrow \quad (-\tau_{1max} \le \tau_1 \le \tau_{1max}) \wedge (-\tau_{4max} \le \tau_4 \le \tau_{4max}) \\ 0 & \qquad otherwise \end{cases} \quad (4.67)
$$

$$kkt_5 = \begin{cases} 1 & \Leftrightarrow \quad (-\tau_{1max} \leq \tau_1 \leq \tau_{1max}) \wedge (-\tau_{3max} \leq \tau_3 \leq \tau_{3max}) \\ 0 & otherwise \end{cases} \tag{4.68}$$

$$kkt_6 = \begin{cases} 1 & \Leftrightarrow \quad (-\tau_{1max} \leq \tau_1 \leq \tau_{1max}) \wedge (-\tau_{2max} \leq \tau_2 \leq \tau_{2max}) \\ 0 & otherwise \end{cases} \tag{4.69}$$

In this solution, Eq. (4.62) is represented as the maximum value of 24 terms. Each term in Eq. (4.62) is obtained as the product of Eq. (4.63) (evaluated with different values of τ_1, τ_2, τ_3 and τ_4) and a penalization term (kkt_n) as shown in Eqs. (4.64) to (4.69).

To evaluate the 24 terms in Eq. (4.62), the components τ_1, τ_2, τ_3 and τ_4 need to be obtained as a function of the constant values of saturation ($\tau_{n_{max}}$), the desired moment at the end effector of the manipulator (M_{i_z}) and the desired angle of application of the force (θ) using Eqs. (4.70) to (4.81).

$$\tau_1(\tau_3, \tau_4, M_{i_z}, \theta) = \frac{(M_{i_z} - \tau_3\, a_{3,3} - \tau_4\, a_{3,4})\, v_b(\theta) + (\tau_3\, v_c(\theta) + \tau_4\, v_d(\theta))\, a_{3,2}}{a_{3,1}\, v_b(\theta) - a_{3,2}\, v_a(\theta)} \tag{4.70}$$

$$\tau_2(\tau_3, \tau_4, M_{i_z}, \theta) = \frac{(M_{i_z} - \tau_3\, a_{3,3} - \tau_4\, a_{3,4})\, v_a(\theta) + (\tau_3\, v_c(\theta) + \tau_4\, v_d(\theta))\, a_{3,1}}{a_{3,2}\, v_a(\theta) - a_{3,1}\, v_b(\theta)} \tag{4.71}$$

$$\tau_1(\tau_2, \tau_4, M_{i_z}, \theta) = \frac{(M_{i_z} - \tau_2\, a_{3,2} - \tau_4\, a_{3,4})\, v_c(\theta) + (\tau_2\, v_b(\theta) + \tau_4\, v_d(\theta))\, a_{3,3}}{a_{3,1}\, v_c(\theta) - a_{3,3}\, v_a(\theta)} \tag{4.72}$$

$$\tau_3(\tau_2, \tau_4, M_{i_z}, \theta) = \frac{(M_{i_z} - \tau_2\, a_{3,2} - \tau_4\, a_{3,4})\, v_a(\theta) + (\tau_2\, v_b(\theta) + \tau_4\, v_d(\theta))\, a_{3,1}}{a_{3,3}\, v_a(\theta) - a_{3,1}\, v_c(\theta)} \tag{4.73}$$

$$\tau_1(\tau_2, \tau_3, M_{i_z}, \theta) = \frac{(M_{i_z} - \tau_2\, a_{3,2} - \tau_3\, a_{3,3})\, v_d(\theta) + (\tau_2\, v_b(\theta) + \tau_3\, v_c(\theta))\, a_{3,4}}{a_{3,1}\, v_d(\theta) - a_{3,4}\, v_a(\theta)} \tag{4.74}$$

$$\tau_4(\tau_2,\tau_3,M_{i_z},\theta)=\frac{(M_{i_z}-\tau_2\,a_{3,2}-\tau_3\,a_{3,3})\,v_a(\theta)+(\tau_2\,v_b(\theta)+\tau_3\,v_c(\theta))\,a_{3,1}}{a_{3,4}\,v_a(\theta)-a_{3,1}\,v_d(\theta)} \tag{4.75}$$

$$\tau_2(\tau_1,\tau_4,M_{i_z},\theta)=\frac{(M_{i_z}-\tau_1\,a_{3,1}-\tau_4\,a_{3,4})\,v_c(\theta)+(\tau_1\,v_a(\theta)+\tau_4\,v_d(\theta))\,a_{3,3}}{a_{3,2}\,v_c(\theta)-a_{3,3}\,v_b(\theta)} \tag{4.76}$$

$$\tau_3(\tau_1,\tau_4,M_{i_z},\theta)=\frac{(M_{i_z}-\tau_1\,a_{3,1}-\tau_4\,a_{3,4})\,v_b(\theta)+(\tau_1\,v_a(\theta)+\tau_4\,v_d(\theta))\,a_{3,2}}{a_{3,3}\,v_b(\theta)-a_{3,2}\,v_c(\theta)} \tag{4.77}$$

$$\tau_2(\tau_1,\tau_3,M_{i_z},\theta)=\frac{(M_{i_z}-\tau_1\,a_{3,1}-\tau_3\,a_{3,3})\,v_d(\theta)+(\tau_1\,v_a(\theta)+\tau_3\,v_c(\theta))\,a_{3,4}}{a_{3,2}\,v_d(\theta)-a_{3,4}\,v_b(\theta)} \tag{4.78}$$

$$\tau_4(\tau_1,\tau_3,M_{i_z},\theta)=\frac{(M_{i_z}-\tau_1\,a_{3,1}-\tau_3\,a_{3,3})\,v_b(\theta)+(\tau_1\,v_a(\theta)+\tau_3\,v_c(\theta))\,a_{3,2}}{a_{3,4}\,v_b(\theta)-a_{3,2}\,v_d(\theta)} \tag{4.79}$$

$$\tau_3(\tau_1,\tau_2,M_{i_z},\theta)=\frac{(M_{i_z}-\tau_1\,a_{3,1}-\tau_2\,a_{3,2})\,v_d(\theta)+(\tau_1\,v_a(\theta)+\tau_2\,v_b(\theta))\,a_{3,4}}{a_{3,3}\,v_d(\theta)-a_{3,4}\,v_c(\theta)} \tag{4.80}$$

$$\tau_4(\tau_1,\tau_2,M_{i_z},\theta)=\frac{(M_{i_z}-\tau_1\,a_{3,1}-\tau_2\,a_{3,2})\,v_c(\theta)+(\tau_1\,v_a(\theta)+\tau_2\,v_b(\theta))\,a_{3,3}}{a_{3,4}\,v_c(\theta)-a_{3,3}\,v_d(\theta)} \tag{4.81}$$

The mathematical closed-form solution to obtain the force capability in manipulators with $C_N = 4$ presented herein represents another important result obtained in this study. It should be noted that the twelve kinematic variables $(a_{1,1}, ..., a_{3,4})$ were obtained from the solution of the direct static problem presented in Eq. (4.3), and the terms $v_a(\theta)$, $v_b(\theta)$, $v_c(\theta)$ and $v_d(\theta)$ are obtained as shown in Eqs. (4.82) to (4.85). At this point it is important to highlight that although variables $v_a(\theta)$ to $v_d(\theta)$ appeared previously in sections 4.3 and 4.4, in this section these variables assume new values as shown in Eqs. (4.82) to (4.85) in order to solve the force capability in manipulators with $C_N = 4$.

$$v_a(\theta) = a_{2,1} - a_{1,1}\tan(\theta) \quad (4.82)$$
$$v_b(\theta) = a_{2,2} - a_{1,2}\tan(\theta) \quad (4.83)$$
$$v_c(\theta) = a_{2,3} - a_{1,3}\tan(\theta) \quad (4.84)$$
$$v_d(\theta) = a_{2,4} - a_{1,4}\tan(\theta) \quad (4.85)$$

4.6 MATHEMATICAL CLOSED-FORM SOLUTION TO OBTAIN THE FORCE CAPABILITY IN MANIPULATORS WITH $C_N = 5$

In a similar way as in section 4.4 and 4.5, the mathematical closed-form solution to obtain the force capability in manipulators with $C_N = 5$ can be obtained by using an optimization process. In this section the mathematical closed-form solution to obtain the force capability in manipulators with $C_N = 5$ is presented directly as shown in Eqs. (4.86) to (4.122).

$$\begin{aligned} F_{app}(\theta, M_{i_z}) = \max[&f_{e_1}(\tau_1,\tau_2,\tau_3,\tau_4(\tau_1,\tau_2,\tau_3),\tau_5(\tau_1,\tau_2,\tau_3)) \cdot kkt_1; \cdots \\ &\cdots f_{e_2}(\tau_1,\tau_2,\tau_3(\tau_1,\tau_2,\tau_4),\tau_4,\tau_5(\tau_1,\tau_2,\tau_4)) \cdot kkt_2; \cdots \\ &\cdots f_{e_3}(\tau_1,\tau_2(\tau_1,\tau_3,\tau_4),\tau_3,\tau_4,\tau_5(\tau_1,\tau_3,\tau_4)) \cdot kkt_3; \cdots \\ &\cdots f_{e_4}(\tau_1(\tau_2,\tau_3,\tau_4),\tau_2,\tau_3,\tau_4,\tau_5(\tau_2,\tau_3,\tau_4)) \cdot kkt_4; \cdots \\ &\cdots f_{e_5}(\tau_1,\tau_2,\tau_3(\tau_1,\tau_2,\tau_5),\tau_4(\tau_1,\tau_2,\tau_5),\tau_5) \cdot kkt_5; \cdots \\ &\cdots f_{e_6}(\tau_1,\tau_2(\tau_1,\tau_3,\tau_5),\tau_3,\tau_4(\tau_1,\tau_3,\tau_5),\tau_5) \cdot kkt_6; \cdots \\ &\cdots f_{e_7}(\tau_1(\tau_2,\tau_3,\tau_5),\tau_2,\tau_3,\tau_4(\tau_2,\tau_3,\tau_5),\tau_5) \cdot kkt_7; \cdots \\ &\cdots f_{e_8}(\tau_1,\tau_2(\tau_1,\tau_4,\tau_5),\tau_3(\tau_1,\tau_4,\tau_5),\tau_4,\tau_5) \cdot kkt_8; \cdots \\ &\cdots f_{e_9}(\tau_1(\tau_2,\tau_4,\tau_5),\tau_2,\tau_3(\tau_2,\tau_4,\tau_5),\tau_4,\tau_5) \cdot kkt_9; \cdots \\ &\cdots f_{e_{10}}(\tau_1(\tau_3,\tau_4,\tau_5),\tau_2(\tau_3,\tau_4,\tau_5),\tau_3,\tau_4,\tau_5) \cdot kkt_{10}] \end{aligned} \quad (4.86)$$

where

$$\begin{aligned} f_{e_n}(\tau_1,\tau_2,\tau_3,\tau_4,\tau_5) = ((a_{1,1}\tau_1 + a_{1,2}\tau_2 + a_{1,3}\tau_3 + a_{1,4}\tau_4 + a_{1,5}\tau_5)^2 + \cdots \\ \cdots + (a_{2,1}\tau_1 + a_{2,2}\tau_2 + a_{2,3}\tau_3 + a_{2,4}\tau_4 + a_{2,5}\tau_5)^2)^{\frac{1}{2}} \end{aligned} \quad (4.87)$$

$$kkt_1 = \begin{cases} 1 & \Leftrightarrow \quad (-\tau_{4max} \leq \tau_4 \leq \tau_{4max}) \wedge (-\tau_{5max} \leq \tau_5 \leq \tau_{5max}) \\ 0 & otherwise \end{cases} \tag{4.88}$$

$$kkt_2 = \begin{cases} 1 & \Leftrightarrow \quad (-\tau_{3max} \leq \tau_3 \leq \tau_{3max}) \wedge (-\tau_{5max} \leq \tau_5 \leq \tau_{5max}) \\ 0 & otherwise \end{cases} \tag{4.89}$$

$$kkt_3 = \begin{cases} 1 & \Leftrightarrow \quad (-\tau_{2max} \leq \tau_2 \leq \tau_{2max}) \wedge (-\tau_{5max} \leq \tau_5 \leq \tau_{5max}) \\ 0 & otherwise \end{cases} \tag{4.90}$$

$$kkt_4 = \begin{cases} 1 & \Leftrightarrow \quad (-\tau_{1max} \leq \tau_1 \leq \tau_{1max}) \wedge (-\tau_{5max} \leq \tau_5 \leq \tau_{5max}) \\ 0 & otherwise \end{cases} \tag{4.91}$$

$$kkt_5 = \begin{cases} 1 & \Leftrightarrow \quad (-\tau_{3max} \leq \tau_3 \leq \tau_{3max}) \wedge (-\tau_{4max} \leq \tau_4 \leq \tau_{4max}) \\ 0 & otherwise \end{cases} \tag{4.92}$$

$$kkt_6 = \begin{cases} 1 & \Leftrightarrow \quad (-\tau_{2max} \leq \tau_2 \leq \tau_{2max}) \wedge (-\tau_{4max} \leq \tau_4 \leq \tau_{4max}) \\ 0 & otherwise \end{cases} \tag{4.93}$$

$$kkt_7 = \begin{cases} 1 & \Leftrightarrow \quad (-\tau_{1max} \leq \tau_1 \leq \tau_{1max}) \wedge (-\tau_{4max} \leq \tau_4 \leq \tau_{4max}) \\ 0 & otherwise \end{cases} \tag{4.94}$$

$$kkt_8 = \begin{cases} 1 & \Leftrightarrow \quad (-\tau_{2max} \leq \tau_2 \leq \tau_{2max}) \wedge (-\tau_{3max} \leq \tau_3 \leq \tau_{3max}) \\ 0 & otherwise \end{cases} \tag{4.95}$$

$$kkt_9 = \begin{cases} 1 & \Leftrightarrow \quad (-\tau_{1max} \leq \tau_1 \leq \tau_{1max}) \wedge (-\tau_{3max} \leq \tau_3 \leq \tau_{3max}) \\ 0 & otherwise \end{cases} \tag{4.96}$$

$$kkt_{10} = \begin{cases} 1 & \Leftrightarrow \quad (-\tau_{1max} \leq \tau_1 \leq \tau_{1max}) \wedge (-\tau_{2max} \leq \tau_2 \leq \tau_{2max}) \\ 0 & otherwise \end{cases} \tag{4.97}$$

In this solution, Eq. (4.86) is represented as the maximum value of 10 terms. Each term in Eq. (4.86) is obtained as the product of Eq. (4.87) evaluated with different values of saturation for τ_1, τ_2, τ_3, τ_4 and τ_5 and a penalization term (kkt_n) as shown in Eqs. (4.88) to (4.97). In order to exemplify the choose of the different values of saturation for the actuated joints τ_n, consider the first element in Eq. (4.86), where $f_{e_1}(\tau_1, \tau_2, \tau_3, \tau_4(\tau_1, \tau_2, \tau_3), \tau_5(\tau_1, \tau_2, \tau_3))$ is a composed function that needs to be evaluated by all the possible saturation values of τ_1, τ_2 and τ_3. The possible values of saturation for τ_1, τ_2 and τ_3 are shown in Table. 1, and the elements τ_4 and τ_5 need to be calculated as a function of these saturated elements and the imposed moment (M_{i_z}) and the desired direction (θ) as shown in Eqs. (4.116) and (4.117). The same process needs to be followed in order to evaluate all the elements in Eq. (4.86) but saturating the independent values τ_n for each element F_{e_n} in these equation.

Case	$\boldsymbol{\tau_1}$	$\boldsymbol{\tau_2}$	$\boldsymbol{\tau_3}$
1	$-\tau_{1max}$	$-\tau_{2max}$	$-\tau_{3max}$
2	$-\tau_{1max}$	$-\tau_{2max}$	τ_{3max}
3	$-\tau_{1max}$	τ_{2max}	$-\tau_{3max}$
4	$-\tau_{1max}$	τ_{2max}	τ_{3max}
5	τ_{1max}	$-\tau_{2max}$	$-\tau_{3max}$
6	τ_{1max}	$-\tau_{2max}$	τ_{3max}
7	τ_{1max}	τ_{2max}	$-\tau_{3max}$
8	τ_{1max}	τ_{2max}	τ_{3max}

Table 3 – Saturation values of τ_1, τ_2 and τ_3 in the first element of Eq. 4.86.

$$\tau_1(\tau_3, \tau_4, \tau_5, M_{i_z}, \theta) = \frac{(M_{i_z} - \tau_3\, a_{3,3} - \tau_4\, a_{3,4} - \tau_5\, a_{3,5})\, v_b(\theta)}{a_{3,1}\, v_b(\theta) - a_{3,2}\, v_a(\theta)} + \cdots$$
$$\cdots + \frac{(\tau_3\, v_c(\theta) + \tau_4\, v_d(\theta) + \tau_5\, v_e(\theta))\, a_{3,2}}{a_{3,1}\, v_b(\theta) - a_{3,2}\, v_a(\theta)} \tag{4.98}$$

$$\tau_2(\tau_3,\tau_4,\tau_5,M_{i_z},\theta) = \frac{(M_{i_z} - \tau_3\, a_{3,3} - \tau_4\, a_{3,4} - \tau_5\, a_{3,5})\, v_a(\theta)}{a_{3,2}\, v_a(\theta) - a_{3,1}\, v_b(\theta)} + \cdots$$
$$\cdots + \frac{(\tau_3\, v_c(\theta) + \tau_4\, v_d(\theta) + \tau_5\, v_e(\theta))\, a_{3,1}}{a_{3,2}\, v_a(\theta) - a_{3,1}\, v_b(\theta)} \quad (4.99)$$

$$\tau_1(\tau_2,\tau_4,\tau_5,M_{i_z},\theta) = \frac{(M_{i_z} - \tau_2\, a_{3,2} - \tau_4\, a_{3,4} - \tau_5\, a_{3,5})\, v_c(\theta)}{a_{3,1}\, v_c(\theta) - a_{3,3}\, v_a(\theta)} + \cdots$$
$$\cdots + \frac{(\tau_2\, v_b(\theta) + \tau_4\, v_d(\theta) + \tau_5\, v_e(\theta))\, a_{3,3}}{a_{3,1}\, v_c(\theta) - a_{3,3}\, v_a(\theta)} \quad (4.100)$$

$$\tau_3(\tau_2,\tau_4,\tau_5,M_{i_z},\theta) = \frac{(M_{i_z} - \tau_2\, a_{3,2} - \tau_4\, a_{3,4} - \tau_5\, a_{3,5})\, v_a(\theta)}{a_{3,3}\, v_a(\theta) - a_{3,1}\, v_c(\theta)} + \cdots$$
$$\cdots + \frac{(\tau_2\, v_b(\theta) + \tau_4\, v_d(\theta) + \tau_5\, v_e(\theta))\, a_{3,1}}{a_{3,3}\, v_a(\theta) - a_{3,1}\, v_c(\theta)} \quad (4.101)$$

$$\tau_1(\tau_2,\tau_3,\tau_5,M_{i_z},\theta) = \frac{(M_{i_z} - \tau_2\, a_{3,2} - \tau_3\, a_{3,3} - \tau_5\, a_{3,5})\, v_d(\theta)}{a_{3,1}\, v_d(\theta) - a_{3,4}\, v_a(\theta)} + \cdots$$
$$\cdots + \frac{(\tau_2\, v_b(\theta) + \tau_3\, v_c(\theta) + \tau_5\, v_e(\theta))\, a_{3,4}}{a_{3,1}\, v_d(\theta) - a_{3,4}\, v_a(\theta)} \quad (4.102)$$

$$\tau_4(\tau_2,\tau_3,\tau_5,M_{i_z},\theta) = \frac{(M_{i_z} - \tau_2\, a_{3,2} - \tau_3\, a_{3,3} - \tau_5\, a_{3,5})\, v_a(\theta)}{a_{3,4}\, v_a(\theta) - a_{3,1}\, v_d(\theta)} + \cdots$$
$$\cdots + \frac{(\tau_2\, v_b(\theta) + \tau_3\, v_c(\theta) + \tau_5\, v_e(\theta))\, a_{3,1}}{a_{3,4}\, v_a(\theta) - a_{3,1}\, v_d(\theta)} \quad (4.103)$$

$$\tau_1(\tau_2,\tau_3,\tau_4,M_{i_z},\theta) = \frac{(M_{i_z} - \tau_2\, a_{3,2} - \tau_3\, a_{3,3} - \tau_4\, a_{3,4})\, v_e(\theta)}{a_{3,1}\, v_e(\theta) - a_{3,5}\, v_a(\theta)} + \cdots$$
$$\cdots + \frac{(\tau_2\, v_b(\theta) + \tau_3\, v_c(\theta) + \tau_4\, v_d(\theta))\, a_{3,5}}{a_{3,1}\, v_e(\theta) - a_{3,5}\, v_a(\theta)} \quad (4.104)$$

$$\tau_5(\tau_2,\tau_3,\tau_4,M_{i_z},\theta) = \frac{(M_{i_z} - \tau_2\, a_{3,2} - \tau_3\, a_{3,3} - \tau_4\, a_{3,4})\, v_a(\theta)}{a_{3,5}\, v_a(\theta) - a_{3,1}\, v_e(\theta)} + \cdots$$
$$\cdots + \frac{(\tau_2\, v_b(\theta) + \tau_3\, v_c(\theta) + \tau_4\, v_d(\theta))\, a_{3,1}}{a_{3,5}\, v_a(\theta) - a_{3,1}\, v_e(\theta)} \quad (4.105)$$

$$\tau_2(\tau_1,\tau_4,\tau_5,M_{i_z},\theta) = \frac{(M_{i_z} - \tau_1\, a_{3,1} - \tau_4\, a_{3,4} - \tau_5\, a_{3,5})\, v_c(\theta)}{a_{3,2}\, v_c(\theta) - a_{3,3}\, v_b(\theta)} + \cdots$$
$$\cdots + \frac{(\tau_1\, v_a(\theta) + \tau_4\, v_d(\theta) + \tau_5\, v_e(\theta))\, a_{3,3}}{a_{3,2}\, v_c(\theta) - a_{3,3}\, v_b(\theta)} \quad (4.106)$$

$$\tau_3(\tau_1,\tau_4,\tau_5,M_{i_z},\theta) = \frac{(M_{i_z} - \tau_1\, a_{3,1} - \tau_4\, a_{3,4} - \tau_5\, a_{3,5})\, v_b(\theta)}{a_{3,3}\, v_b(\theta) - a_{3,2}\, v_c(\theta)} + \cdots$$
$$\cdots + \frac{(\tau_1\, v_a(\theta) + \tau_4\, v_d(\theta) + \tau_5\, v_e(\theta))\, a_{3,2}}{a_{3,3}\, v_b(\theta) - a_{3,2}\, v_c(\theta)} \quad (4.107)$$

$$\tau_2(\tau_1,\tau_3,\tau_5,M_{i_z},\theta) = \frac{(M_{i_z} - \tau_1\, a_{3,1} - \tau_3\, a_{3,3} - \tau_5\, a_{3,5})\, v_d(\theta)}{a_{3,2}\, v_d(\theta) - a_{3,4}\, v_b(\theta)} + \cdots$$
$$\cdots + \frac{(\tau_1\, v_a(\theta) + \tau_3\, v_c(\theta) + \tau_5\, v_e(\theta))\, a_{3,4}}{a_{3,2}\, v_d(\theta) - a_{3,4}\, v_b(\theta)} \quad (4.108)$$

$$\tau_4(\tau_1,\tau_3,\tau_5,M_{i_z},\theta) = \frac{(M_{i_z} - \tau_1\, a_{3,1} - \tau_3\, a_{3,3} - \tau_5\, a_{3,5})\, v_b(\theta)}{a_{3,4}\, v_b(\theta) - a_{3,2}\, v_d(\theta)} + \cdots$$
$$\cdots + \frac{(\tau_1\, v_a(\theta) + \tau_3\, v_c(\theta) + \tau_5\, v_e(\theta))\, a_{3,2}}{a_{3,4}\, v_b(\theta) - a_{3,2}\, v_d(\theta)} \quad (4.109)$$

$$\tau_2(\tau_1,\tau_3,\tau_4,M_{i_z},\theta) = \frac{(M_{i_z} - \tau_1\, a_{3,1} - \tau_3\, a_{3,3} - \tau_4\, a_{3,4})\, v_e(\theta)}{a_{3,2}\, v_e(\theta) - a_{3,5}\, v_b(\theta)} + \cdots$$
$$\cdots + \frac{(\tau_1\, v_a(\theta) + \tau_3\, v_c(\theta) + \tau_4\, v_d(\theta))\, a_{3,5}}{a_{3,2}\, v_e(\theta) - a_{3,5}\, v_b(\theta)} \quad (4.110)$$

$$\tau_5(\tau_1,\tau_3,\tau_4,M_{i_z},\theta) = \frac{(M_{i_z} - \tau_1\, a_{3,1} - \tau_3\, a_{3,3} - \tau_4\, a_{3,4})\, v_b(\theta)}{a_{3,5}\, v_b(\theta) - a_{3,2}\, v_e(\theta)} + \cdots$$
$$\cdots + \frac{(\tau_1\, v_a(\theta) + \tau_3\, v_c(\theta) + \tau_4\, v_d(\theta))\, a_{3,2}}{a_{3,5}\, v_b(\theta) - a_{3,2}\, v_e(\theta)} \quad (4.111)$$

$$\tau_3(\tau_1,\tau_2,\tau_5,M_{i_z},\theta) = \frac{(M_{i_z} - \tau_1\, a_{3,1} - \tau_2\, a_{3,2} - \tau_5\, a_{3,5})\, v_d(\theta)}{a_{3,3}\, v_d(\theta) - a_{3,4}\, v_c(\theta)} + \cdots$$
$$\cdots + \frac{(\tau_1\, v_a(\theta) + \tau_2\, v_b(\theta) + \tau_5\, v_e(\theta))\, a_{3,4}}{a_{3,3}\, v_d(\theta) - a_{3,4}\, v_c(\theta)} \quad (4.112)$$

$$\tau_4(\tau_1,\tau_2,\tau_5,M_{i_z},\theta)=\frac{(M_{i_z}\ -\tau_1\,a_{3,1}-\tau_2\,a_{3,2}-\tau_5\,a_{3,5})\,v_c(\theta)}{a_{3,4}\,v_c(\theta)-a_{3,3}\,v_d(\theta)}+\cdots$$
$$\cdots+\frac{(\tau_1\,v_a(\theta)+\tau_2\,v_b(\theta)+\tau_5\,v_e(\theta))\,a_{3,3}}{a_{3,4}\,v_c(\theta)-a_{3,3}\,v_d(\theta)} \quad (4.113)$$

$$\tau_3(\tau_1,\tau_2,\tau_4,M_{i_z},\theta)=\frac{(M_{i_z}-\tau_1\,a_{3,1}-\tau_2\,a_{3,2}-\tau_4\,a_{3,4})\,v_e(\theta)}{a_{3,3}\,v_e(\theta)-a_{3,5}\,v_c(\theta)}+\cdots$$
$$\cdots+\frac{(\tau_1\,v_a(\theta)+\tau_2\,v_b(\theta)+\tau_4\,v_d(\theta))\,a_{3,5}}{a_{3,3}\,v_e(\theta)-a_{3,5}\,v_c(\theta)} \quad (4.114)$$

$$\tau_5(\tau_1,\tau_2,\tau_4,M_{i_z},\theta)=\frac{(M_{i_z}-\tau_1\,a_{3,1}-\tau_2\,a_{3,2}-\tau_4\,a_{3,4})\,v_c(\theta)}{a_{3,5}\,v_c(\theta)-a_{3,3}\,v_e(\theta)}+\cdots$$
$$\cdots+\frac{(\tau_1\,v_a(\theta)+\tau_2\,v_b(\theta)+\tau_4\,v_d(\theta))\,a_{3,3}}{a_{3,5}\,v_c(\theta)-a_{3,3}\,v_e(\theta)} \quad (4.115)$$

$$\tau_4(\tau_1,\tau_2,\tau_3,M_{i_z},\theta)=\frac{(M_{i_z}-\tau_1\,a_{3,1}-\tau_2\,a_{3,2}-\tau_3\,a_{3,3})\,v_e(\theta)}{a_{3,4}\,v_e(\theta)-a_{3,5}\,v_d(\theta)}+\cdots$$
$$\cdots+\frac{(\tau_1\,v_a(\theta)+\tau_2\,v_b(\theta)+\tau_3\,v_c(\theta))\,a_{3,5}}{a_{3,4}\,v_e(\theta)-a_{3,5}\,v_d(\theta)} \quad (4.116)$$

$$\tau_5(\tau_1,\tau_2,\tau_3,M_{i_z},\theta)=\frac{(M_{i_z}-\tau_1\,a_{3,1}-\tau_2\,a_{3,2}-\tau_3\,a_{3,3})\,v_d(\theta)}{a_{3,5}\,v_d(\theta)-a_{3,4}\,v_e(\theta)}+\cdots$$
$$\cdots+\frac{(\tau_1\,v_a(\theta)+\tau_2\,v_b(\theta)+\tau_3\,v_c(\theta))\,a_{3,4}}{a_{3,5}\,v_d(\theta)-a_{3,4}\,v_e(\theta)} \quad (4.117)$$

The mathematical closed-form solution to obtain the force capability in manipulators with $C_N = 5$ presented herein represents another important result obtained in this study. It should be noted that the fifteen kinematic variables $(a_{1,1},...,a_{3,5})$ were obtained from the solution of the direct static problem presented in Eq. (4.4), and the terms $v_a(\theta)$, $v_b(\theta)$, $v_c(\theta)$, $v_d(\theta)$ and $v_e(\theta)$ are obtained as shown in Eqs. (4.118) to (4.122). At this point it is important to highlight that although variables $v_a(\theta)$ to $v_d(\theta)$ appeared previously in section 4.5, in this section these variables assume new values as shown in Eqs. (4.118) to (4.121) in order to solve the force capability in manipulators with $C_N = 5$.

$$v_a(\theta) = a_{2,1} - a_{1,1}\tan(\theta) \quad (4.118)$$
$$v_b(\theta) = a_{2,2} - a_{1,2}\tan(\theta) \quad (4.119)$$
$$v_c(\theta) = a_{2,3} - a_{1,3}\tan(\theta) \quad (4.120)$$
$$v_d(\theta) = a_{2,4} - a_{1,4}\tan(\theta) \quad (4.121)$$
$$v_e(\theta) = a_{2,5} - a_{1,5}\tan(\theta) \quad (4.122)$$

4.7 MATHEMATICAL CLOSED-FORM SOLUTION TO OBTAIN THE FORCE CAPABILITY IN MANIPULATORS WITH $C_N = 6$

Similarly as in Sections 4.4, 4.5 and 4.6, the mathematical closed-form solution to obtain the force capability in manipulators with $C_N = 6$ was obtained by using an optimization procedure. This section shows in a direct way the mathematical closed-form solution to obtain the force capability in manipulators with $C_N = 6$. This mathematical closed-form solution is presented in Eqs. (4.123) to (4.175).

$$\begin{aligned}
F_{app}(\theta, M_{i_z}) = \max[&f_{e_1}(\tau_1,\tau_2,\tau_3,\tau_4,\tau_5(\tau_1,\tau_2,\tau_3,\tau_4),\tau_6(\tau_1,\tau_2,\tau_3,\tau_4))\cdot kkt_1;\cdots\\
&\cdots f_{e_2}(\tau_1,\tau_2,\tau_3,\tau_4(\tau_1,\tau_2,\tau_3,\tau_5),\tau_5,\tau_6(\tau_1,\tau_2,\tau_3,\tau_5))\cdot kkt_2;\cdots\\
&\cdots f_{e_3}(\tau_1,\tau_2,\tau_3(\tau_1,\tau_2,\tau_4,\tau_5),\tau_4,\tau_5,\tau_6(\tau_1,\tau_2,\tau_4,\tau_5))\cdot kkt_3;\cdots\\
&\cdots f_{e_4}(\tau_1,\tau_2(\tau_1,\tau_3,\tau_4,\tau_5),\tau_3,\tau_4,\tau_5,\tau_6(\tau_1,\tau_3,\tau_4,\tau_5))\cdot kkt_4;\cdots\\
&\cdots f_{e_5}(\tau_1(\tau_2,\tau_3,\tau_4,\tau_5),\tau_2,\tau_3,\tau_4,\tau_5,\tau_6(\tau_2,\tau_3,\tau_4,\tau_5))\cdot kkt_5\cdots\\
&\cdots f_{e_6}(\tau_1,\tau_2,\tau_3,\tau_4(\tau_1,\tau_2,\tau_3,\tau_6),\tau_5(\tau_1,\tau_2,\tau_3,\tau_6),\tau_6)\cdot kkt_6;\cdots\\
&\cdots f_{e_7}(\tau_1,\tau_2,\tau_3(\tau_1,\tau_2,\tau_4,\tau_6),\tau_4,\tau_5(\tau_1,\tau_2,\tau_4,\tau_6),\tau_6)\cdot kkt_7;\cdots\\
&\cdots f_{e_8}(\tau_1,\tau_2(\tau_1,\tau_3,\tau_4,\tau_6),\tau_3,\tau_4,\tau_5(\tau_1,\tau_3,\tau_4,\tau_6),\tau_6)\cdot kkt_8;\cdots\\
&\cdots f_{e_9}(\tau_1(\tau_2,\tau_3,\tau_4,\tau_6),\tau_2,\tau_3,\tau_4,\tau_5(\tau_2,\tau_3,\tau_4,\tau_6),\tau_6)\cdot kkt_9;\cdots\\
&\cdots f_{e_{10}}(\tau_1,\tau_2,\tau_3(\tau_1,\tau_2,\tau_5,\tau_6),\tau_4(\tau_1,\tau_2,\tau_5,\tau_6),\tau_5,\tau_6)\cdot kkt_{10};\cdots\\
&\cdots f_{e_{11}}(\tau_1,\tau_2(\tau_1,\tau_3,\tau_5,\tau_6),\tau_3,\tau_4(\tau_1,\tau_3,\tau_5,\tau_6),\tau_5,\tau_6)\cdot kkt_{11};\cdots\\
&\cdots f_{e_{12}}(\tau_1(\tau_2,\tau_3,\tau_5,\tau_6),\tau_2,\tau_3,\tau_4(\tau_2,\tau_3,\tau_5,\tau_6),\tau_5,\tau_6)\cdot kkt_{12};\cdots\\
&\cdots f_{e_{13}}(\tau_1,\tau_2(\tau_1,\tau_4,\tau_5,\tau_6),\tau_3(\tau_1,\tau_4,\tau_5,\tau_6),\tau_4,\tau_5,\tau_6)\cdot kkt_{13};\cdots\\
&\cdots f_{e_{14}}(\tau_1(\tau_2,\tau_4,\tau_5,\tau_6),\tau_2,\tau_3(\tau_2,\tau_4,\tau_5,\tau_6),\tau_4,\tau_5,\tau_6)\cdot kkt_{14};\cdots\\
&\cdots f_{e_{15}}(\tau_1(\tau_3,\tau_4,\tau_5,\tau_6),\tau_2(\tau_3,\tau_4,\tau_5,\tau_6),\tau_3,\tau_4,\tau_5,\tau_6)\cdot kkt_{15}] \quad (4.123)
\end{aligned}$$

where

$$f_{e_n}(\tau_1,\tau_2,\tau_3,\tau_4,\tau_5,\tau_6) = ((a_{1,1}\tau_1+a_{1,2}\tau_2+a_{1,3}\tau_3+a_{1,4}\tau_4+a_{1,5}\tau_5+a_{1,6}\tau_6)^2+\cdots$$
$$\cdots+(a_{2,1}\tau_1+a_{2,2}\tau_2+a_{2,3}\tau_3+a_{2,4}\tau_4+a_{2,5}\tau_5+a_{2,6}\tau_6)^2)^{\frac{1}{2}} \quad (4.124)$$

$$kkt_1 = \begin{cases} 1 & \Leftrightarrow \quad (-\tau_{5max} \leq \tau_5 \leq \tau_{5max}) \wedge (-\tau_{6max} \leq \tau_6 \leq \tau_{6max}) \\ 0 & otherwise \end{cases} \quad (4.125)$$

$$kkt_2 = \begin{cases} 1 & \Leftrightarrow \quad (-\tau_{4max} \leq \tau_4 \leq \tau_{4max}) \wedge (-\tau_{6max} \leq \tau_6 \leq \tau_{6max}) \\ 0 & otherwise \end{cases} \quad (4.126)$$

$$kkt_3 = \begin{cases} 1 & \Leftrightarrow \quad (-\tau_{3max} \leq \tau_3 \leq \tau_{3max}) \wedge (-\tau_{6max} \leq \tau_6 \leq \tau_{6max}) \\ 0 & otherwise \end{cases} \quad (4.127)$$

$$kkt_4 = \begin{cases} 1 & \Leftrightarrow \quad (-\tau_{2max} \leq \tau_2 \leq \tau_{2max}) \wedge (-\tau_{6max} \leq \tau_6 \leq \tau_{6max}) \\ 0 & otherwise \end{cases} \quad (4.128)$$

$$kkt_5 = \begin{cases} 1 & \Leftrightarrow \quad (-\tau_{1max} \leq \tau_1 \leq \tau_{1max}) \wedge (-\tau_{6max} \leq \tau_6 \leq \tau_{6max}) \\ 0 & otherwise \end{cases} \quad (4.129)$$

$$kkt_6 = \begin{cases} 1 & \Leftrightarrow \quad (-\tau_{4max} \leq \tau_4 \leq \tau_{4max}) \wedge (-\tau_{5max} \leq \tau_5 \leq \tau_{5max}) \\ 0 & otherwise \end{cases} \quad (4.130)$$

$$kkt_7 = \begin{cases} 1 & \Leftrightarrow \quad (-\tau_{3max} \leq \tau_3 \leq \tau_{3max}) \wedge (-\tau_{5max} \leq \tau_5 \leq \tau_{5max}) \\ 0 & otherwise \end{cases} \quad (4.131)$$

$$kkt_8 = \begin{cases} 1 & \Leftrightarrow \quad (-\tau_{2max} \leq \tau_2 \leq \tau_{2max}) \wedge (-\tau_{5max} \leq \tau_5 \leq \tau_{5max}) \\ 0 & otherwise \end{cases} \quad (4.132)$$

$$kkt_9 = \begin{cases} 1 & \Leftrightarrow \quad (-\tau_{1max} \leq \tau_1 \leq \tau_{1max}) \wedge (-\tau_{5max} \leq \tau_5 \leq \tau_{5max}) \\ 0 & otherwise \end{cases} \tag{4.133}$$

$$kkt_{10} = \begin{cases} 1 & \Leftrightarrow \quad (-\tau_{3max} \leq \tau_3 \leq \tau_{3max}) \wedge (-\tau_{4max} \leq \tau_4 \leq \tau_{4max}) \\ 0 & otherwise \end{cases} \tag{4.134}$$

$$kkt_{11} = \begin{cases} 1 & \Leftrightarrow \quad (-\tau_{2max} \leq \tau_2 \leq \tau_{2max}) \wedge (-\tau_{4max} \leq \tau_4 \leq \tau_{4max}) \\ 0 & otherwise \end{cases} \tag{4.135}$$

$$kkt_{12} = \begin{cases} 1 & \Leftrightarrow \quad (-\tau_{1max} \leq \tau_1 \leq \tau_{1max}) \wedge (-\tau_{4max} \leq \tau_4 \leq \tau_{4max}) \\ 0 & otherwise \end{cases} \tag{4.136}$$

$$kkt_{13} = \begin{cases} 1 & \Leftrightarrow \quad (-\tau_{2max} \leq \tau_2 \leq \tau_{2max}) \wedge (-\tau_{3max} \leq \tau_3 \leq \tau_{3max}) \\ 0 & otherwise \end{cases} \tag{4.137}$$

$$kkt_{14} = \begin{cases} 1 & \Leftrightarrow \quad (-\tau_{1max} \leq \tau_1 \leq \tau_{1max}) \wedge (-\tau_{3max} \leq \tau_3 \leq \tau_{3max}) \\ 0 & otherwise \end{cases} \tag{4.138}$$

$$kkt_{15} = \begin{cases} 1 & \Leftrightarrow \quad (-\tau_{1max} \leq \tau_1 \leq \tau_{1max}) \wedge (-\tau_{2max} \leq \tau_2 \leq \tau_{2max}) \\ 0 & otherwise \end{cases} \tag{4.139}$$

In this new solution, Eq. (4.123) is represented as the maximum value of fifteen elements where each element in these equation is obtained as the product of Eq. (4.124) evaluated with different values of saturation for τ_1, τ_2, τ_3, τ_4, τ_5 and τ_6 and a penalization term (kkt_n) as shown in Eqs. (4.125) to (4.139). In order to exemplify the choose of the different values of saturation for the actuated joints τ_n, consider the first element in Eq. (4.123) similarly as was done in Section 4.6, where $f_{e_1}(\tau_1, \tau_2, \tau_3, \tau_4, \tau_5(\tau_1, \tau_2, \tau_3, \tau_4), \tau_6(\tau_1, \tau_2, \tau_3, \tau_4))$ is a composed function that needs to be evaluated by all the possible saturation values of τ_1, τ_2, τ_3 and τ_4. The possible values of saturation for τ_1, τ_2, τ_3 and τ_4 are shown in Table. 2, and the elements τ_5 and τ_6 need to be calculated as a function of these saturated elements and the imposed

moment (M_{i_z}) and the desired direction (θ) as shown in Eqs. (4.168) and (4.169). The same process needs to be followed in order to evaluate all the elements in Eq. (4.123) but saturating the independent values τ_n for each element f_{e_n} in these equation.

Case	$\boldsymbol{\tau_1}$	$\boldsymbol{\tau_2}$	$\boldsymbol{\tau_3}$	$\boldsymbol{\tau_4}$
1	$-\tau_{1max}$	$-\tau_{2max}$	$-\tau_{3max}$	$-\tau_{4max}$
2	$-\tau_{1max}$	$-\tau_{2max}$	$-\tau_{3max}$	τ_{4max}
3	$-\tau_{1max}$	$-\tau_{2max}$	τ_{3max}	$-\tau_{4max}$
4	$-\tau_{1max}$	$-\tau_{2max}$	τ_{3max}	τ_{4max}
5	$-\tau_{1max}$	τ_{2max}	$-\tau_{3max}$	$-\tau_{4max}$
6	$-\tau_{1max}$	τ_{2max}	$-\tau_{3max}$	τ_{4max}
7	$-\tau_{1max}$	τ_{2max}	τ_{3max}	$-\tau_{4max}$
8	$-\tau_{1max}$	τ_{2max}	τ_{3max}	τ_{4max}
9	τ_{1max}	$-\tau_{2max}$	$-\tau_{3max}$	$-\tau_{4max}$
10	τ_{1max}	$-\tau_{2max}$	$-\tau_{3max}$	τ_{4max}
11	τ_{1max}	$-\tau_{2max}$	τ_{3max}	$-\tau_{4max}$
12	τ_{1max}	$-\tau_{2max}$	τ_{3max}	τ_{4max}
13	τ_{1max}	τ_{2max}	$-\tau_{3max}$	$-\tau_{4max}$
14	τ_{1max}	τ_{2max}	$-\tau_{3max}$	τ_{4max}
15	τ_{1max}	τ_{2max}	τ_{3max}	$-\tau_{4max}$
16	τ_{1max}	τ_{2max}	τ_{3max}	τ_{4max}

Table 4 – Saturation values of τ_1, τ_2, τ_3 and τ_4 in the first element of Eq. 4.123.

$$\tau_1(\tau_3,\tau_4,\tau_5,\tau_6,M_{i_z},\theta) = \frac{(M_{i_z} - \tau_3\, a_{3,3} - \tau_4\, a_{3,4} - \tau_5\, a_{3,5} - \tau_6\, a_{3,6})\, v_b(\theta)}{a_{3,1}\, v_b(\theta) - a_{3,2}\, v_a(\theta)} + \cdots$$
$$\cdots + \frac{(\tau_3\, v_c(\theta) + \tau_4\, v_d(\theta) + \tau_5\, v_e(\theta) + \tau_6\, v_f(\theta))\, a_{3,2}}{a_{3,1}\, v_b(\theta) - a_{3,2}\, v_a(\theta)} \quad (4.140)$$

$$\tau_2(\tau_3,\tau_4,\tau_5,\tau_6,M_{i_z},\theta) = \frac{(M_{i_z} - \tau_3\, a_{3,3} - \tau_4\, a_{3,4} - \tau_5\, a_{3,5} - \tau_6\, a_{3,6})\, v_a(\theta)}{a_{3,2}\, v_a(\theta) - a_{3,1}\, v_b(\theta)} + \cdots$$
$$\cdots + \frac{(\tau_3\, v_c(\theta) + \tau_4\, v_d(\theta) + \tau_5\, v_e(\theta) + \tau_6\, v_f(\theta))\, a_{3,1}}{a_{3,2}\, v_a(\theta) - a_{3,1}\, v_b(\theta)} \quad (4.141)$$

$$\tau_1(\tau_2,\tau_4,\tau_5,\tau_6,M_{i_z},\theta) = \frac{(M_{i_z} - \tau_2\, a_{3,2} - \tau_4\, a_{3,4} - \tau_5\, a_{3,5} - \tau_6\, a_{3,6})\, v_c(\theta)}{a_{3,1}\, v_c(\theta) - a_{3,3}\, v_a(\theta)} + \cdots$$
$$\cdots + \frac{(\tau_2\, v_b(\theta) + \tau_4\, v_d(\theta) + \tau_5\, v_e(\theta) + \tau_6\, v_f(\theta))\, a_{3,3}}{a_{3,1}\, v_c(\theta) - a_{3,3}\, v_a(\theta)} \quad (4.142)$$

$$\tau_3(\tau_2,\tau_4,\tau_5,\tau_6,M_{i_z},\theta) = \frac{(M_{i_z} - \tau_2\, a_{3,2} - \tau_4\, a_{3,4} - \tau_5\, a_{3,5} - \tau_6\, a_{3,6})\, v_a(\theta)}{a_{3,3}\, v_a(\theta) - a_{3,1}\, v_c(\theta)} + \cdots$$
$$\cdots + \frac{(\tau_2\, v_b(\theta) + \tau_4\, v_d(\theta) + \tau_5\, v_e(\theta) + \tau_6\, v_f(\theta))\, a_{3,1}}{a_{3,3}\, v_a(\theta) - a_{3,1}\, v_c(\theta)} \quad (4.143)$$

$$\tau_1(\tau_2,\tau_3,\tau_5,\tau_6,M_{i_z},\theta) = \frac{(M_{i_z} - \tau_2\, a_{3,2} - \tau_3\, a_{3,3} - \tau_5\, a_{3,5} - \tau_6\, a_{3,6})\, v_d(\theta)}{a_{3,1}\, v_d(\theta) - a_{3,4}\, v_a(\theta)} + \cdots$$
$$\cdots + \frac{(\tau_2\, v_b(\theta) + \tau_3\, v_c(\theta) + \tau_5\, v_e(\theta) + \tau_6\, v_f(\theta))\, a_{3,4}}{a_{3,1}\, v_d(\theta) - a_{3,4}\, v_a(\theta)} \quad (4.144)$$

$$\tau_4(\tau_2,\tau_3,\tau_5,\tau_6,M_{i_z},\theta) = \frac{(M_{i_z} - \tau_2\, a_{3,2} - \tau_3\, a_{3,3} - \tau_5\, a_{3,5} - \tau_6\, a_{3,6})\, v_a(\theta)}{a_{3,4}\, v_a(\theta) - a_{3,1}\, v_d(\theta)} + \cdots$$
$$\cdots + \frac{(\tau_2\, v_b(\theta) + \tau_3\, v_c(\theta) + \tau_5\, v_e(\theta) + \tau_6\, v_f(\theta))\, a_{3,1}}{a_{3,4}\, v_a(\theta) - a_{3,1}\, v_d(\theta)} \quad (4.145)$$

$$\tau_1(\tau_2,\tau_3,\tau_4,\tau_6,M_{i_z},\theta) = \frac{(M_{i_z} - \tau_2\, a_{3,2} - \tau_3\, a_{3,3} - \tau_4\, a_{3,4} - \tau_6\, a_{3,6})\, v_e(\theta)}{a_{3,1}\, v_e(\theta) - a_{3,5}\, v_a(\theta)} + \cdots$$
$$\cdots + \frac{(\tau_2\, v_b(\theta) + \tau_3\, v_c(\theta) + \tau_4\, v_d(\theta) + \tau_6\, v_f(\theta))\, a_{3,5}}{a_{3,1}\, v_e(\theta) - a_{3,5}\, v_a(\theta)} \quad (4.146)$$

$$\tau_5(\tau_2,\tau_3,\tau_4,\tau_6,M_{i_z},\theta) = \frac{(M_{i_z} - \tau_2\, a_{3,2} - \tau_3\, a_{3,3} - \tau_4\, a_{3,4} - \tau_6\, a_{3,6})\, v_a(\theta)}{a_{3,5}\, v_a(\theta) - a_{3,1}\, v_e(\theta)} + \cdots$$
$$\cdots + \frac{(\tau_2\, v_b(\theta) + \tau_3\, v_c(\theta) + \tau_4\, v_d(\theta) + \tau_6\, v_f(\theta))\, a_{3,1}}{a_{3,5}\, v_a(\theta) - a_{3,1}\, v_e(\theta)} \quad (4.147)$$

$$\tau_1(\tau_2,\tau_3,\tau_4,\tau_5,M_{i_z},\theta) = \frac{(M_{i_z} - \tau_2\, a_{3,2} - \tau_3\, a_{3,3} - \tau_4\, a_{3,4} - \tau_5\, a_{3,5})\, v_f(\theta)}{a_{3,1}\, v_f(\theta) - a_{3,6}\, v_a(\theta)} + \cdots$$
$$\cdots + \frac{(\tau_2\, v_b(\theta) + \tau_3\, v_c(\theta) + \tau_4\, v_d(\theta) + \tau_5\, v_e(\theta))\, a_{3,6}}{a_{3,1}\, v_f(\theta) - a_{3,6}\, v_a(\theta)} \quad (4.148)$$

$$\tau_6(\tau_2,\tau_3,\tau_4,\tau_5,M_{i_z},\theta)=\frac{(M_{i_z}-\tau_2\,a_{3,2}-\tau_3\,a_{3,3}-\tau_4\,a_{3,4}-\tau_5\,a_{3,5})\,v_a(\theta)}{a_{3,6}\,v_a(\theta)-a_{3,1}\,v_f(\theta)}+\cdots$$
$$\cdots+\frac{(\tau_2\,v_b(\theta)+\tau_3\,v_c(\theta)+\tau_4\,v_d(\theta)+\tau_5\,v_e(\theta))\,a_{3,1}}{a_{3,6}\,v_a(\theta)-a_{3,1}\,v_f(\theta)} \quad (4.149)$$

$$\tau_2(\tau_1,\tau_4,\tau_5,\tau_6,M_{i_z},\theta)=\frac{(M_{i_z}-\tau_1\,a_{3,1}-\tau_4\,a_{3,4}-\tau_5\,a_{3,5}-\tau_6\,a_{3,6})\,v_c(\theta)}{a_{3,2}\,v_c(\theta)-a_{3,3}\,v_b(\theta)}+\cdots$$
$$\cdots+\frac{(\tau_1\,v_a(\theta)+\tau_4\,v_d(\theta)+\tau_5\,v_e(\theta)+\tau_6\,v_f(\theta))\,a_{3,3}}{a_{3,2}\,v_c(\theta)-a_{3,3}\,v_b(\theta)} \quad (4.150)$$

$$\tau_3(\tau_1,\tau_4,\tau_5,\tau_6,M_{i_z},\theta)=\frac{(M_{i_z}-\tau_1\,a_{3,1}-\tau_4\,a_{3,4}-\tau_5\,a_{3,5}-\tau_6\,a_{3,6})\,v_b(\theta)}{a_{3,3}\,v_b(\theta)-a_{3,2}\,v_c(\theta)}+\cdots$$
$$\cdots+\frac{(\tau_1\,v_a(\theta)+\tau_4\,v_d(\theta)+\tau_5\,v_e(\theta)+\tau_6\,v_f(\theta))\,a_{3,2}}{a_{3,3}\,v_b(\theta)-a_{3,2}\,v_c(\theta)} \quad (4.151)$$

$$\tau_2(\tau_1,\tau_3,\tau_5,\tau_6,M_{i_z},\theta)=\frac{(M_{i_z}-\tau_1\,a_{3,1}-\tau_3\,a_{3,3}-\tau_5\,a_{3,5}-\tau_6\,a_{3,6})\,v_d(\theta)}{a_{3,2}\,v_d(\theta)-a_{3,4}\,v_b(\theta)}+\cdots$$
$$\cdots+\frac{(\tau_1\,v_a(\theta)+\tau_3\,v_c(\theta)+\tau_5\,v_e(\theta)+\tau_6\,v_f(\theta))\,a_{3,4}}{a_{3,2}\,v_d(\theta)-a_{3,4}\,v_b(\theta)} \quad (4.152)$$

$$\tau_4(\tau_1,\tau_3,\tau_5,\tau_6,M_{i_z},\theta)=\frac{(M_{i_z}-\tau_1\,a_{3,1}-\tau_3\,a_{3,3}-\tau_5\,a_{3,5}-\tau_6\,a_{3,6})\,v_b(\theta)}{a_{3,4}\,v_b(\theta)-a_{3,2}\,v_d(\theta)}+\cdots$$
$$\cdots+\frac{(\tau_1\,v_a(\theta)+\tau_3\,v_c(\theta)+\tau_5\,v_e(\theta)+\tau_6\,v_f(\theta))\,a_{3,2}}{a_{3,4}\,v_b(\theta)-a_{3,2}\,v_d(\theta)} \quad (4.153)$$

$$\tau_2(\tau_1,\tau_3,\tau_4,\tau_6,M_{i_z},\theta)=\frac{(M_{i_z}-\tau_1\,a_{3,1}-\tau_3\,a_{3,3}-\tau_4\,a_{3,4}-\tau_6\,a_{3,6})\,v_e(\theta)}{a_{3,2}\,v_e(\theta)-a_{3,5}\,v_b(\theta)}+\cdots$$
$$\cdots+\frac{(\tau_1\,v_a(\theta)+\tau_3\,v_c(\theta)+\tau_4\,v_d(\theta)+\tau_6\,v_f(\theta))\,a_{3,5}}{a_{3,2}\,v_e(\theta)-a_{3,5}\,v_b(\theta)} \quad (4.154)$$

$$\tau_5(\tau_1,\tau_3,\tau_4,\tau_6,M_{i_z},\theta)=\frac{(M_{i_z}-\tau_1\,a_{3,1}-\tau_3\,a_{3,3}-\tau_4\,a_{3,4}-\tau_6\,a_{3,6})\,v_b(\theta)}{a_{3,5}\,v_b(\theta)-a_{3,2}\,v_e(\theta)}+\cdots$$
$$\cdots+\frac{(\tau_1\,v_a(\theta)+\tau_3\,v_c(\theta)+\tau_4\,v_d(\theta)+\tau_6\,v_f(\theta))\,a_{3,2}}{a_{3,5}\,v_b(\theta)-a_{3,2}\,v_e(\theta)} \quad (4.155)$$

$$\tau_2(\tau_1,\tau_3,\tau_4,\tau_5,M_{i_z},\theta) = \frac{(M_{i_z} - \tau_1\, a_{3,1} - \tau_3\, a_{3,3} - \tau_4\, a_{3,4} - \tau_5\, a_{3,5})\, v_f(\theta)}{a_{3,2}\, v_f(\theta) - a_{3,6}\, v_b(\theta)} + \cdots$$
$$\cdots + \frac{(\tau_1\, v_a(\theta) + \tau_3\, v_c(\theta) + \tau_4\, v_d(\theta) + \tau_5\, v_e(\theta))\, a_{3,6}}{a_{3,2}\, v_f(\theta) - a_{3,6}\, v_b(\theta)} \quad (4.156)$$

$$\tau_6(\tau_1,\tau_3,\tau_4,\tau_5,M_{i_z},\theta) = \frac{(M_{i_z} - \tau_1\, a_{3,1} - \tau_3\, a_{3,3} - \tau_4\, a_{3,4} - \tau_5\, a_{3,5})\, v_b(\theta)}{a_{3,6}\, v_b(\theta) - a_{3,2}\, v_f(\theta)} + \cdots$$
$$\cdots + \frac{(\tau_1\, v_a(\theta) + \tau_3\, v_c(\theta) + \tau_4\, v_d(\theta) + \tau_5\, v_e(\theta))\, a_{3,2}}{a_{3,6}\, v_b(\theta) - a_{3,2}\, v_f(\theta)} \quad (4.157)$$

$$\tau_3(\tau_1,\tau_2,\tau_5,\tau_6,M_{i_z},\theta) = \frac{(M_{i_z} - \tau_1\, a_{3,1} - \tau_2\, a_{3,2} - \tau_5\, a_{3,5} - \tau_6\, a_{3,6})\, v_d(\theta)}{a_{3,3}\, v_d(\theta) - a_{3,4}\, v_c(\theta)} + \cdots$$
$$\cdots + \frac{(\tau_1\, v_a(\theta) + \tau_2\, v_b(\theta) + \tau_5\, v_e(\theta) + \tau_6\, v_f(\theta))\, a_{3,4}}{a_{3,3}\, v_d(\theta) - a_{3,4}\, v_c(\theta)} \quad (4.158)$$

$$\tau_4(\tau_1,\tau_2,\tau_5,\tau_6,M_{i_z},\theta) = \frac{(M_{i_z} - \tau_1\, a_{3,1} - \tau_2\, a_{3,2} - \tau_5\, a_{3,5} - \tau_6\, a_{3,6})\, v_c(\theta)}{a_{3,4}\, v_c(\theta) - a_{3,3}\, v_d(\theta)} + \cdots$$
$$\cdots + \frac{(\tau_1\, v_a(\theta) + \tau_2\, v_b(\theta) + \tau_5\, v_e(\theta) + \tau_6\, v_f(\theta))\, a_{3,3}}{a_{3,4}\, v_c(\theta) - a_{3,3}\, v_d(\theta)} \quad (4.159)$$

$$\tau_3(\tau_1,\tau_2,\tau_4,\tau_6,M_{i_z},\theta) = \frac{(M_{i_z} - \tau_1\, a_{3,1} - \tau_2\, a_{3,2} - \tau_4\, a_{3,4} - \tau_6\, a_{3,6})\, v_e(\theta)}{a_{3,3}\, v_e(\theta) - a_{3,5}\, v_c(\theta)} + \cdots$$
$$\cdots + \frac{(\tau_1\, v_a(\theta) + \tau_2\, v_b(\theta) + \tau_4\, v_d(\theta) + \tau_6\, v_f(\theta))\, a_{3,5}}{a_{3,3}\, v_e(\theta) - a_{3,5}\, v_c(\theta)} \quad (4.160)$$

$$\tau_5(\tau_1,\tau_2,\tau_4,\tau_6,M_{i_z},\theta) = \frac{(M_{i_z} - \tau_1\, a_{3,1} - \tau_2\, a_{3,2} - \tau_4\, a_{3,4} - \tau_6\, a_{3,6})\, v_c(\theta)}{a_{3,5}\, v_c(\theta) - a_{3,3}\, v_e(\theta)} + \cdots$$
$$\cdots + \frac{(\tau_1\, v_a(\theta) + \tau_2\, v_b(\theta) + \tau_4\, v_d(\theta) + \tau_6\, v_f(\theta))\, a_{3,3}}{a_{3,5}\, v_c(\theta) - a_{3,3}\, v_e(\theta)} \quad (4.161)$$

$$\tau_3(\tau_1,\tau_2,\tau_4,\tau_5,M_{i_z},\theta) = \frac{(M_{i_z} - \tau_1\, a_{3,1} - \tau_2\, a_{3,2} - \tau_4\, a_{3,4} - \tau_5\, a_{3,5})\, v_f(\theta)}{a_{3,3}\, v_f(\theta) - a_{3,6}\, v_c(\theta)} + \cdots$$
$$\cdots + \frac{(\tau_1\, v_a(\theta) + \tau_2\, v_b(\theta) + \tau_4\, v_d(\theta) + \tau_5\, v_e(\theta))\, a_{3,6}}{a_{3,3}\, v_f(\theta) - a_{3,6}\, v_c(\theta)} \quad (4.162)$$

$$\tau_6(\tau_1,\tau_2,\tau_4,\tau_5,M_{i_z},\theta)=\frac{(M_{i_z}-\tau_1\,a_{3,1}-\tau_2\,a_{3,2}-\tau_4\,a_{3,4}-\tau_5\,a_{3,5})\,v_c(\theta)}{a_{3,6}\,v_c(\theta)-a_{3,3}\,v_f(\theta)}+\cdots$$
$$\cdots+\frac{(\tau_1\,v_a(\theta)+\tau_2\,v_b(\theta)+\tau_4\,v_d(\theta)+\tau_5\,v_e(\theta))\,a_{3,3}}{a_{3,6}\,v_c(\theta)-a_{3,3}\,v_f(\theta)} \quad (4.163)$$

$$\tau_4(\tau_1,\tau_2,\tau_3,\tau_6,M_{i_z},\theta)=\frac{(M_{i_z}-\tau_1\,a_{3,1}-\tau_2\,a_{3,2}-\tau_3\,a_{3,3}-\tau_6\,a_{3,6})\,v_e(\theta)}{a_{3,4}\,v_e(\theta)-a_{3,5}\,v_d(\theta)}+\cdots$$
$$\cdots+\frac{(\tau_1\,v_a(\theta)+\tau_2\,v_b(\theta)+\tau_3\,v_c(\theta)+\tau_6\,v_f(\theta))\,a_{3,5}}{a_{3,4}\,v_e(\theta)-a_{3,5}\,v_d(\theta)} \quad (4.164)$$

$$\tau_5(\tau_1,\tau_2,\tau_3,\tau_6,M_{i_z},\theta)=\frac{(M_{i_z}-\tau_1\,a_{3,1}-\tau_2\,a_{3,2}-\tau_3\,a_{3,3}-\tau_6\,a_{3,6})\,v_d(\theta)}{a_{3,5}\,v_d(\theta)-a_{3,4}\,v_e(\theta)}+\cdots$$
$$\cdots+\frac{(\tau_1\,v_a(\theta)+\tau_2\,v_b(\theta)+\tau_3\,v_c(\theta)+\tau_6\,v_f(\theta))\,a_{3,4}}{a_{3,5}\,v_d(\theta)-a_{3,4}\,v_e(\theta)} \quad (4.165)$$

$$\tau_4(\tau_1,\tau_2,\tau_3,\tau_5,M_{i_z},\theta)=\frac{(M_{i_z}-\tau_1\,a_{3,1}-\tau_2\,a_{3,2}-\tau_3\,a_{3,3}-\tau_5\,a_{3,5})\,v_f(\theta)}{a_{3,4}\,v_f(\theta)-a_{3,6}\,v_d(\theta)}+\cdots$$
$$\cdots+\frac{(\tau_1\,v_a(\theta)+\tau_2\,v_b(\theta)+\tau_3\,v_c(\theta)+\tau_5\,v_e(\theta))\,a_{3,6}}{a_{3,4}\,v_f(\theta)-a_{3,6}\,v_d(\theta)} \quad (4.166)$$

$$\tau_6(\tau_1,\tau_2,\tau_3,\tau_5,M_{i_z},\theta)=\frac{(M_{i_z}-\tau_1\,a_{3,1}-\tau_2\,a_{3,2}-\tau_3\,a_{3,3}-\tau_5\,a_{3,5})\,v_d(\theta)}{a_{3,6}\,v_d(\theta)-a_{3,4}\,v_f(\theta)}+\cdots$$
$$\cdots+\frac{(\tau_1\,v_a(\theta)+\tau_2\,v_b(\theta)+\tau_3\,v_c(\theta)+\tau_5\,v_e(\theta))\,a_{3,4}}{a_{3,6}\,v_d(\theta)-a_{3,4}\,v_f(\theta)} \quad (4.167)$$

$$\tau_5(\tau_1,\tau_2,\tau_3,\tau_4,M_{i_z},\theta)=\frac{(M_{i_z}-\tau_1\,a_{3,1}-\tau_2\,a_{3,2}-\tau_3\,a_{3,3}-\tau_4\,a_{3,4})\,v_f(\theta)}{a_{3,5}\,v_f(\theta)-a_{3,6}\,v_e(\theta)}+\cdots$$
$$\cdots+\frac{(\tau_1\,v_a(\theta)+\tau_2\,v_b(\theta)+\tau_3\,v_c(\theta)+\tau_4\,v_d(\theta))\,a_{3,6}}{a_{3,5}\,v_f(\theta)-a_{3,6}\,v_e(\theta)} \quad (4.168)$$

$$\tau_6(\tau_1,\tau_2,\tau_3,\tau_4,M_{i_z},\theta)=\frac{(M_{i_z}-\tau_1\,a_{3,1}-\tau_2\,a_{3,2}-\tau_3\,a_{3,3}-\tau_4\,a_{3,4})\,v_e(\theta)}{a_{3,6}\,v_e(\theta)-a_{3,5}\,v_f(\theta)}+\cdots$$
$$\cdots+\frac{(\tau_1\,v_a(\theta)+\tau_2\,v_b(\theta)+\tau_3\,v_c(\theta)+\tau_4\,v_d(\theta))\,a_{3,5}}{a_{3,6}\,v_e(\theta)-a_{3,5}\,v_f(\theta)} \quad (4.169)$$

The mathematical closed-form solution to obtain the force capability in manipulators with $C_N = 6$ presented herein represents the last important result obtained in this chapter. It should be noted that the eighteen kinematic variables $(a_{1,1}, ..., a_{3,6})$ were obtained from the solution of the direct static problem presented in Eq. (4.5), and the terms $v_a(\theta)$, $v_b(\theta)$, $v_c(\theta)$, $v_d(\theta)$, $v_e(\theta)$ and $v_f(\theta)$ are obtained now as shown in Eqs. (4.170) to (4.175). Similarly as in the previous sections, it is important to highlight that although variables $v_a(\theta)$ to $v_e(\theta)$ appeared previously, in this section these variables assume new values as shown in Eqs. (4.170) to (4.174) in order to solve the force capability in manipulators with $C_N = 6$.

$$v_a(\theta) = a_{2,1} - a_{1,1}\tan(\theta) \quad (4.170)$$
$$v_b(\theta) = a_{2,2} - a_{1,2}\tan(\theta) \quad (4.171)$$
$$v_c(\theta) = a_{2,3} - a_{1,3}\tan(\theta) \quad (4.172)$$
$$v_d(\theta) = a_{2,4} - a_{1,4}\tan(\theta) \quad (4.173)$$
$$v_e(\theta) = a_{2,5} - a_{1,5}\tan(\theta) \quad (4.174)$$
$$v_f(\theta) = a_{2,6} - a_{1,6}\tan(\theta) \quad (4.175)$$

4.8 APPLICATIONS AND RESULTS OF THE PROPOSED CLOSED-FORM SOLUTIONS

To validate the mathematical closed-form solutions proposed in this chapter six cases were studied, the first is a non-redundantly-actuated 3$\underline{\text{R}}$RR planar parallel manipulator, the second is a redundantly-actuated 4$\underline{\text{R}}$RR planar parallel manipulator, the third is a redundantly-actuated 5$\underline{\text{R}}$RR planar parallel manipulator, the fourth is a redundantly-actuated 6$\underline{\text{R}}$RR planar parallel manipulator, the fifth is a redundantly-actuated 3$\underline{\text{RR}}$R planar parallel manipulator with three of its passive joints actuated, and finally, the sixth is a non-redundantly-actuated 3R$\underline{\text{P}}$R planar parallel manipulator. The first four planar parallel manipulators studied herein were shown in Figs. 19(a), 19(b), 19(c) and 19(d) respectively, the fifth studied manipulator is shown in Fig. 21 and the sixth studied manipulator is shown in Fig. 22. In these parallel manipulators, the fixed and moving platforms are formed by regular polygons with 3, 4, 5 and 6 sides joined by using the same number of legs. Each leg has three rotational joints whose axes are perpendicular to the $(x - y)$ plane, and some of their joints in each leg are actuated

according to its net degree of constraint (C_N).

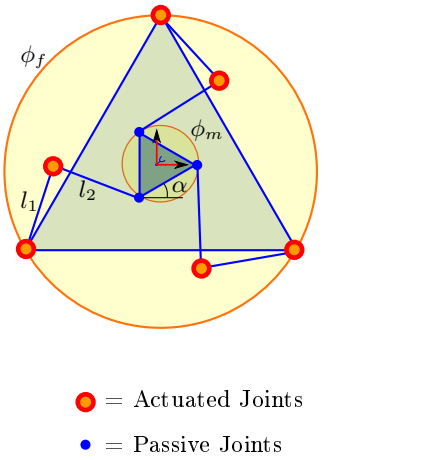

Figure 21 – Redundantly-actuated 3$\underline{\text{R}}$RR planar parallel manipulator ($C_N = 6$).

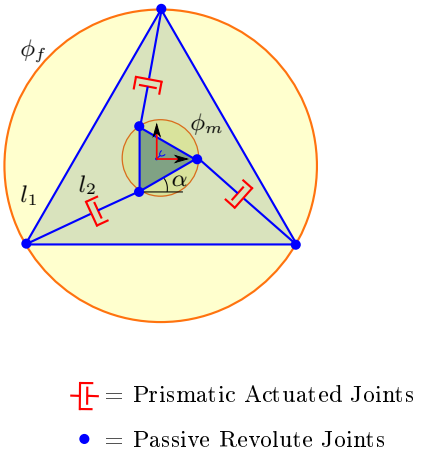

Figure 22 – Non-Redundantly-actuated 3R$\underline{\text{P}}$R planar parallel manipulator ($C_N = 3$).

Notice that in the planar parallel manipulators shown in Figs. 19(a), 19(b), 19(c), 19(d), and in Fig. 21 and 22, all of them have a circular envelopment around their moving and fixed platform. These

circular envelopments were constructed in order to normalize the geometry of the studied manipulators. In this study, the fixed and moving platform of the parallel manipulators are circumscribed about circles with diameters $\phi_f = 1$ [m] and $\phi_m = 0.3$ [m] respectively. In all the studied manipulators herein, the legs are formed or by two links with lengths l_1 and l_2 either a variable distance d_1, the end effector of the manipulator is located in the geometrical center of the moving platform (E) and the angle of orientation (α) represents the orientation of the moving platform (MEJIA; SIMAS; MARTINS, 2014b, 2014c). Here, the link lengths in each leg were specified as $l_1 = l_2 = 0.6$ [m] and $d_1 = 0.7$ [m], the end effector of the manipulator is located in $E = (0, 0)$ [m], the moving platform is oriented in $\alpha = 0°$ and the maximum torque for each actuated joint of the manipulator is imposed as $\tau_{max} = \pm\ 100$ [Nm].

Due that the closed-form solutions shown in Sections 4.4, 4.5, 4.6 and 4.7 allow us to know the maximum force (F_{app}) with a prescribed moment (M_{i_z}) that can be applied or sustained in a given direction (θ). If all the possible directions of the desired angle θ are considered as $0° \leq \theta \leq 360°$, a force capability polygon can be constructed as a polar representation of the maximum force with a prescribed moment at the end effector of the manipulator. Considering the imposed moment $M_{i_z} = 0$, the force capability polygon for the 3$\underline{\text{R}}$RR non-redundant planar parallel manipulator (PPM) is obtained as shown in Fig. 23, the force capability polygon for the 4$\underline{\text{R}}$RR redundant planar parallel manipulator (RPPM) is obtained as shown in Fig. 24, the force capability polygon for the 5$\underline{\text{R}}$RR RPPM is obtained as shown in Fig. 25, the force capability polygon for the 6$\underline{\text{R}}$RR RPPM is obtained as shown in Fig. 26, the force capability polygon for the 3$\underline{\text{R}}$RR RPPM with three of its passive joints actuated is obtained as shown in Fig. 27 and finally the force capability polygon for the 3R$\underline{\text{P}}$R PPM is obtained as shown in Fig. 28.

Following the same strategy that we used previously, it is possible to obtain different wrench capability polygons for different values of the imposed moment at the end effector of the manipulator. If a three-dimensional representation of several wrench capability polygons is plotted, a complete mapping of the wrench capability at the end effector of the manipulator can be obtained. This kind of graphic representation is called the ***wrench capability polytope***.

The wrench capability polytope of the studied manipulators are shown in Figs. 29, 30, 31, 32 and 33. In Fig. 29 the wrench capability polytope of the 3$\underline{\text{R}}$RR PPM is shown. In Fig. 30 the wrench capab-

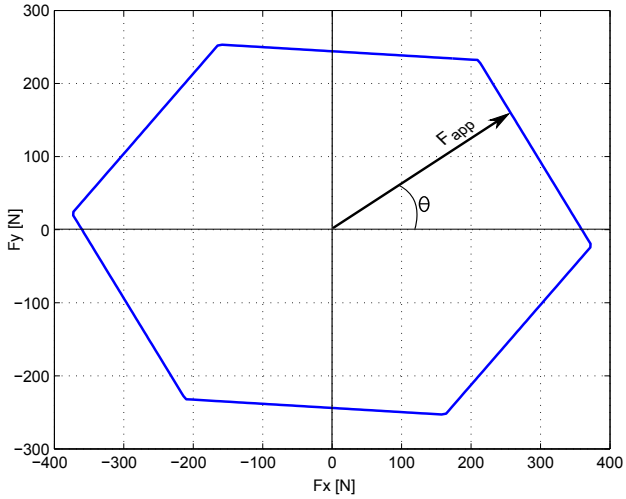

Figure 23 – Force capability polygons for a non-Redundantly-actuated 3$\underline{\text{R}}$RR planar parallel manipulator ($C_N = 3$).

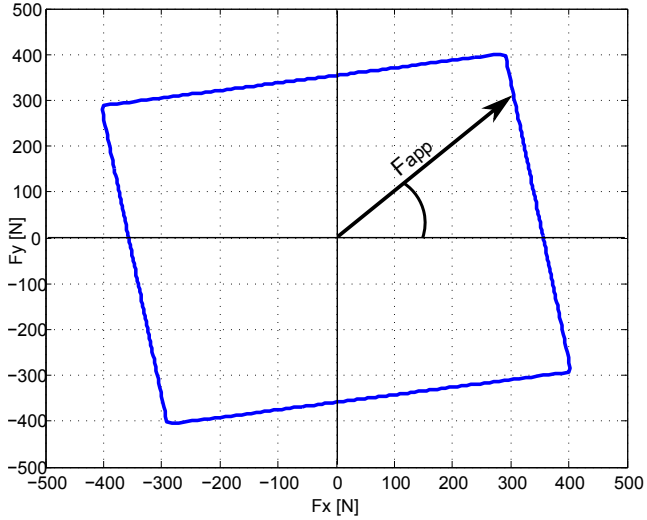

Figure 24 – Force capability polygons for a Redundantly-actuated 4$\underline{\text{R}}$RR planar parallel manipulator ($C_N = 4$).

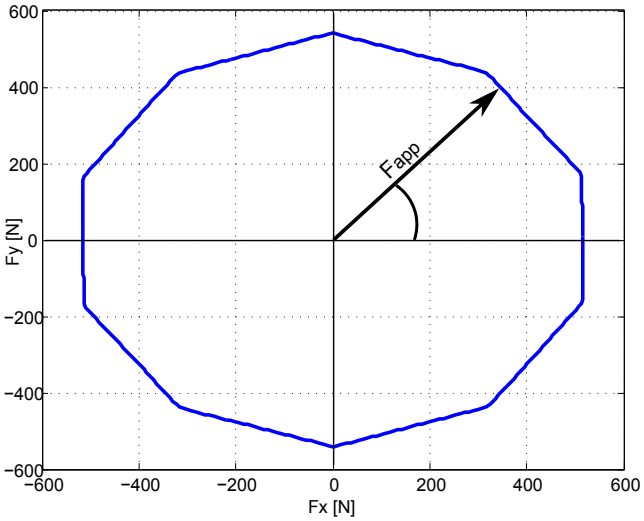

Figure 25 – Force capability polygons for a Redundantly-actuated 5$\underline{\text{R}}$RR planar parallel manipulator ($C_N = 5$).

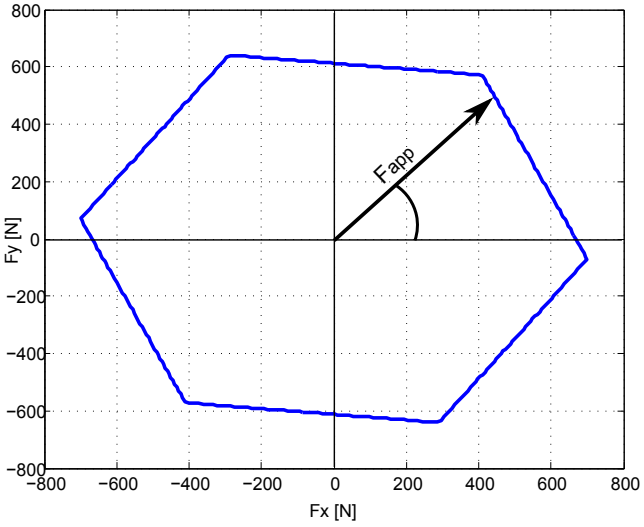

Figure 26 – Force capability polygons for a Redundantly-actuated 6$\underline{\text{R}}$RR planar parallel manipulator ($C_N = 6$).

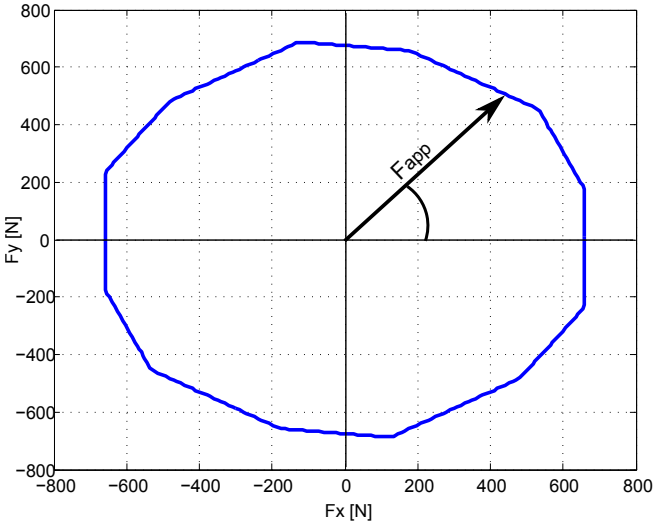

Figure 27 – Force capability polygons for a Redundantly-actuated 3$\underline{\text{RR}}$R planar parallel manipulator ($C_N = 6$).

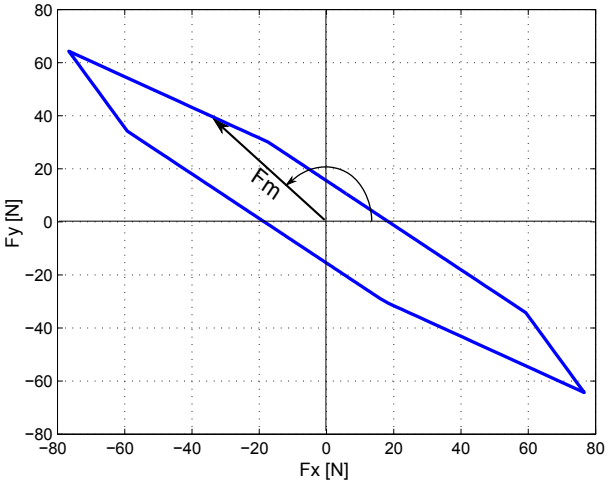

Figure 28 – Force capability polygons for a non-Redundantly-actuated 3R$\underline{\text{P}}$R planar parallel manipulator ($C_N = 3$).

ility polytope of the 4RRR RPPM is shown. In Fig. 31 the wrench capability polytope of the 5RRR RPPM is shown. In Fig. 32 the wrench capability polytope of the 6RRR RPPM is shown, in Fig. 33, the wrench capability polytope of the 3RRR planar parallel manipulator with three of its passive joints actuated is shown and finally, in Fig. 34, the wrench capability polytope of the 3RPR planar parallel manipulator is shown.

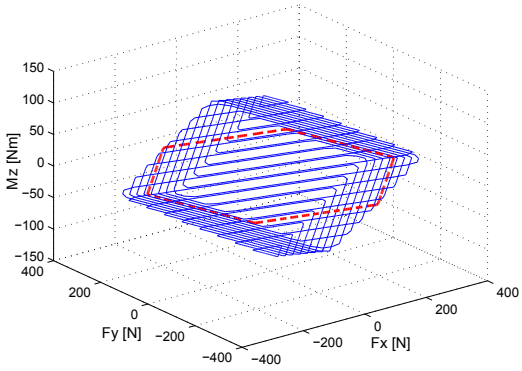

Figure 29 – Force capability polytope for the studied PPM 3RRR

4.9 QUADRATIC PROGRAMMING APPROACH

A special case of the *NLP* arises when the objective functional f is quadratic and the constraints h, g are linear in $x \in \mathbb{R}^n$. Such an NLP is called a Quadratic Programming *(QP)* problem. Its general form is

$$\textit{minimize} \quad f(x) := \frac{1}{2} x^T H x - b x^T, \quad \textbf{over} \quad x \in \mathbb{R}^n \tag{4.176}$$

$$\begin{aligned} \textit{subject to} \quad A_1(x) &= c & (4.177)\\ A_2(x) &\leqslant d & (4.178) \end{aligned}$$

where $H \in \mathbb{R}^{n \times n}$, $m \leq n$ is symmetric, $A_1 \in \mathbb{R}^{m \times n}$, $A_2 \in \mathbb{R}^{p \times n}$ and $b \in \mathbb{R}^n$, $c \in \mathbb{R}^m$, $d \in \mathbb{R}^p$.

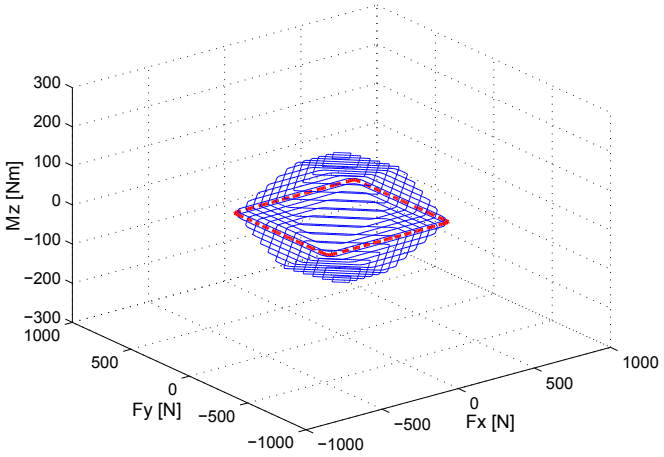

Figure 30 – Force capability polytope for the studied RPPM 4RRR

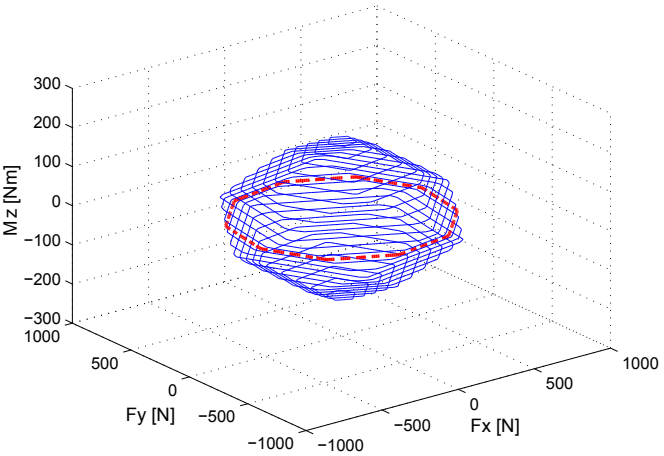

Figure 31 – Force capability polytope for the studied RPPM 5RRR RPPM

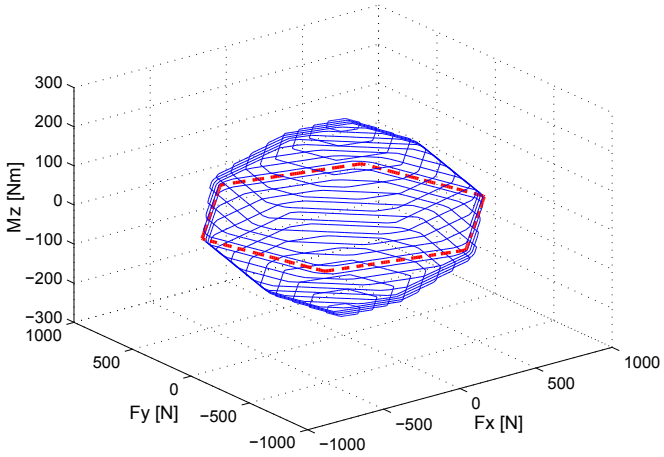

Figure 32 – Force capability polytope for the studied RPPM 6RRR RPPM

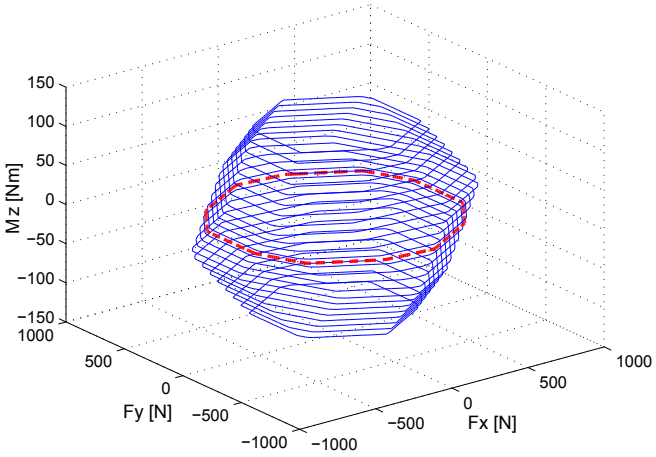

Figure 33 – Force capability polytope for the studied 3RRR planar parallel manipulator with three of its passive joints actuated.

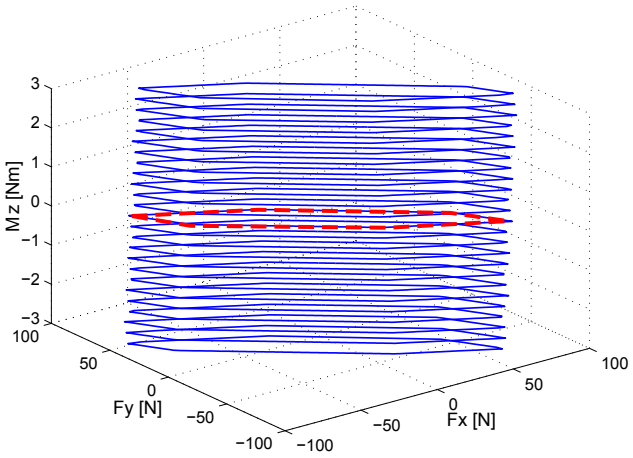

Figure 34 – Force capability polytope for the studied 3RPR planar parallel manipulator.

If the force capability problem previously shown in Eqs. 4.13 to 4.18 is re-formulated in order to eliminate the non-linear constraint of direction of the application of the force shown in 4.14, the optimization problem lies on a quadratic programming case and can be solved alternatively by using several computing tools freely available as Octave, GeoGebra, Mathematica, Matlab, among others.

At this point it is very important to remark that by using the quadratic programming approach, the maximum wrench in a manipulator is obtained only for a limited number of directions, and without consider a direction of application, it is not possible to guarantee that this maximum value of wrench can be applied in all directions and it is not possible to prevent overloading or even it is possible damaging the manipulator or the objects to be manipulated. In this way, it is necessary to be very carefully with the results obtained by using this approach.

by using the quadratic programming approach, and in order to exemplify, the wrench capability optimization problem for a manipulator with $C_N = 3$ can be re-formulated as:

$$\begin{aligned} &minimize: \quad f(\tau_1,\tau_2,\tau_3) = -F^2 = -\left(F_x^2 + F_y^2\right) = \dots \\ &\dots = -\left((a_{1,1}\tau_1 + a_{1,2}\tau_2 + a_{1,3}\tau_3)^2 + (a_{2,1}\tau_1 + a_{2,2}\tau_2 + a_{2,3}\tau_3)^2\right) \end{aligned} \tag{4.179}$$

$$\begin{aligned} subject\ to: \ h_1(\tau_1,\tau_2,\tau_3) &: a_{3,1}\tau_1 + a_{3,2}\tau_2 + a_{3,3}\tau_3 - M_{i_z} = 0 && (4.180)\\ g_1(\tau_1) &: -\tau_{1max} \leqslant \tau_1 \leqslant \tau_{1max} && (4.181)\\ g_2(\tau_2) &: -\tau_{2max} \leqslant \tau_2 \leqslant \tau_{2max} && (4.182)\\ g_3(\tau_3) &: -\tau_{3max} \leqslant \tau_3 \leqslant \tau_{3max} && (4.183) \end{aligned}$$

where the objective function, can be rewritten as:

$$f(\tau_1,\tau_2,\tau_3) = -c_1(\tau_1)^2 - c_2(\tau_2)^2 - c_3(\tau_3)^2 - c_4\tau_1\tau_1 - c_5\tau_1\tau_3 - c_6\tau_2\tau_3 \tag{4.184}$$

and the coeficients c_1 to c_6 are expressed as:

$$c_1 = a_{1,1}^2 + a_{2,1}^2 \tag{4.185}$$

$$c_2 = a_{1,2}^2 + a_{2,2}^2 \tag{4.186}$$

$$c_3 = a_{1,3}^2 + a_{2,3}^2 \tag{4.187}$$

$$c_4 = 2a_{1,1}a_{1,2} + 2a_{2,1}a_{2,2} \tag{4.188}$$

$$c_5 = 2a_{1,1}a_{1,3} + 2a_{2,1}a_{2,3} \tag{4.189}$$

$$c_6 = 2a_{1,2}a_{1,3} + 2a_{2,2}a_{2,3} \tag{4.190}$$

And by using the general form of a quadratic programming *(QP)* approach, The wrench capability optimization problem can be re-written as:

$$minimize \quad f(x) := \frac{1}{2}x^T H x - bx^T \tag{4.191}$$

$$\begin{aligned} subject\ to \quad Ax &= M_{i_z} && (4.192)\\ l_b \leq \quad x &\leq u_b && (4.193) \end{aligned}$$

where:

$$H = \begin{bmatrix} -2c_1 & -c_4 & -c_5 \\ -c_4 & -2c_2 & -c_6 \\ -c_5 & -c_6 & -2c_3 \end{bmatrix} \tag{4.194}$$

$$b = \begin{bmatrix} 0 \\ 0 \\ 0 \end{bmatrix} \tag{4.195}$$

$$x = \begin{bmatrix} \tau_1 \\ \tau_2 \\ \tau_3 \end{bmatrix} \tag{4.196}$$

$$A = \begin{bmatrix} a_{3,1} & a_{3,2} & a_{3,3} \end{bmatrix} \tag{4.197}$$

$$l_b = \begin{bmatrix} -\tau_{1_{max}} \\ -\tau_{2_{max}} \\ -\tau_{3_{max}} \end{bmatrix} \tag{4.198}$$

$$u_b = \begin{bmatrix} \tau_{1_{max}} \\ \tau_{2_{max}} \\ \tau_{3_{max}} \end{bmatrix} \tag{4.199}$$

In order to optimize the problem previously defined, any quadratic programming algorithm can be used, in our case, we used a Matlab subroutine as shown below:

$$\text{x} = \text{quadprog}(H,b,[],[],A,M_{i_z},l_b,u_b)$$

At this point, it is important to note that, although only one example using manipulators with $C_N = 3$ was shown, the method can be applied to manipulators with different net degree of constraint (C_N). The elapsed time used to solve the problem in a manipulator with $C_N = 3$ was 0.356512 seconds approximately.

4.10 DISCUSSION ABOUT THE PROPOSED CLOSED-FORM SOLUTIONS

Some important issues regarding the closed-form solutions obtained are related to its simplicity, generality, versatility and computing time. We comment these aspects below.

The closed-form solutions shown in Sections 4.4, 4.5, 4.6 and 4.7 are mathematical expressions that can be evaluated in a finite number of operations, containing constants, variables, well known operations (e.g., $+,-,\times,\div$) and functions (e.g., square root, exponent, maximum, etc.) and thus the evaluation is *simpler compared with other methodologies* found in the literature.

The evaluation of the closed-form solutions is based on a knowledge of the kinematic variables $(a_{1,1}, ..., a_{3,C_N})$ obtained from the solution of the direct static problem (presented in Eqs. (4.2), 4.3), (4.4) and (4.5)), the desired moment and direction of the application of the force at the end effector of the manipulator, and the maximum torque in the actuated joints. Since these characteristics are a common factor in all manipulators with $C_N = 3$, $C_N = 4$, $C_N = 5$ and $C_N = 6$ the proposed solutions represent *general solutions for any manipulator with these net degree of constraint.*

Given that the force capabilities as a function of the desired moment and the fixed force direction can be established relatively easily, it is possible to solve several processes which require an easy redefinition of the task. This allow us to affirm that *the proposed closed-form solutions offers a high degree of versatility.*

Finally, as the effort necessary to evaluate the mathematical closed-form solutions is reduced to the time needed to evaluate some finite operations, *the computing time is less than that associated with other methodologies using heuristic or meta-heuristic approaches described in the literature.*

It should be emphasized that the proposed mathematical closed-form solutions obtained in Sections. 4.4, 4.5, 4.6 and 4.7 work only when the manipulator evaluated has a net degree of constraint value equal to three, four, five or six ($C_N = 3$, $C_N = 4$, $C_N = 5$ or $C_N = 6$). Manipulators with a net degree of constraint values which are not four, five or six ($C_N \neq 3$, $C_N \neq 4$, $C_N \neq 5$ or $C_N \neq 6$) cannot be solved using the mathematical closed-form solutions proposed in this chapter. However, and although it is not common in practice, mathematical closed-form solutions can be constructed in a similiar way in manipulators with a net degree of constraint values greater than six ($C_N > 6$).

The results shown in Figs. 23, 24, 25, 26, 27, 29, 30, 31, 32 and 33 are the same as those obtained by using the method proposed by Mejia *et al.* (MEJIA; SIMAS; MARTINS, 2014b, 2014c) for the same manipulators, using the same dimensions, topological structure, posture and maximum torques at the actuated joints. This allowed us to compare and validate the results obtained using the proposed mathematical closed-form solutions. The comparison showed that the force capabilities obtained were exactly the same as the results reported by Mejia *et al.* (MEJIA; SIMAS; MARTINS, 2014c), but an important difference lies in the computing time used to obtain these results.

Table 5 – Comparison of the computing time required for different strategies in order to solve the force capability problem.

Study case	**Computer used**	**Method used**	**Time needed for one pose**	**Time needed for one direction**
PPM with $C_N = 3$	P4 2.4 GHz	Proposed closed-form solution	0.021407 s	0.000074 s
		Quadratic Programming	0.356512 s	Unknown
		(DE) algorithm	>5400 s	>18 s
	P4 3.2 GHz	Explicit method	0.1 s	Unknown
		Scaling factor method	15 s	Unknown
PPM with $C_N = 4$	P4 2.4 GHz	Proposed closed-form solution	0.4622 s	0.001284 s
		Quadratic Programming	0.6243 s	Unknown
		(DE) algorithm	>7400 s	>21 s
PPM with $C_N = 5$	P4 2.4 GHz	Proposed closed-form solution	1.1894 s	0.003304 s
		Quadratic Programming	1.4623 s	Unknown
		(DE) algorithm	>9000 s	>25 s
PPM with $C_N = 6$	P4 2.4 GHz	Proposed closed-form solution	3.7868 s	0.010519 s
		Quadratic Programming	3.9823 s	Unknown
		(DE) algorithm	>10800 s	>30 s

Using the proposed generalized mathematical closed-form solutions for the manipulators with $C_N = 3$, $C_N = 4$, $C_N = 5$ and $C_N = 6$, the force capability polygon for one pose is completed in 0.021407, 0.4622 seconds, 1.1894 seconds and 3.7868 seconds respectively when running on a P4 2.4 GHz computer.

As a comparison, the same results were obtained using the method proposed by Mejia *et al.* (MEJIA; SIMAS; MARTINS, 2014c) using a differential evolution algorithm *(DE)*, but with a very slow response of more than 5400 seconds for each case when running on a the same P4 2.4 GHz computer.

Another important issue with regard to the computing time of the proposed generalized mathematical closed-form solution is that when the force capability of manipulators with $C_N = 3$, $C_N = 4$, $C_N = 5$ and $C_N = 6$ is evaluated in a fixed direction, the time used in that operation is only 0.000074 seconds, 0.001284 seconds, 0.003304 seconds and 0.010519 seconds respectively (again, when running on a P4 2.4 GHz computer). This response is very fast and allows us to contemplate applications that require a real-time response in terms of the manipulation of the force, such as grasping, polishing, milling, etc. A comparison of the computing times required to solve the force capability problem using several approaches is shown in Table. 5.

5 CONCLUSIONS

This work focuses on the wrench capabilities of planar manipulators, whether it be serial parallel or hybrid and with redundancy or not. In order to solve the wrench capability problem, in this work two new approaches were proposed based in the classic scaling factor method and in classical optimization methods.

These new approaches gave as result a new method called the modified scaling factor method used to solve the wrench capability in planar serial manipulators and four mathematical closed-form solutions to solve the wrench capability problem in planar parallel manipulators with a net degree of constraint equal to three, four, five or six ($C_N = 3$, $C_N = 4$, $C_N = 5$ or $C_N = 6$).

The ***modified scaling factor method*** proposed in this work, was proposed because the ***original scaling factor method*** (NOKLEBY et al., 2005) does not allow the desired moment at the manipulator end effector to be included in an explicit mathematical expression, and an optimization process is required in order to solve the force capability problem. In addition, the computation of the maximum allowed moment is not presented.

The novelty of the ***modified scaling factor method*** lies in the fact that this approach does not require the use of an optimization algorithm, in contrast to the original scaling factor method. Instead, explicit equations are used in order to solve the force capability problem. The avoidance of optimization algorithms results in a simpler, faster and more direct solution to obtain the force capability of manipulators compared with other solutions for the same problem found in the literature.

In the other hand, the proposed ***mathematical closed-form solutions*** were obtained applying classical optimization methods, considering the cases in which the net degree of constraint is equal to the number of actuated joints in the mechanism or manipulator and their values are equal to three, four, five or six ($C_N = 3$, $C_N = 4$, $C_N = 5$ or $C_N = 6$). In robotics, closed-form solutions are often very desirable, because they are faster than numerical solutions and readily identify all possible solutions (SICILIANO; KHATIB, 2008).

The novelty of the mathematical closed-form solutions described in this work lies in the fact that our main results are not methods or numerical algorithms, but mathematical expressions to obtain the force capability in planar redundantly-actuated mechanisms and manipulat-

ors with net degree of constraint equal to three, four, five or six.

An equation is said to be a closed-form solution if it solves a given problem in terms of functions and mathematical operations from a given generally-accepted set (CHOW, 1999). This means that the mathematical closed-form solution reported in this thesis are functions that can be used directly without the use of a method, numerical algorithm or optimization process, implying that their use represent simpler, faster and more direct solutions to obtain the force capability of manipulators compared with other solutions for the same problem found in literature.

The proposed ***modified scaling factor method*** and ***mathematical closed-form solutions*** in combination with the ***Davies method*** constitutes a powerful tool to solve the force capability problem in any mechanism or manipulator (whether it be serial, parallel or hybrid) with a net degree of constraint equal to three, four, five or six ($C_N = 3$, $C_N = 4$, $C_N = 5$ and $C_N = 6$).

A final and very important conclusion is that, once the modified scaling factor method and the mathematical closed-form solutions proposed in this thesis were developed in a symbolic way, the maximization of similar models like the differential kinematics in planar mechanisms can be optimized by using exactly the same methods, but taking care of the correct formulation of the coeficient matrices. In this way, the velocity capacity and the power capacity in planar manipulators can be obtained by using the same methods proposed in this document. The detailed solution for those problems is proposed as future works.

5.1 CONTRIBUTIONS OF THIS WORK

The original contributions of this work can be summarized as shown below:

i. Development of a modified scaling factor method to obtain the wrench capability in manipulators with $C_N = 3$.

ii. Inclusion of a procedure to obtain the maximum imposed moment as a particularization of the modified scaling factor method.

iii. Development of mathematical closed-form solutions to obtain the wrench capability in manipulators with a net degree of constraint equal to three, four, five or six ($C_N = 3$, $C_N = 4$, $C_N = 5$ and $C_N = 6$).

iv. Development of mathematical closed-form solutions to obtain the maximum imposed moment in manipulators with a net degree of constraint equal to three, four, five or six ($C_N = 3$, $C_N = 4$, $C_N = 5$ and $C_N = 6$).

5.2 PUBLICATIONS

Up to the moment to the submission of this thesis, several publications have been generated. These publications are classified and listed below:

Publications in Journal:

i. Journal: Mechanisms and Machine Theory;
Status: Published;
Title: Force capability in general 3 DoF planar mechanisms (MEJIA; SIMAS; MARTINS, 2015b);
Available online from: Apr 29, 2015.

ii. Journal: Mechanisms and Machine Theory;
Status: Under Review;
Title: Determination of force capability of planar mechanisms using a modified scaling factor method (MEJIA; SIMAS; MARTINS, 2015a);
Status Date: Jun 16, 2015.

iii. Journal: Mechanisms and Machine Theory;
Status: Under Review;
Title: Wrench capability in redundant planar parallel manipulators with net degree of constraint equal to four, five or six (MEJIA; SIMAS; MARTINS, 2015c);
Status Date: Dec 01, 2015.

Chapters in Book:

i. Book: Advances on Theory and Practice of Robots and Manipulators;
Status: Published;
Title: Force Capability Polytope of a 3RRR Planar Parallel Manipulator (MEJIA; SIMAS; MARTINS, 2014b);
Available online from: Jun 03, 2014.

ii. Book: Advances in Robot Kinematics;
Status: Published;
Title: Force Capability Polytope of a 4RRR Redundant Planar Parallel Manipulator (MEJIA; SIMAS; MARTINS, 2014c);
Available online from: May 20, 2014.

iii. Book: ABCM Symposium Series in Mechatronics - Vol: 6;
Status: Published;
Title: Force Capability maximization of a 3RRR parallel manipulator by topology optimization;
Available online from: Aug 15, 2014.

Proceedings Congress:

i. Congress: 23^{th} ABCM International Congress of Mechanical Engineering (COBEM 2015);
Status: Published;
Title: Influence of the assembly mode on the force capability in parallel manipulators (MEJIA et al., 2015b);
Available online from: Dez 11, 2015.

ii. Congress: 23^{th} ABCM International Congress of Mechanical Engineering (COBEM 2015);
Status: Published;
Title: Wrench capability polytopes in redundant parallel manipulators (MEJIA et al., 2015d);
Available online from: Dez 11, 2015.

iii. Congress: 23^{th} ABCM International Congress of Mechanical Engineering (COBEM 2015);
Status: Published;
Title: Analysis of wrench capability for cooperative robotic systems (MEJIA et al., 2015a);
Available online from: Dez 11, 2015.

iv. Congress: 14^{th} IFToMM World Congress (IFToMM 2015);
Status: Published;
Title: Modified Scaling Factor Method for the Obtention of the Wrench Capabilities in Cooperative Planar Manipulators (MEJIA et al., 2015c);
Available online from: Oct 30, 2015.

v. Congress: 21^{th} Congreso Iberoamericano de Ingenieria Mecánica (CIBIM 2013);
Status: Published;
Title: Influencia del modo de trabajo de un manipulador paralelo planar sobre su capacidad de fuerza (MEJIA; SIMAS; MARTINS, 2013);
Available online from: Nov 30, 2013.

5.3 FUTURE WORKS

The results presented in this work opened the door to a huge world of possibilities related to the study of the wrench capability in manipulators. Some of these future works are listed below:

i. To include the stiffness and the gravitational forces in the static model of the manipulators;

ii. To include the dynamic behavior into the study of the wrench capability problem;

iii. To extend the proposed methods for spatial mechanisms and manipulators;

iv. To optimize the posture of complex robotic structures as humanoids in order to minimize the energy consumption;

v. To obtain the velocity capacity in planar manipulators;

vi. To obtain the power capacity in planar manipulators;

REFERENCES

ARORA, J. *Introduction to Optimum Design*. San Diego, California: Elsevier Academic Press, 2004.

BALL, R. The theory of screws: A study in the dynamics of a rigid body. *Mathematische Annalen*, Springer-Verlag, v. 9, n. 4, p. 541–553, 1876. ISSN 0025-5831. <http://dx.doi.org/10.1007/BF01442479>.

BALL, R. S. *A treatise on the theory of screws*. [S.l.]: Cambridge :University Press,, 1900. 544 p.

BICCHI, A.; MELCHIORRI, C.; BALLUCHI, D. On the mobility and manipulability of general multiple limb robotic systems. *IEEE Transactions on Robotics and Automation*, v. 11, p. 215–228, 1995.

BUTTOLO, P.; HANNAFORD, B. Advantages of actuation redundancy for the design of haptic displays. *Proceedings of the 1995 ASME International Mechanical Engineering Congress and Exposition-Part 2*, p. 623 – 630, 1995.

CAMPOS, A. *cinemática Diferencial de Manipuladores empregando Cadeias Virtuais*. Tese (Doutorado) — Universidade Federal de Santa Catarina, 2004.

CAZANGI, H. R. *Aplicação do método de Davies para Análise Cinemática e Estática de Mecanismos de Múltiplos Graus de Liberdade*. Tese (Doutorado) — Universidade Federal de Santa Catarina, Brazil, 2008.

CHAND, D. R.; KAPUR, S. S. An algorithm for convex polytopes. *Journal of the Association for Computing Machinery*, v. 17, p. 78–86, 1970.

CHIACCHIO, P. Force polytope and force ellipsoid for redundant manipulators. *Journal of Robotic Systems - 14*, p. 613–620, 1997.

CHIACCHIO, P.; VERCELLI, Y. B.; PIERROT, F. Evaluation of force capabilities for redundant manipulators. *Proceedings of the 1996 IEEE International Conference on Robotics and Automation , Vol. 4*, p. 3520–3525, 1996.

CHIACCHIO, P.; VERCELLI, Y. B.; PIERROT, F. Force polytope and force ellipsoid for redundant manipulators. *Journal of Robotic Systems , Vol. 14, No. 8*, p. 613–620, 1997.

CHOW, T. Y. What is a closed form number. *The American Mathematical Monthly*, v. 106, p. 440–448, 1999.

DAVIDSON, J. K.; HUNT, K. H. *Robots and Screw Theory: Applications of Kinematics and Statics to Robotics*. New York: Oxford University Press Inc., 2004. ISBN 0-19-856245-4.

DAVIES, T. Couplings, coupling networks and their graphs. *Mechanism and Machine Theory*, v. 30, n. 7, p. 991 – 1000, 1995. ISSN 0094-114X. Graphs and Mechanics First International Conference. <http://www.sciencedirect.com/science/article/pii/0094114X9500023R>.

DAVIES, T. H. Mechanical networks I: Passivity and redundancy. *Mechanism and Machine Theory*, p. 95–101, 1983a.

DAVIES, T. H. Mechanical networks II: Formulae for the degrees of mobility and redundancy. *Mechanism and Machine Theory*, p. 102–106, 1983b.

DAVIES, T. H. Mechanical networks III: Wrenches on circuit screws. *Mechanism and Machine Theory*, p. 107–112, 1983c.

DENAVIT, J.; HARTENBERG, R. S. A kinematic notation for lower-pair mechanisms based on matrices. *ASME E, Journal of Applied Mechanics*, v. 22, p. 215–221, 1955.

EBRAHIMI, I.; CARREYERO, J. A.; BORDREAU, R. 3-prrr redundant planar parallel manipulator: Inverse displacement, workspace and singularity analyses. *Mechanism and Machine Theory*, v. 42, p. 1007–1016, 2007.

FINOTELLO, R. et al. Computation of kinetostatic performances of robot manipulators with polytopes. *IEEE International Conference on Robotics and Automation*, p. 3241 – 3246, 1998.

FIRMANI, F.; PODHORODESKI, R. P. Force-unconstrained poses for a redundantly- actuated planar parallel manipulator. *Mechanism and Machine Theory*, v. 39, p. 459–476, 2004.

FIRMANI, F. et al. Wrench capabilities of planar parallel manipulators. part i: Wrench polytopes and performance indices. *Robotica 26*, p. 791 – 802, 2008.

FIRMANI, F. et al. *Wrench Capabilities of Planar Parallel Manipulators and their Effects Under Redundancy.* [S.l.]: INTECH Open Access Publisher, 2008.

GALLINA, P.; ROSATI, G.; ROSSI, A. 3-d.o.f. wire driven planar haptic interface. *Journal of Intelligent and Robotic Systems , Vol. 32, No. 1*, p. 23 – 36, 2001.

GARG, V.; NOKLEBY, S. B.; CARRETERO, J. A. Force-moment capabilities of redundantly-actuated spatial parallel manipulators using two methods. In: . [S.l.: s.n.].

GOGU, G. Mobility of mechanisms: a critical review. *Mechanism and Machine Theory, Vol. 40*, p. 1608 – 1097, 2005.

GROSS, J. L.; YELLEN, J. *Graph Theory and Its Applications, Second Edition (Discrete Mathematics and Its Applications).* [S.l.]: Chapman & Hall/CRC, 2005. ISBN 158488505X.

HUNT, K. H. *Kinematic geometry of mechanisms / by K. H. Hunt.* [S.l.]: Clarendon Press ; Oxford University Press Oxford : New York, 1978. xvii, 465 p. : p. ISBN 0198561245.

HWANG, Y. S.; LEE, J.; HSIA, T. C. Recursive dimension-growing method for computing robotic manipulability polytope. *Proceedings of the 2000 IEEE International Conference on Robotics and Automation*, v. 3, p. 2569–2574, 2000.

IONESCU, T. Terminology for mechanisms and machine science. *Mechanism and Machine Theory, Vol. 38*, p. 7 –10, 2003.

JAZAR, R. N. *Theory of Applied Robotics: Kinematics, Dynamics, and Control.* [S.l.]: Springer Publishing Company, Incorporated, 2007. ISBN 0387324755, 9780387324753.

KHALIFA, H. et al. Parallel, serial and hybrid machine tools and robotics structures: Comparative study on optimum kinematic designs. *Serial and Parallel Robot Manipulators - INTEC*, p. 109 –124, 2012.

KOKKINIS, T.; PADEN, B. Kinetostatic performance limits of cooperating robot manipulators using force-velocity polytopes. *Proceedings of the ASME Winter Annual Meeting*, p. 151–155, 1989.

KRUT, S.; COMPANY, O.; PIERROT, F. Force performance indexes for parallel mechanisms with actuation redundancy, especially for parallel wire-driven manipulators. *Proceedings of 2004 IEEE/RSJ International Conference on Intelligent Robots and Systems , Vol. 4*, p. 3936–3941, 2004.

KRUT, S.; COMPANY, O.; PIERROT, F. Velocity performance indices for parallel mechanisms with actuation redundancy. *Robotica , Vol. 22, No. 2*, p. 129–139, 2004.

KUMAR, V.; WALDRON, K. J. Force distribution in closed kinematic chains. *Proceedings of the 1988 IEEE International Conference on Robotics and Automation*, p. 114 – 119, 1988.

LEE, J. A study on the manipulability measures for robot manipulators. *Proceedings of 1997 IEEE/RSJ International Conference on Intelligent Robots and Systems*, v. 3, p. 1458–1465, 1997.

LEE, J.; SHIM, H. On the dynamic manipulability of cooperating multiple arm robot systems. *Proceedings of 2004 IEEE/RSJ International Conference on Intelligent Robots and Systems , Vol. 2*, p. 2087 – 2092, 2004.

LEE, S.; KIM, S. A self-reconfigurable dual-arm system. *Proceedings of the1991 IEEE International Conference on Robotics and Automation , Vol. 1*, p. 164–169, 1991.

LEE, S.; KIM, S. Kinematic analysis of generalized parallel manipulator systems. *Proceedings of the 32nd IEEE Conference on Decision and Control*, v. 2, p. 1097–1102, 1993.

MEJIA, L. et al. Analysis of wrench capability for cooperative robotic systems. *Proceeding in* 23^{th} *ABCM International Congress of Mechanical Engineering (COBEM 2015)*, 2015.

MEJIA, L. et al. Influence of the assembly mode on the force capability in parallel manipulators. *Proceeding in* 23^{th} *ABCM International Congress of Mechanical Engineering (COBEM 2015)*, 2015.

MEJIA, L. et al. Modified scaling factor method for the obtention of the wrench capabilities in cooperative planar manipulators. *Proceeding in* 14^{th} *IFToMM World Congress (IFToMM 2015)*, 2015.

MEJIA, L. et al. Wrench capability polytopes in redundant parallel manipulators. *Proceeding in* 23^{th} *ABCM International Congress of Mechanical Engineering (COBEM 2015)*, 2015.

MEJIA, L.; SIMAS, H.; MARTINS, D. Influencia del modo de trabajo de un manipulador paralelo planar sobre su capacidad de fuerza. *Proceeding in* 21^{th} *Congreso Iberoamericano de Ingenieria Mecánica (CIBIM 2013)*, 2013.

MEJIA, L.; SIMAS, H.; MARTINS, D. Force capability maximization of a 3RRR parallel manipulator by topology optimization. *ABCM Symposium Series in Mechatronics*, v. 6, p. 568–577, 2014.

MEJIA, L.; SIMAS, H.; MARTINS, D. Force capability polytope of a 3RRR planar parallel manipulator. *Proceedings of Romansy 2014 XX CISM-IFToMM Symposium on Theory and Practice of Robots and Manipulators*, p. 537–545, 2014.

MEJIA, L.; SIMAS, H.; MARTINS, D. Force capability polytope of a 4RRR redundant planar parallel manipulator. *Advances in Robot Kinematics*, p. 87–94, 2014.

MEJIA, L.; SIMAS, H.; MARTINS, D. Determination of force capability of planar mechanisms using a modified scaling factor method. *Submited in Mechanism and Machine Theory*, 2015.

MEJIA, L.; SIMAS, H.; MARTINS, D. Force capability in general 3 dof planar mechanisms. *Mechanism and Machine Theory*, v. 91, p. 120 – 134, 2015.

MEJIA, L.; SIMAS, H.; MARTINS, D. Wrench capability in redundant planar parallel manipulators with net degree of constraint equal to four, five or six. *Submited in Mechanism and Machine Theory*, 2015.

MERLET, J. P. Redundant parallel manipulators. *Journal of Laboratory Robotics and Automation*, v. 8, p. 17–24, 1996.

MORRISON, A. *Optimal dimentional synthesis of planar parallel manipulators whith respect to workspaces*. Dissertação (Mestrado) — University of Pretoria, Pretoria, 2003.

MOZZI, G. *Discorso matematico sopra il rotamiento momentaneo dei corpi*. Naples: Stamperia di Donato Campo, 1763.

NAHON, M. A.; ANGELES, J. Real-time force optimization in parallel kinematic chains under inequality constraints. *IEEE Trans. Robot. Autom. 8(4)*, p. 439 – 450, 1992.

NOKLEBY, S. B. et al. Force moment capabilities of redundantly actuated planar parallel architectures. *12th IFToMM 2007 World Congress*, p. 17 – 21, 2007.

NOKLEBY, S. B. et al. Force capabilities of redundantly-actuated parallel manipulators. *Mechanism and Machine Theory 40*, p. 578 – 599, 2005.

POINSOT, L. Sur la composition des moments et la composition des aires. *J. Éc Polyt. Paris*, v. 6, p. 182–205, 1806.

ROCKAFELLAR, R. T. Convex analysis. *Princeton University Press*, 1997.

ROMANELLI, F. Advanced methods for robot-environment interaction towards an industrial robot aware of its volume. *Journal of Robotics*, p. 1 – 12, 2011.

SHAI, O.; PREISS, K. Graph theory representations of engineering systems and their embedded knowledge. *Artificial Intelligence in Engineering Journal*, p. 273 – 285, 1999.

SICILIANO, B.; KHATIB, O. Springer handbook of robotics. Springer, 2008.

STORN, R.; PRICE, K.; LAMPINEN, J. The motivation for differential evolution. *A Practical Approach to Global Optimization Series*, p. 1–34, 2005.

TAO, J. M.; LUH, J. Y. S. Coordination of two redundant manipulators. *Proceedings of the 1989 IEEE International Conference on Robotics and Automation*, p. 425–430, 1989.

TSAI, L.-W. *Robot Analysis and Design: The Mechanics of Serial and Parallel Manipulators*. 1st. ed. New York, NY, USA: John Wiley & Sons, Inc., 1999. ISBN 0471325937.

VISVANATHAN, V.; MILOR, S. L. An efficient algorithm to determine the image of a parallelepiped under a linear transformation. *Proceedings of 2nd Annual Symposium on Computational Geometry*, p. 207 – 215, 1986.

WANG, J.; GOSELIN, C. M. Kinematic analysis and design of kinematically redundant parallel mechanisms. *Transactions of the ASME, Journal of Mechanical Design*, v. 126, p. 109–118, 2004.

WEIHMANN, L. *Modelagem e otimização de forças e torques aplicados por robôs com redundância cinemática e de atuação em contato com o meio*. Tese (Doutorado) — Universidade Federal de Santa Catarina, Brazil, 2011.

WEIHMANN, L.; MARTINS, D.; COELHO, L. S. Force capabilities of kinematically redundant planar parallel manipulators. *13th World Congress in Mechanism and Machine Science*, p. 483 – 483, 2011.

YANG, A. T. "calculus of screws" in basic questions of design theory. *Elsevier, New York*, p. 266–281, 1974.

YOSHIKAWA, T. Dynamic manipulability of robot manipulators. *Journal of Robotic Systems, Vol 2, No. 1*, p. 113 – 124, 1985.

YOSHIKAWA, T. Manipulability and redundancy control of robotic mechanisms. *in Robotics Research: The Second International Symposium*, p. 1004 – 1009, 1985.

YOSHIKAWA, T. Foundations of robotics: Analysis and control. *The MIT Press, Cambridge, MA, USA*, 1990.

ZHAO, J.; FENG, Z.; DONG, J. Computation of the configuration degree of freedom of a spatial parallel mechanism by using reciprocal screw theory. *Mechanism and Machine Theory*, Elsevier, v. 41, n. 12, p. 1486–1504, 2006.

ZIBIL, A. et al. An explicit method for determining the force moment capabilities of redundantly actuated planar parallel manipulators. *Mech. Design*, p. 1046 – 1056, 2007.

APPENDIX A – Conceptual and analytical tools

Kinematic chain, mechanism, manipulator and robot are common terms found in the literature, and, although these terms can be frequently confused as being synonymous, there exist a significant difference among them. For instance, a kinematic chain is an interconnected system of links in which not a single link is fixed, but such a chain becomes a mechanism when one of the links in the chain is fixed (the fixed link is called a frame or, sometimes, a base link). When a gripper device is attached to such a mechanism, it could be considered a manipulator or a robot (TSAI, 1999).

In order to assist the reader in the understanding of this document, this Appendix introduces some fundamental concepts of the mechanisms theory such as: mobility, coupling, joint, kinematic chain, mechanism, manipulator and robot among others.

As previously noted, kinematic chains and manipulators are constituted by links and joints. These components can be represented in one more abstract way by a graph whose vertices correspond to the links and the edges correspond to the joints. This type of representation will be presented in this document. Also, a brief introduction on kinematics of manipulators will be shown at the end of this Appendix.

A.1 BASIC TERMS AND DEFINITIONS

In the study of mechanisms, manipulators and robots are commonly used the terms coupling, joint, kinematic chain, mechanism, manipulator and robot (DAVIES, 1995). Considering that these terms will be used along the current document, a definition of each of them is shown below. The terminology exposed here is in accordance with the International Federation for the Promotion of Mechanism and Machine Science (IFToMM) and the International Federation of Robotics (IFR). For further information about terminology, see Ionescu (IONESCU, 2003), Tsai (TSAI, 1999) and Hunt (HUNT, 1978).

> **Link:** *1. (IFToMM) Mechanism element (component) carrying kinematic pairing elements. 2. (IFToMM) Element of a linkage.*

> **Coupling:** *1. (IFToMM) Device for joining two moving members, e.g. two shafts at their ends.*

> **Joint:** *1. (IFToMM) Physical realization of a kinematic pair, including connection via intermediate mechanism elements. 2. (IFToMM) Kinematic pair.*

Kinematic pair: *1. (IFToMM) Mechanical model of the connection of two pairing elements having relative motion of a certain type.*

Kinematic chain: *1. (IFToMM) Assemblage of links and joints.*

Closed kinematic chain: *1. (IFToMM) Kinematic chain each link of which is connected with at least two other links.*

Open kinematic chain: *1. (IFToMM) Kinematic chain in which there is at least one link which carries only one kinematic pairing element.*

Loop: *1. (IFToMM) Subset of links that forms a closed circuit.*

Tree: *1. (IFToMM) Kinematic chain that contains no loops.*

Mechanism: *1. (IFToMM) System of bodies designed to convert motions of, and forces on, one or several bodies into constrained motions of, and forces on, other bodies. 2. (IFToMM) Kinematic chain with one of its components (links) taken as a frame.*

Manipulator: *1. (IFToMM) Device for gripping and the controlled movement of objects. 2. (IFR) machine in which the mechanism usually consists of a series of segments, jointed or sliding relative to one another, for the purpose of grasping and/or moving objects (pieces or tools) usually in several degrees of freedom*

Robot: *1. (IFToMM) Mechanical system under automatic control that performs operations such as handling and locomotion. 2. (IFR) An automatically controlled, reprogrammable, multipurpose manipulator programmable in three or more axes, which may be either fixed in place or mobile for use in industrial automation applications.*

Although the terms previously shown can have a conceptual difference, some of them can be used in an analogous way in specific situations. In the calculus of the mobility and the redundancies, for

instance, it is common to use the terms kinematic chain and mechanism indistinctly. In the kinematic and static analysis of manipulators, the term robot can be used without restrictions. Thus, since the conceptual principles are not infringed, some of these terms may be used interchangeably (DAVIES, 1995).

A.2 MOBILITY

manipulators can be represented by a set of links and joints arranged as a serial, parallel or hybrid kinematic chain. In a manipulator one or more links are connected to the ground and at the free end an end effector or gripping device is attached (KHALIFA et al., 2012). Three examples of serial, parallel and hybrid manipulators are shown in Fig. 35. In these examples, the underlining indicates joints which are actuated within each branch.

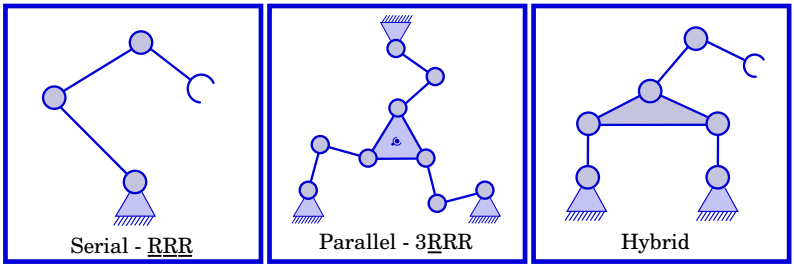

Figure 35 – (a) Serial, (b) parallel and (c) hybrid manipulators

manipulators assembled from a number of links and joints have a significant structural attribute called ***mobility (M)***. Mobility is one of the most fundamental concepts in the kinematic and dynamic modeling of mechanisms and manipulators (KHALIFA et al., 2012).

IFToMM terminology defines the ***mobility (M)*** or ***degrees of freedom (DoF)*** as the number of independent coordinates needed to define the configuration of a kinematic chain or mechanism (GOGU, 2005; IONESCU, 2003). Mobility is used to verify the existence of a mechanism ($\boldsymbol{M > 0}$), to indicate the number of independent parameters in kinematic and dynamic models and to determine the number of inputs needed to drive the mechanism (KHALIFA et al., 2012).

Many formulas have been proposed in the literature for the cal-

culation of mechanism mobility and several of these are reducible to the Chebychev-Grubler-Kutzbach mobility formula given by Eq. (A.1) (GOGU, 2005). Using this formula, the ***mobility M*** of a linkage composed of ***"n" links*** connected with ***"j" joints*** can be determined (KHALIFA et al., 2012).

$$\boldsymbol{M = \lambda(n - j - 1) + \sum_{i=1}^{j} f_i} \tag{A.1}$$

In Eq. (A.1) $\boldsymbol{\lambda}$ represents the dimension of the task space in which the mechanism works (in planar mechanisms $\boldsymbol{\lambda = 3}$ and in spatial mechanisms $\boldsymbol{\lambda = 6}$), and $\boldsymbol{f_i}$ is the ***DoF*** associated with joint $\boldsymbol{i}$ (for instance, prismatic and rotative joints in a planar mechanism have $\boldsymbol{f_i = 1}$). In order to exemplify how the mobility in a mechanism or manipulator can be obtained, below is calculated this property for the parallel manipulator shown in Fig. 35 (b). For all mechanisms shown in Fig. 35 $\boldsymbol{M = 3}$.

A.2.1 Calculus of the mobility in the 3$\underline{\text{R}}$RRR parallel manipulator:

The parallel manipulator shown in Fig. 35 (b) is a manipulator with eight links $\boldsymbol{(n = 8)}$ and nine joints $\boldsymbol{(j = 9)}$. As the manipulator is in a planar system $\boldsymbol{\lambda = 3}$, and as all the joints are rotative the ***DoF*** in each joint is $\boldsymbol{f_i = 1}$. Using the the Chebychev-Grubler-Kutzbach mobility formula given by Eq. (A.1) it is possible to calculate its mobility as shown below:

$$\boldsymbol{M = \lambda(n - j - 1) + \sum_{i=1}^{j} f_i} \tag{A.2}$$

$$\boldsymbol{M = \lambda(n - j - 1) + j} \tag{A.3}$$

$$\boldsymbol{M = 3(8 - 9 - 1) + 9 = 3} \tag{A.4}$$

A.3 GRAPH THEORY APPLIED TO MECHANISMS

A ***graph*** is a structure in which pairs of ***vertices*** are connected by ***edges***. A graph $\boldsymbol{G = (V, E)}$ consists of two finite sets $\boldsymbol{V}$ and $\boldsymbol{E}$

where the elements of $\boldsymbol{V}$ are called the vertices and the elements of $\boldsymbol{E}$ are the edges of $\boldsymbol{G}$. Graphs have natural visual representations in which each vertex is represented by a point or circle and each edge by a line connecting two points. For instance, as shown in Fig. 36, $\boldsymbol{V} = \{1, 2, 3, 4, 5\}$ and $\boldsymbol{E} = \{\{1, 2\}, \{2, 3\}, \{3, 4\}, \{4, 5\}\}$ define a graph with **5** vertices and **4** edges.

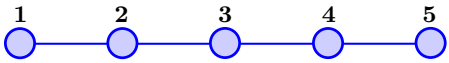

Figure 36 – Example of a graph with **5** vertices and **4** edges.

The general theory of graphs can be used to model many types of relations and processes in physical, biological, social and information systems. Many practical problems can be represented by graphs.

Graph theory is a useful representation because on the one hand the elements of the graph can be defined so as to have a one-to-one correspondence with the elements of many kinds of engineering systems. On the other hand, the theorems and algorithms of graph theory allow one also to represent behavioral properties of the system, such as deformations and forces, or velocities and movements, as properties of the vertices or edges of the graph.

Since a kinematic chain is an assemblage of links and joints, this link and joint assemblage can be represented in a more abstract form known as the ***graph representation***. In a graph representation links are denoted by vertices and joints by edges. To distinguish the differences between pair connections, the edges can be colored or labeled (SHAI; PREISS, 1999). The advantages of using graph representation in mechanisms theory can be summarized as follows (TSAI, 1999):

1. Many network properties of graphs are directly applicable;
2. The structure topology of a mechanism can be uniquely identified. Using graph representation, the similarities and differences between various mechanisms can be clearly identified;
3. A single atlas of graphs can be used to enumerate an enormous amount of mechanisms;
4. Graphs can be used to better organize kinematic and dynamic analysis of mechanisms.

In order to exemplify the graph representation of a mechanical system, Fig. 37 (a) shows a hybrid manipulator that is basically constituted by a serial manipulator assembled on a four bar mechanism. This

hybrid manipulator has seven joints $(j = 7)$ and seven links $(n = 7)$ and its graph representation is shown in Fig. 37 (b). In this representation, the links are identified using numbers (i.e. 0, 1, 2, 3, 4, 5 and 6 respectively), while the joints are identified using letters (i. e. A, B, C, D, E, F and G respectively)

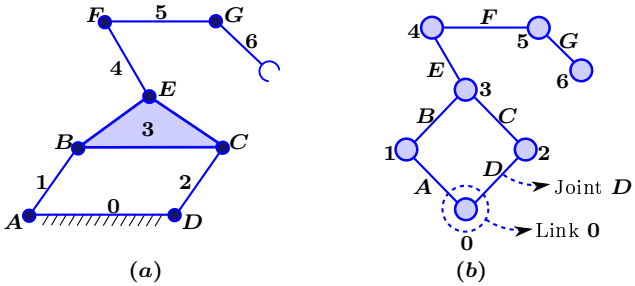

Figure 37 – (a) Hybrid manipulator and its (b) graph representation

In a graph, all types of joints are represented by edges, thus, it is necessary to introduce an additional notation in order to identify what type of joint is being represented in each kinematic chain. In this notation, a number signifies the number of kinematic chains linking the end effector or moving platform to the base, and the set of letters defines the sequence of joints used in each kinematic chain. A revolute joint is denoted by $\boldsymbol{R}$ and a prismatic joint by $\boldsymbol{P}$. Spatial universal and spherical joints are respectively denoted by $\boldsymbol{U}$ (or sometimes $\boldsymbol{RR}$) and $\boldsymbol{S}$. Actuated joints are indicated by underlining *(e.g.* $\underline{\boldsymbol{R}}$, $\underline{\boldsymbol{P}}$, $\underline{\boldsymbol{RR}}$, *etc.)* (MORRISON, 2003).

Following this line of thought, the 3$\underline{\text{R}}$RR planar parallel manipulator shown if Fig. 35(b), is a manipulator with three kinematic chains (legs) connecting the fixed and the mobile platform. Each leg has three rotational joints whose axes are perpendicular to the $(\boldsymbol{x} - \boldsymbol{y})$ plane (because is a planar manipulator), and the first joint in each leg is actuated. In a similar way, the serial planar manipulator $\underline{\text{RRR}}$ shown in Fig. 35 (a) is a manipulator with only one kinematic chain which has three rotational joints, all them actuated.

A graph to which is assigned an orientation to their edges in order to distinguish between its start vertices and arrival vertices is called a ***directed graph*** or ***digraph***, otherwise is called ***undirected graph***.

The possibility of directing a graph is important in the study of the mechanisms when it is desired to represent the static or kinematic

state of a rigid body in relation to its adjacent. In the kinematic analysis, a di-graph indicates the direction of relative movement between adjacent links. In static analysis, the direction of the edges defines if a body is applying an action in the adjacent body or if it is receiving such action. The di-graph works as a sign convention which must be respected in order to obtain correct results.

A correct representation of the restrictions and freedoms allowed in the joints of mechanisms is required in its kinematic and static analysis. This representation can be done through graphs. In order to exemplify this, suppose a revolute joint acting in a spatial system $(\boldsymbol{\lambda = 6})$ and allowing only a rotation around the $\boldsymbol{x}$ axis $(\boldsymbol{\omega_x})$ as shown in Fig. 38 (a), then, this revolute joint will have five constraints on its movement, two rotational constraints around the axis $\boldsymbol{y}$ and $\boldsymbol{z}$ $(\boldsymbol{M_y, M_z})$ and three linear constraints along the main axis $\boldsymbol{x}$, $\boldsymbol{y}$ and $\boldsymbol{z}$ $(\boldsymbol{F_x, F_y, F_z})$. Figure 38 (b) and (c) show the graph representation of this revolute joint in the kinematics and statics analysis respectively.

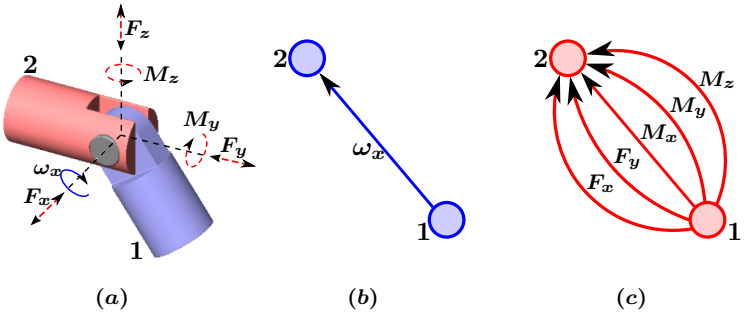

Figure 38 – (a) Revolute joint and its (b) kinematic and (c) static graph representation

Some other concepts of graphs theory directly related to the static and kinematic analysis of mechanisms and robots are mentioned below (CAZANGI, 2008; GROSS; YELLEN, 2005):

Path: *Sequence of vertices* $\boldsymbol{v_1, v_2, v_3, ..., vn}$ *where there is an edge from* $\boldsymbol{v_i}$ *to* $\boldsymbol{v_{i+1}}$.

Cycle: *A path in which the first and last vertices are the same.*

Tree: *1. connected, acyclic graph with a specially designated vertex called the root. 2. It is a graph in which at*

least one path connects each pair of vertices, but does not have circuits.

Spanning tree: *A subgraph of a connected undirected graph that contains all of its vertices and enough of its edges to form a tree. 2. A tree is called a spanning tree if it is a subgraph of any graph, so that contains all vertices of the graph, but only a subset of their edges.*

Branch: *An edge of a spanning tree is called a branch.*

Chord: *an edge in the graph that is not in the spanning tree is called a chord.*

Cut: *A cut of a connected graph is a minimal set of edges whose removal separate the graph into two components (pieces).*

A.4 KINEMATICS OF MANIPULATORS

Kinematics studies the motion of bodies without consideration of the forces or moments that cause the motion. Robot kinematics refers to the analytical study of the motion of a robot manipulator. Formulating the suitable kinematics models for a robot mechanism is very crucial for analyzing the behaviour of manipulators.

Kinematics is the science of geometry in motion. It is restricted to a pure geometrical description of motion by means of position, orientation, and their time derivatives. In robotics, the kinematic descriptions of manipulators and their assigned tasks are utilized to set up the fundamental equations for dynamics and control (JAZAR, 2007).

Because the links in a robotic system are modeled as rigid bodies, the properties of rigid body displacement takes a central place in robotics. Vector and matrix algebra are utilized to develop a systematic and generalized approach to describe and represent the location of the links of a robot with respect to a global fixed reference frame $\boldsymbol{G}$. Since the links of a robot may rotate or translate with respect to each other, body-attached coordinate frames (for instance $\boldsymbol{A}$, $\boldsymbol{B}$, $\boldsymbol{C}$,...,etc) will be established along with the joint axis for each link to find their relative configurations, and within the reference frame $\boldsymbol{G}$. The position of one link $\boldsymbol{B}$ relative to another link $\boldsymbol{A}$ is defined kinematically by a coordinate transformation ${}^{\boldsymbol{A}}\boldsymbol{T}_{\boldsymbol{B}}$ between reference frames attached to the link (JAZAR, 2007).

The direct kinematics problem is reduced to finding a transformation matrix ${}^{G}\boldsymbol{T_B}$ that relates the body attached local coordinate frame $\boldsymbol{B}$ to the global reference coordinate frame $\boldsymbol{G}$. A $\mathbf{3 \times 3}$ rotation matrix is utilized to describe the rotational operations of the local frame with respect to the global frame. The homogeneous coordinates are then introduced to represent position vectors and directional vectors in a three dimensional space. The rotation matrices are expanded to $\mathbf{4 \times 4}$ homogeneous transformation matrices to include both the rotational and translational motions. In the other hand, the inverse kinematics problem is reduced to finding the joint variables for a given configuration of a robot. The determination of the joint variables reduces to solving a set of nonlinear coupled algebraic equations (JAZAR, 2007). The relationship between direct and inverse kinematics is illustrated in Fig. 39.

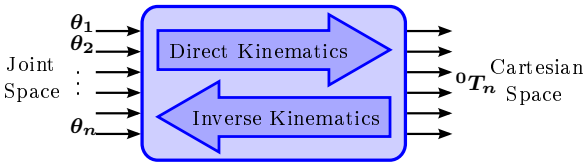

Figure 39 – The schematic representation of direct and inverse kinematics.

Although there is no standard and generally applicable method to solve the direct and inverse kinematic of robots, there are a few analytic and numerical methods that help in the solution of this problem. Some of them are: The geometrical method, The Denavit-Hartenberg (DH) method, the method of successive screw displacements and the dual quaternions method, among others.

This document do not have as main objective to describe or discuss the methods used in order to solve the direct and inverse kinematic problem, however, two basic examples are shown in order to illustrate how the direct and inverse kinematic problem can be solved. The studied manipulators used as example in the current document are a RRR planar serial manipulator and a 3RRR planar parallel manipulator. In the examples, were used the Denavit-Hartenberg (DH) method and the geometric method in order to solve the direct and inverse kinematic problem respectively, but the reader may rely on other methods in order to obtain the same results.

A.4.1 Direct Kinematic of the RRR planar serial manipulator using the Denavit-Hartenberg (DH) method:

As mentioned earlier, a serial manipulator consists of a sequence of links connected by joints. In most industrial manipulators, the links are designed to minimize deflection and consequent loss of accuracy and repeatability, and, in this sense, the links can be assumed to be rigid bodies. It is well-known that a rigid body in $\mathbf{3}\boldsymbol{D}$ space can be described (with respect to another rigid body or a reference coordinate system) completely by six independent parameters, three for the position vector of a point of interest on the link or the origin of a coordinate system attached to the rigid body and three angles for the orientation of the rigid body.

In 1955, Denavit and Hartenberg (DENAVIT; HARTENBERG, 1955), presented a formulation for describing links connected by revolute (R) or prismatic (P) joints which required only four independent parameters and thus leading to more efficient computations. Denavit-Hartenberg (DH) method that uses four parameters is the most common method for describing the robot kinematics. These parameters $\boldsymbol{a_i}$, $\boldsymbol{\alpha_i}$, $\boldsymbol{d_i}$ and $\boldsymbol{\theta_i}$ are the link length, link twist, link offset and joint angle, respectively. A coordinate frame is attached to each joint to determine DH parameters. $\boldsymbol{Z_i}$ axis of the coordinate frame is pointing along the rotary axis or sliding direction of the joints. Fig. 40 shows an example of the four parameters of classic DH convention for a general manipulator.

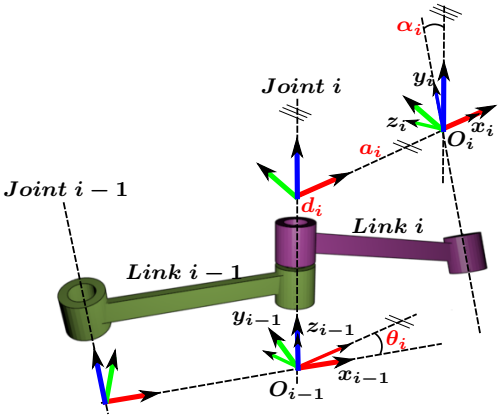

Figure 40 – The four parameters of classic DH convention are shown in red text.

In general terms, Denavit-Hartenberg method is based on the use of the four parameters of classic D-H convention and a $\mathbf{4 \times 4}$ homogeneous transformations matrix that completely describe the position and orientation of the link $\boldsymbol{i}$ with respect to the link $\boldsymbol{i-1}$. In the D-H convention, each homogeneous transformation ${}^{i-1}\boldsymbol{T_i}$ is represented as a product of four basic transformations as shown below:

$$ {}^{i-1}\boldsymbol{T_i} = \boldsymbol{Rot(z,\theta_i) \cdot Trans(z,d_i) \cdot Trans(x,a_i) \cdot Rot(x,\alpha_i)} \tag{A.5} $$

$$ {}^{i-1}\boldsymbol{T_i} = \begin{bmatrix} \boldsymbol{c\theta_i} & \boldsymbol{-s\theta_i} & \mathbf{0} & \mathbf{0} \\ \boldsymbol{s\theta_i} & \boldsymbol{c\theta_i} & \mathbf{0} & \mathbf{0} \\ \mathbf{0} & \mathbf{0} & \mathbf{1} & \mathbf{0} \\ \mathbf{0} & \mathbf{0} & \mathbf{0} & \mathbf{1} \end{bmatrix} \begin{bmatrix} \mathbf{1} & \mathbf{0} & \mathbf{0} & \mathbf{0} \\ \mathbf{0} & \mathbf{1} & \mathbf{0} & \mathbf{0} \\ \mathbf{0} & \mathbf{0} & \mathbf{1} & \boldsymbol{d_i} \\ \mathbf{0} & \mathbf{0} & \mathbf{0} & \mathbf{1} \end{bmatrix} \cdots $$
$$ \cdots \begin{bmatrix} \mathbf{1} & \mathbf{0} & \mathbf{0} & \boldsymbol{a_i} \\ \mathbf{0} & \mathbf{1} & \mathbf{0} & \mathbf{0} \\ \mathbf{0} & \mathbf{0} & \mathbf{1} & \mathbf{0} \\ \mathbf{0} & \mathbf{0} & \mathbf{0} & \mathbf{1} \end{bmatrix} \begin{bmatrix} \mathbf{1} & \mathbf{0} & \mathbf{0} & \mathbf{0} \\ \mathbf{0} & \boldsymbol{c\alpha_i} & \boldsymbol{-s\alpha_i} & \mathbf{0} \\ \mathbf{0} & \boldsymbol{s\alpha_i} & \boldsymbol{c\alpha_i} & \mathbf{0} \\ \mathbf{0} & \mathbf{0} & \mathbf{0} & \mathbf{1} \end{bmatrix} \tag{A.6} $$

$$ {}^{i-1}\boldsymbol{T_i} = \begin{bmatrix} \boldsymbol{c\theta_i} & \boldsymbol{-s\theta_i \cdot c\alpha_i} & \boldsymbol{s\theta_i \cdot s\alpha_i} & \boldsymbol{a_i \cdot c\alpha_i} \\ \boldsymbol{s\theta_i} & \boldsymbol{c\theta_i \cdot c\alpha_i} & \boldsymbol{-c\theta_i \cdot s\alpha_i} & \boldsymbol{a_i \cdot s\alpha_i} \\ \mathbf{0} & \boldsymbol{s\alpha_i} & \boldsymbol{c\alpha_i} & \boldsymbol{d} \\ \mathbf{0} & \mathbf{0} & \mathbf{0} & \mathbf{1} \end{bmatrix} \tag{A.7} $$

To obtain the transformation matrix of a link i with respect to any other link, product of transformation matrices can be used. For example, the link $\boldsymbol{i}$ can be described with respect to the fixed base or reference coordinate system $\mathbf{\{0\}}$ as:

$$ {}^{0}\boldsymbol{T_i} = {}^{0}\,\boldsymbol{T_1}\;{}^{1}\boldsymbol{T_2}\;\ldots\;{}^{i-1}\boldsymbol{T_i} \tag{A.8} $$

To illustrate the concept of Denavit-Hartenberg parameters and link transformation matrices, below is solved the Direct Kinematic of the RRR planar serial manipulator shown in Fig. 41. In this example, all the rotary joint axes are parallel and are pointing out of the paper. The Denavit-Hartenberg parameters are obtained as follows.

The fixed or reference coordinate system, $\mathbf{\{0\}}$, is chosen with its $\boldsymbol{z_0}$ coming out of the paper, and $\boldsymbol{x_0}$ and $\boldsymbol{y_0}$ pointing to the right and top, respectively. For the first coordinate system, the origin $\boldsymbol{O_1}$ and

z_1 are coincident with O_0 and z_0, and x_1 and y_1 are coincident with x_0 and y_0 when θ_1 is zero. The x_1 is along the mutual perpendicular between z_1 and z_2. Similarly, x_2 is along the mutual perpendicular between z_2 and z_3. For the last frame, x_3 is aligned to x_2 when $\theta_3 = 0$. The origin O_2 is located at the intersection of the mutual perpendicular along x_2 and z_2. The origin O_3 is chosen such that d_3 is zero. The origins and the axes of {1}, {2}, and {3} are as shown in Fig. 41.

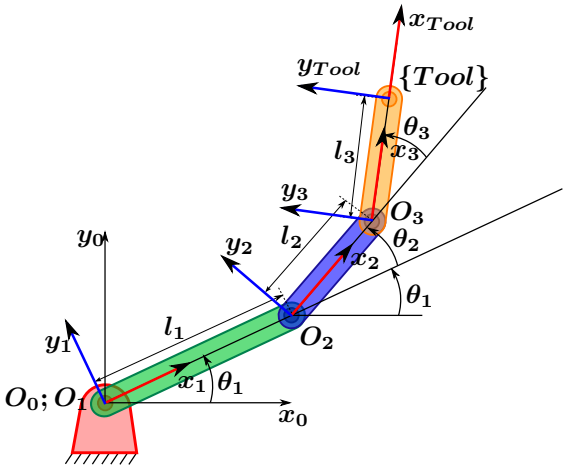

Figure 41 – Illustration of a RRR serial planar manipulator

From the assigned origins and axes, the Denavit-Hartenberg parameters can be obtained by inspection. They are presented in a tabular form below:

Table 6 – The D-H parameters of the RRR planar serial manipulator.

i	α_i	a_i	d_i	θ_i
1	0	0	0	θ_1
2	0	l_1	0	θ_2
3	0	l_2	0	θ_3

In the Table 6, l_1 and l_2 are the link lengths as shown in Fig. 41. It may be noted that the length of the end-effector does not appear in Table 6. To describe the end-effector, we attach a tool frame, {Tool}, aligned to {3} at the mid-point of the parallel jaw gripper. In Fig. 41,

the origin of $\{Tool\}$ is shown at a distance of l_3 from O_3 along X_3. From the DH table, using Eq. A.7, the link transformation matrices can be obtained by substitution. For $i = 1$, $a_i = 0$, $\alpha_i = 0$ and $d_i = 0$. Denoting $\sin(\theta_1)$ and $\cos(\theta_2)$ by s_1 and c_1, respectively, one can get

$$ {}^0T_1 = \begin{bmatrix} c\theta_1 & -s\theta_1 & 0 & 0 \\ s\theta_1 & c\theta_1 & 0 & 0 \\ 0 & 0 & 1 & 0 \\ 0 & 0 & 0 & 1 \end{bmatrix} \tag{A.9} $$

Similarly, for $i = 2$ ($a_i = l_1$, $\alpha_i = 0$, and $d_i = 0$) and for $i = 3$ ($a_i = l_2$, $\alpha_i = 0$ and $d_i = 0$).

$$ {}^1T_2 = \begin{bmatrix} c\theta_2 & -s\theta_2 & 0 & l_1 \\ s\theta_2 & c\theta_2 & 0 & 0 \\ 0 & 0 & 1 & 0 \\ 0 & 0 & 0 & 1 \end{bmatrix} \tag{A.10} $$

$$ {}^2T_3 = \begin{bmatrix} c\theta_3 & -s\theta_3 & 0 & l_2 \\ s\theta_3 & c\theta_3 & 0 & 0 \\ 0 & 0 & 1 & 0 \\ 0 & 0 & 0 & 1 \end{bmatrix} \tag{A.11} $$

To find the transformation matrix ${}^3T_{\{Tool\}}$, the orientation of $\{Tool\}$ is assumed to be the same as the orientation of $\{3\}$ and the origin is at a distance l_3 along x_3. Hence

$$ {}^3T_{\{Tool\}} = \begin{bmatrix} 1 & 0 & 0 & l_3 \\ 0 & 1 & 0 & 0 \\ 0 & 0 & 1 & 0 \\ 0 & 0 & 0 & 1 \end{bmatrix} \tag{A.12} $$

To find the transformation matrix ${}^0T_3$, multiply ${}^0T_1\ {}^1T_2\ {}^2T_3$ resulting in

$$ {}^3T_{\{Tool\}} = \begin{bmatrix} c_{123} & -s_{123} & 0 & l_1c_1 + l_2c_{12} \\ s_{123} & c_{123} & 0 & l_1s_1 + l_2s_{12} \\ 0 & 0 & 1 & 0 \\ 0 & 0 & 0 & 1 \end{bmatrix} \tag{A.13} $$

Finally, to obtain ${}^0T_{\{Tool\}}$, multiply ${}^0T_3\ {}^3T_{\{Tool\}}$ and get

$$ {}^{0}\boldsymbol{T}_{\{\boldsymbol{Tool}\}} = \begin{bmatrix} \boldsymbol{c_{123}} & \boldsymbol{-s_{123}} & \boldsymbol{0} & \boldsymbol{l_1 c_1 + l_2 c_{12} + l_3 c_{123}} \\ \boldsymbol{s_{123}} & \boldsymbol{c_{123}} & \boldsymbol{0} & \boldsymbol{l_1 s_1 + l_2 s_{12} + l_3 s_{123}} \\ \boldsymbol{0} & \boldsymbol{0} & \boldsymbol{1} & \boldsymbol{0} \\ \boldsymbol{0} & \boldsymbol{0} & \boldsymbol{0} & \boldsymbol{1} \end{bmatrix} \quad \text{(A.14)} $$

A.4.2 Inverse Kinematic of the 3RRR planar parallel manipulator using the graphic method:

Parallel manipulators usually consist in a mobile platform connected to a fixed platform by several branches in order to transmit the movement. Generally, the number of branches of parallel manipulators is equal to their degree of freedom (DoF), and the motors are usually located near the fixed base (TSAI, 1999).

In the 3RRR planar parallel manipulator studied in this section, the fixed and mobile platforms are joined by using three branches as shown in Fig. 42. Each branch has three rotational joints whose axes are perpendicular to the $(\boldsymbol{x}-\boldsymbol{y})$ plane, and the first of the three joints in each branch is actuated. Furthermore, the mobile and fixed platforms are formed by equilateral triangles with sides $\boldsymbol{l_m}$ and $\boldsymbol{l_f}$ respectively. The branches are formed by two links with lengths $\boldsymbol{l_1}$ and $\boldsymbol{l_2}$ respectively, the distance between one of the mobile platform vertices and its centroid ($\boldsymbol{E}$) is called $\boldsymbol{l_3}$ and the angle $\boldsymbol{\phi}$ represents the orientation of the mobile platform.

In order to obtain the inverse kinematics of the parallel manipulator, the first step is to obtain the coordinates of the vertices $\boldsymbol{C_1}$, $\boldsymbol{C_2}$ and $\boldsymbol{C_3}$ at the mobile platform as a function of its centroid $\boldsymbol{E}$, the angle of orientation $\boldsymbol{\phi}$ and the lengths $\boldsymbol{l_3}$ and $\boldsymbol{l_m}$. The obtention of the coordinates of the vertices $\boldsymbol{C_1}$, $\boldsymbol{C2}$ and $\boldsymbol{C_3}$ is supported by Fig. 43 and is shown in Eqs. A.15, A.16 and A.17.

$$ \boldsymbol{C_1 = (C_{1x}, C_{1y}) = (E_x - l_3 \cdot \cos(\phi + 30°), E_y - l_3 \cdot \sin(\phi + 30°))} \quad \text{(A.15)} $$

$$ \boldsymbol{C_2 = (C_{2x}, C_{2y}) = (C_{1x} + l_m \cdot \cos(\phi), C_{1y} + l_m \cdot \sin(\phi)} \quad \text{(A.16)} $$

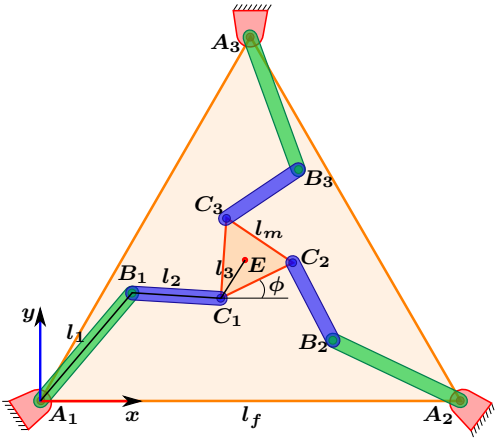

Figure 42 – Illustration of a RRR parallel planar manipulator

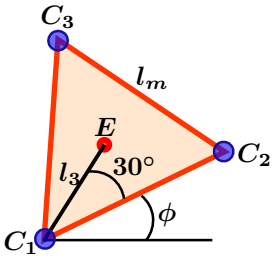

Figure 43 – Schematic representation of the mobile platform in a RRR parallel planar manipulator.

$$\boldsymbol{C_3 = (C_{3x}, C_{3y}) = (C_{1x}+l_m \cdot \cos(\phi+60°), C_{1y}+l_m \cdot \sin(\phi+60°)} \tag{A.17}$$

From Fig. 42, it is possible to observe that the origin of the system is located in $\boldsymbol{A_1}$. it allows us to calculate in a simple way the position of the joints $\boldsymbol{A_1}$, $\boldsymbol{A_2}$ and $\boldsymbol{A_3}$ as shown below in Eqs. A.18, A.19 and A.20.

$$\boldsymbol{A_1 = (A_{1x}, A_{1y}) = (0, 0)} \tag{A.18}$$

$$\boldsymbol{A_2 = (A_{2x}, A_{2y}) = (l_f, 0)} \tag{A.19}$$

$$\boldsymbol{A_3} = (\boldsymbol{A_{3x}}, \boldsymbol{A_{3y}}) = (\boldsymbol{l_f} \cdot \mathbf{cos}(\mathbf{60°}), \boldsymbol{l_f} \cdot \mathbf{sin}(\mathbf{60°})) \tag{A.20}$$

And finally, the position of the joints $\boldsymbol{B_1}$, $\boldsymbol{B_2}$ and $\boldsymbol{B_3}$ can be calculated using simple trigonometric relations. In order to exemplify the procedure, the leg $\boldsymbol{A_1B_1C_1}$ is shown in Fig. 44 and the calculus for the position of the joint $\boldsymbol{B_1}$ is shown below in Eqs. A.21 to A.25. Similar procedures can be used in order to obtain the position of the joints $\boldsymbol{B_2}$ and $\boldsymbol{B_3}$, even if the assembly mode is different to such as shown in Fig. 44.

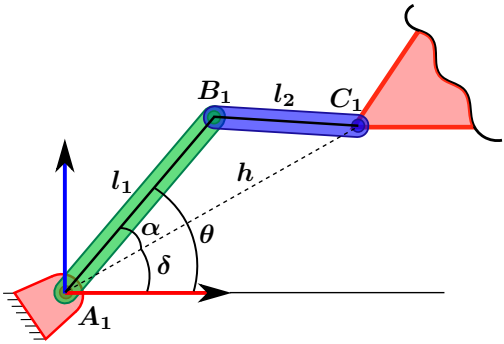

Figure 44 – Schematic representation of the leg $\boldsymbol{A_1B_1C_1}$ in the RRR parallel planar manipulator.

$$\boldsymbol{B_1} = (\boldsymbol{B_{1x}}, \boldsymbol{B_{1y}}) = (\boldsymbol{l_1} \cdot \mathbf{cos}(\boldsymbol{\theta}), \boldsymbol{l_1} \cdot \mathbf{sin}(\boldsymbol{\theta})) \tag{A.21}$$

where

$$\boldsymbol{\theta} = \boldsymbol{\delta} + \boldsymbol{\alpha} \tag{A.22}$$

$$\boldsymbol{\delta} = \mathbf{arctan}\left(\frac{\boldsymbol{C_{1y}}}{\boldsymbol{C_{1x}}}\right) \tag{A.23}$$

$$\boldsymbol{\alpha} = \mathbf{arccos}\left(\frac{\boldsymbol{h^2} + \boldsymbol{l_1^2} - \boldsymbol{l_2^2}}{\boldsymbol{2 l_1 h}}\right) \tag{A.24}$$

$$\boldsymbol{h} = \sqrt{\boldsymbol{C_{1x}^2} + \boldsymbol{C_{1y}^2}} \tag{A.25}$$

APPENDIX B – Static analysis of mechanisms and manipulators

In the static analysis of manipulators, the goal is to determine the force and moment requirements for the joints in relation to the wrenches applied at the end effector. It is possible to apply forces and moments at the joints of the mechanism to analyze the wrenches obtained at the end effector, or to apply external wrenches at the end effector to calculate the forces and moments required at the joints to balance these external forces.

There are several methodologies which allow us to obtain a complete static analysis of manipulators; however, in this thesis the formalism presented by Davies (DAVIES, 1983c) is used as the primary mathematical tool to analyze the mechanisms statically. In this Appendix, the Davies method is presented together to its main conceptual tools. The dynamic effects given by the gravitational force, acceleration, inertia, among others are not considered herein, and only the instantaneous kinematics and statics of mechanisms constituted by rigid bodies are taken into account.

The Davies method provides a systematic way to relate the joint forces and moments in closed kinematic chains (CAZANGI, 2008). This method is based on ***graph theory***, ***screw theory*** and the ***Kirchhoff cut-set law*** and it can be used to obtain the statics of a manipulator as a matricial expression (CAZANGI, 2008).

In the current document the Davies method is widely used because the obtention of the static model of a manipulator or mechanism is simple and easily adaptable, furthermore, it is not necessary to use a pseudo-inverse as in other methodologies. Additionally, the Davies method together with the proposed methods in this thesis constitute a powerful tool to solve the force capability problem in mechanisms and manipulators.

The Davies method uses the graph theory and the Kirchhoff cut-set law in order to represent the relation between the unknown variables, however, the physical characteristics (mechanical quantities), such as forces, moments, etc., are included in the formulation through screws. Therefore, the screw theory is presented for the static case in Sections B.1 and B.2.

The Davies method appears in many publications in the literature and further explanations regarding its use can be found in (DAVIES, 1983a, 1983b, 1983c; CAZANGI, 2008; WEIHMANN, 2011).

B.1 THEORETICAL REVIEW ON THE SCREW THEORY

Screw theory is the algebra and calculus of pairs of vectors, such as forces and moments and angular and linear velocity, that arise in the kinematics and dynamics of rigid bodies (YANG, 1974). The mathematical framework for application in kinematics and statics of mechanisms was initially formulated by Mozzi (MOZZI, 1763) and later systematized by Ball (BALL, 1876, 1900). The screw theory has been an important object of study in recent decades and it has found in the study of mechanisms and robotics a fertile field for their application (DAVIDSON; HUNT, 2004).

In the same way that a point (geometric element) can be used to represent a particle of mass, and a directed line (geometric element) can be used to represent a moment, a screw (geometric element) can also be useful in the representation of mechanical quantities (CAMPOS, 2004).

Geometrically, a screw $\$$ is nothing else than a line $\boldsymbol{l}$ together with a scalar pitch $\boldsymbol{\lambda}$:

$$\$:= (\boldsymbol{l}, \boldsymbol{\lambda}) \tag{B.1}$$

Since the dimension of the space of lines is four, the dimension of the space of screws is five. Note that a screw, as a line, does not have any module information a priori. If this module information is given as we did with the line, we get a six-dimensional space of measurable screws. If the line $\boldsymbol{l}$ representing the screw $\$$ is defined by using a unit vector, the screw is said to be a normalized screw $\hat{\$}$. A screw can be conveniently expressed by using the six Plücker's homogeneous coordinates as shown in the following equation:

$$\$ = \begin{pmatrix} \vec{\boldsymbol{S}} \\ ------ \\ \vec{\boldsymbol{S}}_{\boldsymbol{0}} \times \vec{\boldsymbol{S}} + h\vec{\boldsymbol{S}} \end{pmatrix} = \begin{pmatrix} \boldsymbol{L} \\ \boldsymbol{M} \\ \boldsymbol{N} \\ ------ \\ \boldsymbol{P^* = P + hL} \\ \boldsymbol{Q^* = Q + hM} \\ \boldsymbol{R^* = R + hN} \end{pmatrix} \tag{B.2}$$

In Eq. B.2, $\vec{\boldsymbol{S}}$ is the direction vector along the axis of the screw,

$\vec{S_0}$ is the position vector at any point of the screw axis relative to the origin of the coordinate system (O_{xyz}) and L, M, N, P^*, Q^* and R^* are the Plücker's homogeneous coordinates (ZHAO; FENG; DONG, 2006). In screw notation, the components are often separated by markers (dotted in a matrix form) to facilitate distinction of the pair of vectors.

A screw that is used in order to describe the differential kinematic of mechanisms is commonly called a ***"Twist"***, and a screw that is used in order to describe the statics of mechanisms is commonly called a ***"Wrench"***. The following section presents a review of the screws used in the static analysis of mechanisms and manipulators.

B.2 THE SCREW IN THE STATICS: "THE WRENCH"

The force and torque vectors that arise in applying Newton's laws to a rigid body can be assembled into a screw called a wrench $(\$^A)$. A force has a point of application and a line of action, therefore it defines the Plücker coordinates of a line in space and has zero pitch. A torque, on the other hand, is a pure moment that is not bound to a line in space and is an infinite pitch screw. The ratio of these two magnitudes defines the pitch of the screw (POINSOT, 1806). In static analysis, depending on the point chosen to define the equilibrium equations, the forces may also generate a torque regarding this point (DAVIES, 1995).

The wrench is composed of a vector $\vec{R}$ that is the force acting along the normalized action line $\vec{S}^A$ and a vector $\vec{T_P}$ representing the torque calculated at a specific point of the body. The components (L, M, P) of the force vector $\vec{R}$, represent the forces in the directions of each of the main axes x, y and z of the reference coordinate system. The torque $\vec{T_P}$ is composed by the couple $\vec{T}$ (whose axis is parallel to $\vec{S}^A$) and the moment due to the action of the force $\vec{R}$, calculated by the cross product between the vectors $\vec{S_0}$ and $\vec{R}$ (see Fig. 45). The components (P^*, Q^*, R^*) of the moment T_P represent the moments about each of the main axes x, y and z of the reference coordinate system. The vector $\vec{S}^A$ is a unit vector and corresponds to the screw's axis of actuation, finally, the vector S_0 is the position vector of a point on the screw axis $(\vec{S}_A)$, relative to the point P that was chosen to define the equilibrium equations (DAVIES, 1995).

The torque $\vec{T}$ has units $[force] \times [length]$ and can be related to the force $\vec{R}$ through the pitch of the screw (h) employing Eq. B.3.

$$\vec{T} = h\vec{R} \tag{B.3}$$

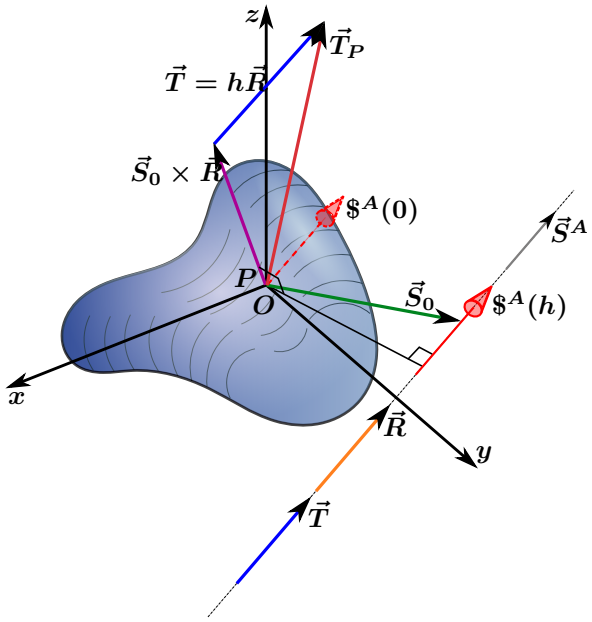

Figure 45 – Wrench determination on a rigid body

As seen in Eq. (B.4) it is possible to normalize the wrench, separating it into a geometric component $\widehat{\$}^{\boldsymbol{A}}$ without an associated dimension and a scalar component $\boldsymbol{\psi}$ with units of force. The actions transferred or constrained by a joint connecting two consecutive links can be represented through a wrench. Because generally the scalar that defines the action axis does not point at one of the main directions of the coordinate system, it is usual to represent each constraint through a wrench called the unitary wrench. The resulting wrench is the summation of the existing unit wrenches. Constraints can be decomposed into three forces $(\boldsymbol{Fx}, \boldsymbol{Fy}, \boldsymbol{Fz})$ and three moments $(\boldsymbol{Mx}, \boldsymbol{My}, \boldsymbol{Mz})$ for the main axes $\boldsymbol{x}$, $\boldsymbol{y}$ and $\boldsymbol{z}$ respecting the conventions of a $\boldsymbol{O_{XYZ}}$ right-handed coordinate system as shown in Fig. 46.

If the wrench represents a pure force, the pitch of the wrench is zero $(\boldsymbol{h = 0})$, and the component $(\vec{\boldsymbol{T}}_{\boldsymbol{P}})$ representing the torque is reduced to $\vec{\boldsymbol{S}}_{\boldsymbol{0}} \times \vec{\boldsymbol{R}}$. Knowing the coordinates $\boldsymbol{p_x}$, $\boldsymbol{p_y}$, and $\boldsymbol{p_z}$ determining the vector $\vec{\boldsymbol{S}}_{\boldsymbol{0}}$, each constraint can be written as a unit wrench and the magnitude of each force has dimensions as shown in Eq. B.5.

$$\$ = \begin{pmatrix} \vec{T_P} \\ -- \\ \vec{R} \end{pmatrix} = \begin{pmatrix} P^* \\ Q^* \\ R^* \\ -- \\ L \\ M \\ N \end{pmatrix} = \begin{pmatrix} \vec{S_0} \times \vec{R} + h\vec{R} \\ ------ \\ \vec{R} \end{pmatrix} = \dots$$

$$\dots \begin{pmatrix} (\vec{S_0} \times \vec{S^A} + h\vec{S^A})\psi \\ ------ \\ \vec{S^A}\psi \end{pmatrix} = \begin{pmatrix} (\vec{S_0} \times \vec{S^A} + h\vec{S^A}) \\ ------ \\ \vec{S^A} \end{pmatrix} \psi = \hat{\$}^A \psi \tag{B.4}$$

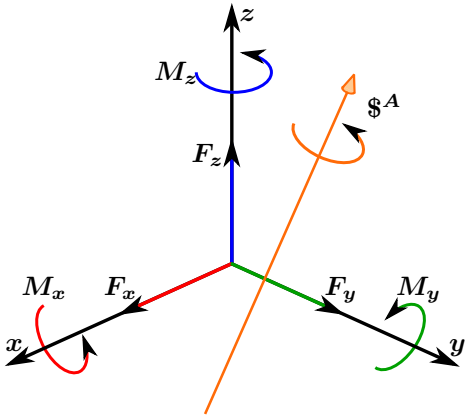

Figure 46 – Wrench decomposition on a right-handed coordinate system

If the wrench represents a couple (pure moment), the pitch of the wrench is considered infinite ($h = \infty$) and the force $\vec{R}$ is zero. Therefore, only exist the component $\vec{T}$ of the wrench which can be decomposed in the three main directions of the reference system as shown in Eq. B.6, where the magnitudes of each unit wrench is [$force$] × [$length$].

$$\$ = \begin{bmatrix} \vec{T_P} \\ -- \\ \vec{R} \end{bmatrix} = \begin{bmatrix} \vec{S_0} \times \vec{R} \\ - - - \\ F_x \\ F_y \\ F_z \end{bmatrix} = \begin{bmatrix} -p_z F_y + p_y F_z \\ p_z F_x - p_x F_z \\ -p_y F_x + p_x F_y \\ - - - - - - \\ F_x \\ F_y \\ F_z \end{bmatrix} = \ldots$$

$$\ldots = \begin{bmatrix} 0 \\ p_z \\ -p_y \\ -- \\ 1 \\ 0 \\ 0 \end{bmatrix} F_x + \begin{bmatrix} -p_z \\ 0 \\ p_x \\ -- \\ 0 \\ 1 \\ 0 \end{bmatrix} F_y + \begin{bmatrix} p_y \\ -p_x \\ 0 \\ -- \\ 0 \\ 0 \\ 1 \end{bmatrix} F_z \tag{B.5}$$

$$\$ = \begin{bmatrix} \vec{T} \\ -- \\ 0 \end{bmatrix} = \begin{bmatrix} M_x \\ M_y \\ M_z \\ -- \\ 0 \\ 0 \\ 0 \end{bmatrix} = \begin{bmatrix} M_x \\ 0 \\ 0 \\ -- \\ 0 \\ 0 \\ 0 \end{bmatrix} + \begin{bmatrix} 0 \\ M_y \\ 0 \\ -- \\ 0 \\ 0 \\ 0 \end{bmatrix} + \begin{bmatrix} 0 \\ 0 \\ M_z \\ -- \\ 0 \\ 0 \\ 0 \end{bmatrix} = \ldots$$

$$\ldots = \begin{bmatrix} 1 \\ 0 \\ 0 \\ -- \\ 0 \\ 0 \\ 0 \end{bmatrix} M_x + \begin{bmatrix} 0 \\ 1 \\ 0 \\ -- \\ 0 \\ 0 \\ 0 \end{bmatrix} M_y + \begin{bmatrix} 0 \\ 0 \\ 1 \\ -- \\ 0 \\ 0 \\ 0 \end{bmatrix} M_z \tag{B.6}$$

In static analysis of mechanisms using the Davies method, it is desirable that all existing wrenches are represented over the same point (generally the origin system), avoiding the need to transform the coordinates to determine the equilibrium equations (DAVIES, 1995).

B.3 SUMMARY OF THE DAVIES METHOD

The Davies method for static analysis can be described in a simplified way through the following steps:

1. Given a mechanism, draw its kinematic chain identifying all of its *"n"* links and *"e"* direct couplings.

2. Draw the coupling graph *"G_C"* for the mechanism with the links of the mechanism as the vertices of the graph, and the joints of the mechanism as the edges of the graph.

3. Generate the action graph *"G_A"* from *"G_C"* through unfolding single actions from direct couplings. In this step, each edge of *"G_C"* representing a coupling is replaced in *"G_A"* by c constraint edges in parallel.

   - Assign positive directions to each edge with an arrow pointing from the minor to major vertex.
   - Locate the number of cuts ($k = n - 1$) and chords ($c = e - n + 1$) in the action graph and depict them.

4. Write the cut-set matrix $[Q_N]_{k,e}$ with suitable signs.

5. Write a wrench $\$_J$ for each edge from G_A as follows:

$$\$_J == \begin{bmatrix} 0 \\ p_z \\ -p_y \\ -- \\ 1 \\ 0 \\ 0 \end{bmatrix} J_{Fx} + \begin{bmatrix} -p_z \\ 0 \\ p_x \\ -- \\ 0 \\ 1 \\ 0 \end{bmatrix} J_{Fy} + \begin{bmatrix} p_y \\ -p_x \\ 0 \\ -- \\ 0 \\ 0 \\ 1 \end{bmatrix} J_{Fz} + \ldots$$

$$\ldots + \begin{bmatrix} 1 \\ 0 \\ 0 \\ -- \\ 0 \\ 0 \\ 0 \end{bmatrix} J_{Mx} + \begin{bmatrix} 0 \\ 1 \\ 0 \\ -- \\ 0 \\ 0 \\ 0 \end{bmatrix} J_{My} + \begin{bmatrix} 0 \\ 0 \\ 1 \\ -- \\ 0 \\ 0 \\ 0 \end{bmatrix} J_{Mz} \tag{B.7}$$

6. Replace each wrench $\$_J$ in the cut-set matrix $[Q_N]_{k,e}$ in order to obtain the generalized action matrix $[A_N]_{3k,e}$

7. Operate algebraically the generalized action matrix $[A_N]_{3k,e}$ in order to statically solve the system.

B.4 NET DEGREE OF CONSTRAINT (C_N)

The net degree of constraint (C_N) is an intrinsic property obtained from the Davies method and is defined as the number of primary variables needed to solve the static problem. The net degree of constraint (C_N) can be directly obtained from the action graph of the mechanism, and it can be computed as shown in Eq. (B.8).

$$C_N = C - \lambda k \tag{B.8}$$

where C represents the total number of internal constraints of the mechanism, λ represents the dimension of the task space in which the mechanism works (in planar mechanisms $\lambda = 3$) and k is the number of cuts in the action graph. In order to exemplify the computational process to obtain the net degree of constraint, suppose the planar serial manipulator shown in Fig. 47 (a) and depicted by the action graph shown in Fig. 47 (b). In the action graph, the vertices of the graph represent the links of the manipulator and the edges of the graph represent the actions at the joints of the manipulator.

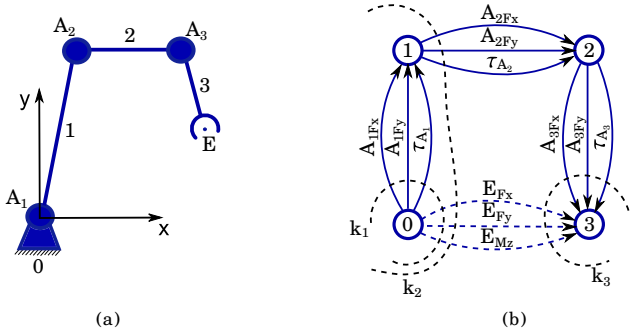

Figure 47 – (a). Planar serial manipulator with 3 DoF. (b). Action graph of the planar serial manipulator

From the action graph shown in Fig. 47 (b). it is possible to observe that the total number of internal constraints is equal to twelve

($\boldsymbol{C = 12}$), represented as the twelve arrows in the graph, the number of cuts in the graph is equal to three $\boldsymbol{k = 3}$ ($\boldsymbol{k_1, k_2, k_3}$) and due that the manipulator is a planar system the dimension of the task space is $\boldsymbol{\lambda = 3}$. By using Eq. (B.8), it is possible to obtain the net degree of constraint as shown below:

$$\boldsymbol{C_N = C - \lambda k = 12 - 3 \cdot 3 = 12 - 9 = 3} \tag{B.9}$$

B.4.1 Static models of mechanisms and manipulators

In planar manipulators, once the Davies method has been applied in order to obtain their inverse statics, it is possible to represent the $\boldsymbol{N}$ primary actions $[\boldsymbol{\tau_1, \tau_2, ..., \tau_N}]^{\boldsymbol{T}}$ as a generalized function of a coefficient matrix $[\boldsymbol{A}]$ and the wrenches at the end effector $[\boldsymbol{F_x, F_y, M_z}]^{\boldsymbol{T}}$, as shown in Eq. (B.10).

$$\begin{bmatrix} \boldsymbol{\tau_1} \\ \boldsymbol{\tau_2} \\ \vdots \\ \boldsymbol{\tau_N} \end{bmatrix} = \begin{bmatrix} \boldsymbol{a_{1,1}} & \boldsymbol{a_{1,2}} & \boldsymbol{a_{1,3}} \\ \boldsymbol{a_{2,1}} & \boldsymbol{a_{2,2}} & \boldsymbol{a_{2,3}} \\ \vdots & \vdots & \vdots \\ \boldsymbol{a_{N,1}} & \boldsymbol{a_{N,2}} & \boldsymbol{a_{N,3}} \end{bmatrix} \cdot \begin{bmatrix} \boldsymbol{F_x} \\ \boldsymbol{F_y} \\ \boldsymbol{M_z} \end{bmatrix} \tag{B.10}$$

In Eq. (B.10) the $\boldsymbol{a_{1,1}, \ldots, a_{N,3}}$ elements represent kinematic expressions as a function of the manipulator joint positions, the $\boldsymbol{\tau_1, \tau_2, ..., \tau_N}$ elements represent the actions (forces/moments) of the actuated joints and the elements $\boldsymbol{F_x, F_y, M_z}$ represent the wrenches at the end effector. In this way, the serial manipulator shown in Fig. 47 (a) (that is a manipulator with a net degree of constraint equal to three ($\boldsymbol{C_N = 3}$)), can have their inverse static model as shown in Eq. (B.11), and the serial manipulator shown in Fig. 48 (that is a manipulator with a net degree of constraint equal to three ($\boldsymbol{C_N = 3}$)), can have their inverse static model as shown in Eq. (B.12).

$$\begin{bmatrix} \boldsymbol{\tau_{A_1}} \\ \boldsymbol{\tau_{A_2}} \\ \boldsymbol{\tau_{A_3}} \end{bmatrix} = \begin{bmatrix} \boldsymbol{a_{1,1}} & \boldsymbol{a_{1,2}} & \boldsymbol{a_{1,3}} \\ \boldsymbol{a_{2,1}} & \boldsymbol{a_{2,2}} & \boldsymbol{a_{2,3}} \\ \boldsymbol{a_{3,1}} & \boldsymbol{a_{3,2}} & \boldsymbol{a_{3,3}} \end{bmatrix} \cdot \begin{bmatrix} \boldsymbol{E_{F_x}} \\ \boldsymbol{E_{F_y}} \\ \boldsymbol{E_{M_z}} \end{bmatrix} \tag{B.11}$$

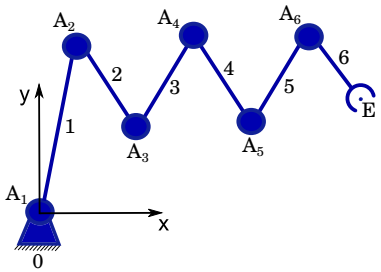

Figure 48 – Planar serial manipulator with 6 DoF.

$$\begin{bmatrix} \tau_{A_1} \\ \tau_{A_2} \\ \tau_{A_3} \\ \tau_{A_4} \\ \tau_{A_5} \\ \tau_{A_6} \end{bmatrix} = \begin{bmatrix} a_{1,1} & a_{1,2} & a_{1,3} \\ a_{2,1} & a_{2,2} & a_{2,3} \\ a_{3,1} & a_{3,2} & a_{3,3} \\ a_{4,1} & a_{4,2} & a_{4,3} \\ a_{5,1} & a_{5,2} & a_{5,3} \\ a_{6,1} & a_{6,2} & a_{6,3} \end{bmatrix} \cdot \begin{bmatrix} E_{F_x} \\ E_{F_y} \\ E_{M_z} \end{bmatrix} \tag{B.12}$$

In the other hand, in planar manipulators which the direct statics has been solved using the Davies method, it is possible to represent the wrenches at the end effector $[F_x, F_y, M_z]^T$ as a generalized function of a coefficient matrix $[A]$ and the N primary actions $[\tau_1, \tau_2, ..., \tau_N]^T$, as shown in Eq. (B.13).

$$\begin{bmatrix} F_x \\ F_y \\ M_z \end{bmatrix} = \begin{bmatrix} a_{1,1} & a_{1,2} & \cdots & a_{1,N} \\ a_{2,1} & a_{2,2} & \cdots & a_{2,N} \\ a_{3,1} & a_{3,2} & \cdots & a_{3,N} \end{bmatrix} \cdot \begin{bmatrix} \tau_1 \\ \tau_2 \\ \vdots \\ \tau_N \end{bmatrix} \tag{B.13}$$

Similarly as in the inverse statics, In Eq. (B.13) the $a_{1,1}, \ldots, a_{3,N}$ elements represent kinematic expressions as a function of the manipulator joint positions, the $\tau_1, \tau_2, ..., \tau_N$ elements represent the actions of the actuated joints and the elements F_x, F_y, M_z represent the wrenches at the end effector. In this way, the parallel manipulator shown in Fig. 49 (a) (that is a manipulator with a net degree of con-

straint equal to three $\boldsymbol{C_N = 3}$), can have their direct static model as shown in Eq. (B.14), and the parallel manipulator shown in Fig. 49(b) (that is a manipulator with a net degree of constraint equal to six $\boldsymbol{C_N = 6}$), can be statically modelled as shown in Eq. (B.15).

$$\begin{bmatrix} F_x \\ F_y \\ M_z \end{bmatrix} = \begin{bmatrix} a_{1,1} & a_{1,2} & a_{1,3} \\ a_{2,1} & a_{2,2} & a_{2,3} \\ a_{3,1} & a_{3,2} & a_{3,3} \end{bmatrix} \cdot \begin{bmatrix} \tau_1 \\ \tau_2 \\ \tau_3 \end{bmatrix} \tag{B.14}$$

$$\begin{bmatrix} F_x \\ F_y \\ M_z \end{bmatrix} = \begin{bmatrix} a_{1,1} & a_{1,2} & a_{1,3} & a_{1,4} & a_{1,5} & a_{1,6} \\ a_{2,1} & a_{2,2} & a_{2,3} & a_{2,4} & a_{2,5} & a_{2,6} \\ a_{3,1} & a_{3,2} & a_{3,3} & a_{3,4} & a_{3,5} & a_{3,6} \end{bmatrix} \cdot \begin{bmatrix} \tau_1 \\ \tau_2 \\ \tau_3 \\ \tau_4 \\ \tau_5 \\ \tau_6 \end{bmatrix} \tag{B.15}$$

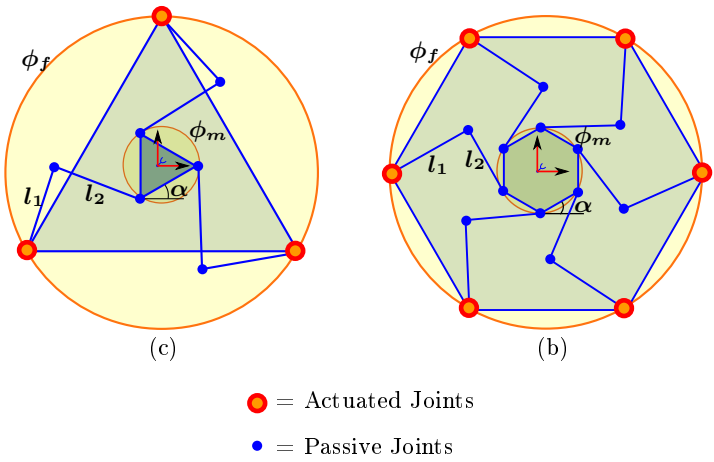

Figure 49 – (a). Non-Redundantly-actuated 3$\underline{\text{R}}$RR planar parallel manipulator ($\boldsymbol{C_N = 3}$). (b). Redundantly-actuated 6$\underline{\text{R}}$RR planar parallel manipulator ($\boldsymbol{C_N = 6}$).

It should be emphasized that although so far, it has been shown

only a few examples of manipulators with $\boldsymbol{C_N = 3}$ and $\boldsymbol{C_N = 6}$, these are not the only mechanisms with this property, in fact, there is a huge number of them.

APPENDIX C – Global Optimization

Engineering consists of a number of well established activities, including analysis, design, fabrication, research, and the development of systems. The process of designing and fabricating systems has been developed over centuries and it is maybe the major field in the engineering profession. The existence of many complex systems, such as buildings, bridges, highways, automobiles, airplanes, space vehicles, robots and others, is an excellent testimonial for this process. However, the evolution of these systems has been slow. The entire process has been both time-consuming and costly, requiring substantial human and material resources (ARORA, 2004).

The design of complex systems requires data processing and a large number of calculations. In the recent past, a revolution in computer technology and numerical computations has taken place. Today's computers can perform complex calculations and process large amounts of data rapidly. The engineering design and optimization processes benefit greatly from this revolution because they require a large number of calculations. Better systems can now be designed by analyzing and optimizing various options in a short time. This is highly desirable because better designed systems cost less, have more capability, and are easy to maintain and operate (ARORA, 2004).

The design of systems can be formulated as problems of optimization in which a measure of performance is to be optimized while satisfying all constraints. Many numerical methods of optimization have been developed and used to design better systems (ARORA, 2004).

In simple terms, optimization is an attempt to maximize the desirable properties of a system while simultaneously minimizing the undesirable characteristics (STORN; PRICE; LAMPINEN, 2005). Formally, mathematical optimization ***(MO)*** is defined as a process which involves: *(i)* the formulation and *(ii)* the solution of a constrained optimization problem of the general mathematical form (STORN; PRICE; LAMPINEN, 2005):

$$\boldsymbol{minimize}\ \ \boldsymbol{f(x)},\ \ \boldsymbol{x} = [\boldsymbol{x_1}, \boldsymbol{x_2}, \boldsymbol{x_3}, \ldots, \boldsymbol{x_n}]^{\boldsymbol{T}} \in \mathbb{R}^{\boldsymbol{n}} \tag{C.1}$$

$$\boldsymbol{subject\ to} \quad \boldsymbol{h_i(x)} = \boldsymbol{0}, \quad \boldsymbol{i = 1, \ldots, n_e} \tag{C.2}$$

$$\boldsymbol{g_j(x)} \leqslant \boldsymbol{0}, \quad \boldsymbol{j = 1, \ldots, n_g} \tag{C.3}$$

where $\boldsymbol{f(x)}$, $\boldsymbol{h_i(x)}$ and $\boldsymbol{g_j(x)}$ are scalar functions of the real column vector $\boldsymbol{x}$.

The continuous components x_i of $x = [x_1, x_2, x_3, \ldots, x_n]^T$ are the ***design variables***, $f(x)$ is the objective function, $h_i(x)$ denotes the respective ***equality constraint functions*** and $g_j(x)$ the ***inequality constraint functions*** (STORN; PRICE; LAMPINEN, 2005). The optimum vector x that solves the problem is denoted by x^* with a corresponding optimum function value $f(x^*)$ (STORN; PRICE; LAMPINEN, 2005).

In some optimization problems, the objective is to maximize a function (rather than minimize it). In these cases, the maximization of a function is obtained by the minimization of its negative (*e.g. maximization of a function* $f(x) = (d_1x_1 + d_2x_2 + ... + d_nx_n)$ *is equivalent to minimization of its negative,* $-f(x) = -(d_1x_1 + d_2x_2 + ... + d_nx_n)$) (ARORA, 2004).

In general, constrained optimization problems can have several local minima. The existence of a single global minimum is guaranteed only under certain circumstances. The necessary conditions for a minimum in the constrained problem are obtained by using the Lagrange multiplier method (ARORA, 2004). Considering the special case of equality constraints only and using the ***Lagrange multiplier technique***, the Lagrangian function can be defined as:

$$\mathcal{L}(x, \lambda) = f(x) + \sum_{j=1}^{n_e} \lambda_j h_j(x) \tag{C.4}$$

where λ_j are unknown *Lagrange multipliers for equality constraints.* The necessary conditions for a stationary point are:

$$\frac{\partial \mathcal{L}}{\partial x_i} = \frac{\partial f}{\partial x_i} + \sum_{j=1}^{n_e} \lambda_j \frac{\partial h_j}{\partial x_i} = 0, \quad i = 1, \ldots, n \tag{C.5}$$

$$\frac{\partial \mathcal{L}}{\partial \lambda_j} = h_j(x) = 0, \quad j = 1, \ldots, n_e \tag{C.6}$$

These conditions, however, apply only at a regular point, that is, at a point where the gradients of the constraints are linearly independent. If constraint gradients that are linearly dependent exist, then it is possible to remove some constraints without affecting the solution. At a regular point, Eqs. (C.5) and (C.6) represent $n + n_e$ equations for the n_e Lagrange multipliers and the n coordinates of the stationary point (ARORA, 2004).

The situation is somewhat more complicated when inequality constraints are present. To apply the *Lagrange multiplier method* it is necessary to transform the inequality constraints to equality constraints by adding *slack variables* (ARORA, 2004). That is, the inequality constraints are written as:

$$g_j(x) + {s_j}^2 = 0, \qquad j = 1, \ldots, n_g \tag{C.7}$$

where s_j is a *slack variable* which measures how far the j^{th} constraint is from being critical. The Lagrangian function can be formed as:

$$\mathcal{L}(x, \mu, s) = f + \sum_{j=1}^{n_g} \mu_j (g_j + {s_j}^2) \tag{C.8}$$

where μ_j are unknown *Lagrange multipliers for inequality constraints.* Differentiating the Lagrangian function with respect to x, μ and s we obtain:

$$\frac{\partial \mathcal{L}}{\partial x_i} = \frac{\partial f}{\partial x_i} + \sum_{j=1}^{n_g} \mu_j \frac{\partial g_j}{\partial x_i} = 0, \qquad i = 1, \ldots, n \tag{C.9}$$

$$\frac{\partial \mathcal{L}}{\partial \mu_j} = g_j(x) + {s_j}^2 = 0, \qquad j = 1, \ldots, n_g \tag{C.10}$$

$$\frac{\partial \mathcal{L}}{\partial s_j} = 2\mu_j s_j = 0, \qquad j = 1, \ldots, n_g \tag{C.11}$$

Equations (C.10) and (C.11) imply that when an inequality constraint is not critical (and thus the corresponding slack variable is non-zero) then the Lagrange multiplier μ_j associated with the constraint is zero. Equations (C.9) to (C.11) are the necessary conditions for a stationary regular point. Note that for inequality constraints a regular point is one where the gradients of the active constraints are linearly independent (ARORA, 2004). These conditions are modified slightly to yield the necessary conditions for a minimum and are known as the *Karush-Kuhn-Tucker conditions (KKT)* (ARORA, 2004).

The Karush-Kuhn-Tucker conditions (KKT) conditions can be sumarized as shown below:

$$\frac{\partial h(x,\lambda)}{\partial x_j} = 0 \quad for \quad j = 1,...,n \tag{C.12}$$

$$\lambda_i g_i(x) = 0 \quad for \quad i = 1,...,n_g \tag{C.13}$$

$$g_i(x) \leq 0 \quad for \quad i = 1,...,n_g \tag{C.14}$$

$$\lambda_i \geq 0 \quad for \quad i = 1,...,n_g \tag{C.15}$$

where Eq. (C.12) is known as the parallel gradient condition, Eq. (C.13) is known as the ortogonality condition, Eq. (C.14) are the conditions for the satisfaction of the original constraints and Eq. (C.15) is known as the Lagrange multiplier nonnegativity condition.

C.1 EXAMPLES:

To illustrate the optimization process using the Karush-Kuhn-Tucker conditions, three simple examples will be shown below in order to help the reader to understand how the optimization process can be developed by using the KKT conditions. The first of these examples shows an optimization problem without constraints, The second example shows an optimization with equality constraints, and finally the third of these examples shows an optimization with equality and inequality constraints.

C.1.1 Example 1: Optimization without constraints.

In this very simple example we optimize an objective function without considering any constraint as shown in Eq. C.16. That means that the variables x_1, x_2, x_3 and x_4 can assume any value in $\mathbb{R}^4$.

$$minimize: \quad f(x_1,x_2,x_3,x_4) = x_1^2 + x_2^2 + x_3^2 + x_4^2 \tag{C.16}$$

To solve this optimization problem it is necessary to define a Lagrangian function $(\mathcal{L})$ first as shown below in Eq. C.17. Differentiating the Lagrangian function $(\mathcal{L})$ with respect to x_1, x_2, x_3 and x_4 and equating to zero allow us to obtain Eqs. C.18 to C.21. These equations allow us to construct a mathematical system whose solution will solve the optimization problem. In this example the solution is

obtained by using a very simple gradient approximation.

$$\mathcal{L}(x_1, x_2, x_3, x_4) = f(x_1, x_2, x_3, x_4) = x_1^2 + x_2^2 + x_3^2 + x_4^2 \quad \text{(C.17)}$$

$$\frac{\partial \mathcal{L}}{\partial x_1} = 2x_1 = 0 \quad \text{(C.18)}$$

$$\frac{\partial \mathcal{L}}{\partial x_2} = 2x_2 = 0 \quad \text{(C.19)}$$

$$\frac{\partial \mathcal{L}}{\partial x_3} = 2x_3 = 0 \quad \text{(C.20)}$$

$$\frac{\partial \mathcal{L}}{\partial x_4} = 2x_4 = 0 \quad \text{(C.21)}$$

Solving Eqs. C.18 to C.21 it is possible to determine the solution to the optimization problem as: $x_1 = x_2 = x_3 = x_4 = 0$ and $f(x_1, x_2, x_3, x_4) = 0$.

In order to graphically represent this results, consider for example a 2-dimensional plane in 4-dimensional space as shown in Fig 50. In that figure it is possible to observe that the optimum values for the x_1 and x_4 variables are located at the origin. this analysis can be extended to any other pair of variables in a similar way. A similar graphical analysis will be done below for examples 2 and 3 but including constraints.

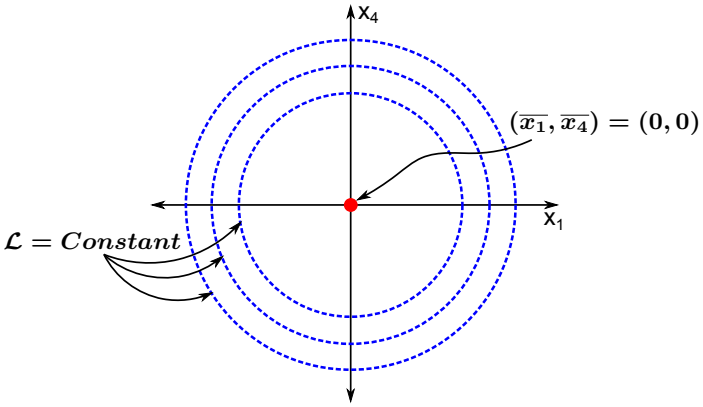

Figure 50 – Example 1 represented in two dimensions

C.1.2 Example 2: Optimization with equality constraints.

In this example we will optimize the same objective function shown in Eq. C.16 and rewritten in Eq. C.22, but considering an equality constraint as shown in Eq. C.23. That means that the variables x_1, x_2, x_3 and x_4 can assume only values satisfying the equality constraint C.23. The optimization problem can be described as:

$$\textit{minimize}: \quad f(x_1, x_2, x_3, x_4) = x_1^2 + x_2^2 + x_3^2 + x_4^2 \tag{C.22}$$

$$\textit{subject to}: \quad h(x_1, x_2, x_3, x_4) = x_1 + x_2 + x_3 + x_4 = 1 \tag{C.23}$$

To solve this optimization problem it is necessary to define a Lagrangian function ($\mathcal{L}$) first as shown below in Eq. C.24. Differentiating the Lagrangian function ($\mathcal{L}$) with respect to x_1, x_2, x_3, x_4 and λ and equating to zero allow us to obtain Eqs. C.25 to C.29. These equations allow us to construct a mathematical system whose solution will solve the optimization problem.

$$\mathcal{L}(x_1, x_2, x_3, x_4, \lambda) = x_1^2 + x_2^2 + x_3^2 + x_4^2 + \lambda(1 - x_1 - x_2 - x_3 - x_4) \tag{C.24}$$

$$\frac{\partial \mathcal{L}}{\partial x_1} = 2x_1 - \lambda = 0 \tag{C.25}$$

$$\frac{\partial \mathcal{L}}{\partial x_2} = 2x_2 - \lambda = 0 \tag{C.26}$$

$$\frac{\partial \mathcal{L}}{\partial x_3} = 2x_3 - \lambda = 0 \tag{C.27}$$

$$\frac{\partial \mathcal{L}}{\partial x_4} = 2x_4 - \lambda = 0 \tag{C.28}$$

$$\frac{\partial \mathcal{L}}{\partial \lambda} = 1 - x_1 - x_2 - x_3 - x_4 = 0 \tag{C.29}$$

Solving Eqs. C.25 to C.29 it is possible to determine the solution to the optimization problem as:

$$x_1 = x_2 = x_3 = x_4 = \frac{\lambda}{2} \tag{C.30}$$

$$x_1 + x_2 + x_3 + x_4 = 4\left(\frac{\lambda}{2}\right) = 1 \quad or \quad \lambda = \frac{1}{2} \tag{C.31}$$

so:

$$x_1 = x_2 = x_3 = x_4 = \frac{1}{4} \quad and \quad f(x_1, x_2, x_3, x_4) = \frac{1}{4} \tag{C.32}$$

In order to graphically represent this results, consider for example a 2-dimensional plane in 4-dimensional space as shown in Fig 51. In that figure it is possible to observe that the optimum values for the x_1 and x_4 variables are located on the curve defined by the constraint equation and satisfying the condition $x_1 = x_2 = \frac{\lambda}{2}$. This analysis can be extended to any other pair of variables in a similar way.

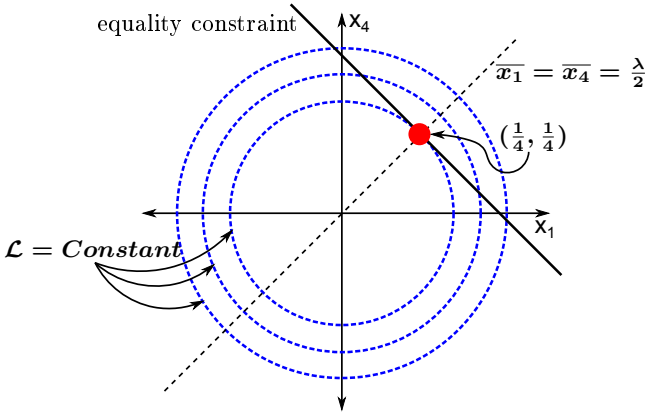

Figure 51 – Example 2 represented in two dimensions

C.1.3 Example 3: Optimization with equality and inequality constraints.

In this example we will optimize the same objective function shown in Eq. C.16 and rewritten in Eq. C.33, but considering an

equality constraint and an inequality constraint as shown in Eqs. C.34 and C.35. That means that the variables x_1, x_2, x_3 and x_4 can assume only values satisfying those equality and inequality constraints simultaneously. The optimization problem can be described as:

$$\textit{minimize}: \quad f(x_1, x_2, x_3, x_4) = x_1^2 + x_2^2 + x_3^2 + x_4^2 \tag{C.33}$$

$$\textit{subject to}: \quad h(x_1, x_2, x_3, x_4) = x_1 + x_2 + x_3 + x_4 = 1 \tag{C.34}$$

$$g(x_1, x_2, x_3, x_4) = x_4 \leq A \tag{C.35}$$

in which A is a parameter that we will play with.

Figures 52 and 53 illustrate two possible versions of this problem, depending on the value of A. (The shaded regions are the forbidden values of x, the places where $x_4 > A$).

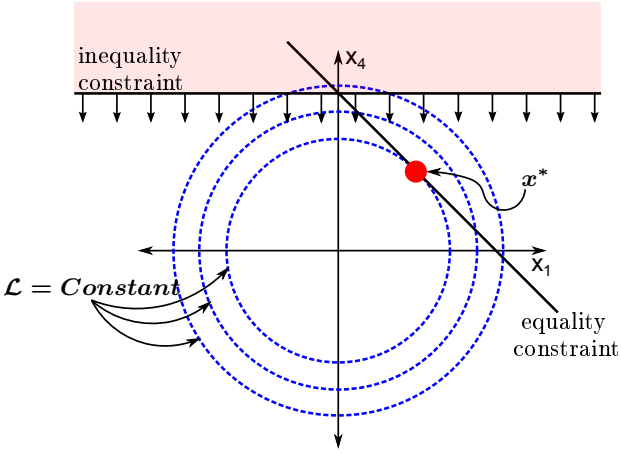

Figure 52 – Example 3 represented in two dimensions with A large

As previously discussed, optimization problems are somewhat more complicated when inequality constraints are presents due that inequality constraints need to be transformed into equality constraints. This transformation is done by using slack variables, and for the present example the Lagrangian function is expressed as shown in Eq. C.36.

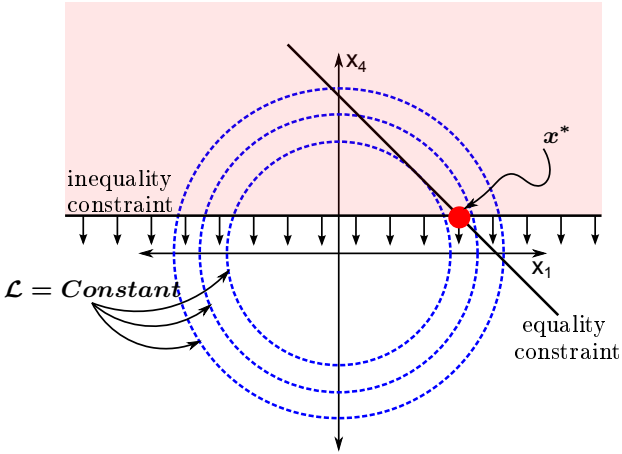

Figure 53 – Example 3 represented in two dimensions with $\boldsymbol{A}$ small

$$\mathcal{L}(x_1, x_2, x_3, x_4, \lambda, \mu) = x_1^2 + x_2^2 + x_3^2 + x_4^2 + \ldots \\ \ldots + \lambda(1 - x_1 - x_2 - x_3 - x_4) + \mu(x_4 - A) \quad \text{(C.36)}$$

Then, the necessary conditions for an optimal solution in the nonlinear problem are satisfied through the *Karush-Kuhn-Tucker conditions (KKT)* as shown below:

$$\frac{\partial \mathcal{L}}{\partial x} = 0 \quad \text{(C.37)}$$

$$x_1 + x_2 + x_3 + x_4 = 1 \quad \text{(C.38)}$$

$$x_4 \leq A \quad \text{(C.39)}$$

$$\mu \geq 0 \quad \text{(C.40)}$$

$$\mu(x_4 - A) = 0 \quad \text{(C.41)}$$

From Eq. C.37:

$$\frac{\partial \mathcal{L}}{\partial x} = \begin{bmatrix} x_1 - \lambda \\ x_2 - \lambda \\ x_3 - \lambda \\ x_4 - \lambda + \mu \end{bmatrix} = \begin{bmatrix} 0 \\ 0 \\ 0 \\ 0 \end{bmatrix} \quad \text{(C.42)}$$

Therefore

$$x_1 = x_2 = x_3 = \frac{\lambda}{2}, \quad x_4 = \frac{\lambda - \mu}{2} \tag{C.43}$$

so, from Eq C.38:

$$x_1 + x_2 + x_3 + x_4 = 4\left(\frac{\lambda}{2}\right) - \frac{\mu}{2} = 1 \tag{C.44}$$

or

$$4\lambda - \mu = 2 \quad or \quad \lambda = \frac{2 + \mu}{4} \tag{C.45}$$

Therefore:

$$x_1 = x_2 = x_3 = \frac{2 + \mu}{8} = \frac{1}{4} + \frac{\mu}{8}, \quad x_4 = \frac{2 + \mu}{8} - \frac{\mu}{2} = \frac{1}{4} - \frac{3\mu}{8} \tag{C.46}$$

From Eq. C.39 we have:

$$\frac{1}{4} - \frac{3\mu}{8} \leq A \quad or \quad \frac{3\mu}{8} \geq \frac{1}{4} - A \tag{C.47}$$

From the general equations previously constructed, it is possible to analyze the behavior of the optimization problem as a function of the imposed value for A. this analysis can be divided into three cases as shown below:

Case 1: This is the interior case illustrated in Fig. 52 where we assume that $A > \frac{1}{4}$. Since $\frac{1}{4} - A \leq 0$, Eq. C.47 implies that Eq. C.40 is automatically satisfied. From Eq. C.46 we have

$$x_1 = x_2 = x_3 \geq \frac{1}{4}, \quad x_4 = 1 - (x_1 + x_2 + x_3) \leq \frac{1}{4} \tag{C.48}$$

More information can be obtained using the results in Eq. C.46 due that the condition in Eq. C.41 can only be satisfied if $\mu = 0$. Therefore:

$$x_1 = x_2 = x_3 = x_4 = \frac{1}{4} \tag{C.49}$$

which is consistent with the answer to Example 2 and common

sense. Example 2 says that this is optimal; if we also require that $\boldsymbol{x_4}$ is less than $\boldsymbol{A}$ and $\boldsymbol{A}$ is greater than $\frac{\mathbf{1}}{\mathbf{4}}$, we haven't changed anything. Note that the optimal $\boldsymbol{\mathcal{L}}$ is again 1/4.

Case 2: In this case, we analyse the limit situation where $\boldsymbol{A} = \frac{\mathbf{1}}{\mathbf{4}}$. This behaves like Case 1. The unconstrained optimum lies on the boundary. Therefore, if we ignored the inequality constraint, we would get the same $\boldsymbol{x^*}$.

Case 3: In this case we consider $\boldsymbol{A} < \frac{\mathbf{1}}{\mathbf{4}}$. If $\boldsymbol{x_4}$ were strictly less than $\boldsymbol{A}$, then Eq. C.41 would require that $\boldsymbol{\mu = 0}$. But then Eq. C.25 would imply $\boldsymbol{x} = \frac{\mathbf{1}}{\mathbf{4}}$, which violates Eq. C.39. Therefore $\boldsymbol{x_4 = A}$ and:

$$\boldsymbol{x_1 = x_2 = x_3 = \frac{1}{3}(1 - A)} \tag{C.50}$$

Also

$$\boldsymbol{\mathcal{L} = 3\left(\frac{1}{9}(1 - A)^2\right) + A^2 = \frac{1}{3}(1 - A)^2 + A^2} \tag{C.51}$$

or

$$\boldsymbol{\mathcal{L} = \frac{1}{3}(4A^2 - 2A + 1)} \tag{C.52}$$

In a generalized form, the results obtained in Example 3 can be expressed mathematically as a composed function of $\boldsymbol{\mathcal{L}}$ as function of $\boldsymbol{A}$ as shown in Eq. C.53 and represented graphically in Fig. 54.

$$\boldsymbol{\mathcal{L} = \begin{cases} \frac{1}{4} & \Leftrightarrow \quad A \geq \frac{1}{4} \\ \frac{1}{3}(4A^2 - 2A + 1) & otherwise \end{cases}} \tag{C.53}$$

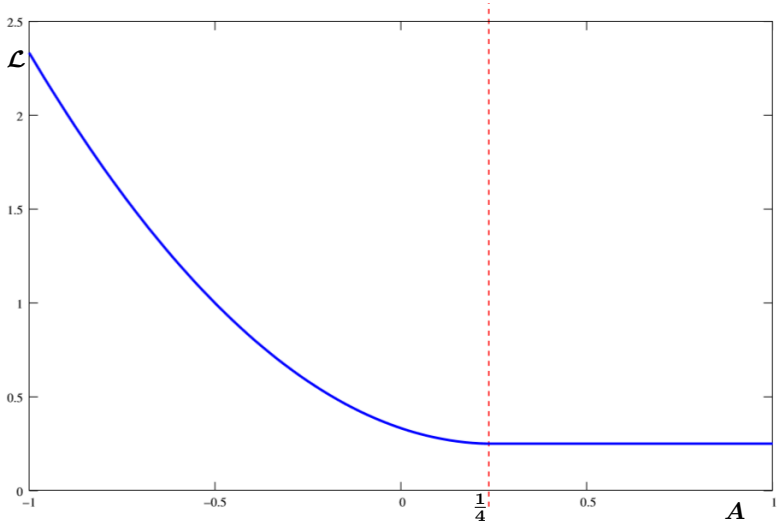

Figure 54 – Graphical representation of $\mathcal{L}$ vs A for Example 3.